Summer 2007

Development of a liquid injection propane system for spark-ignited engines via fuel temperature control

Brian Charles Applegate

Department:

DEVELOPMENT OF A LIQUID INJECTION PROPANE SYSTEM FOR SPARK-IGNITED ENGINES VIA FUEL TEMPERATURE CONTROL

by

BRIAN CHARLES APPLEGATE

A THESIS

Presented to the Faculty of the Graduate School of the

UNIVERSITY OF MISSOURI-ROLLA

In Partial Fulfillment of the Requirements for the Degree

MASTER OF SCIENCE IN MECHANICAL ENGINEERING

2007

Approved by

_____	_____
James A. Drallmeier, Advisor	Virgil Flanigan

_____

Chris Ramsay

ABSTRACT

This thesis entails the development of a liquid injected propane fuel system. Propane fuel offers opportunities in emissions reductions and lower carbon dioxide production per kilogram of fuel. However, drawbacks to the fuel include current storage in a saturated state. The storage method allows higher fuel volume density storage to minimize storage size. This method of storing the fuel presents fuel metering challenges resultant from the variable density of the two-phase flow. Traditionally, the fuel is flashed in a vaporizing heat exchanger and then pumped to the engine as a vapor. The vapor fuel is more voluminous than gasoline and thus reduces the volumetric efficiency of the engine. As a result of the reduced volumetric efficiency, a drop in engine power is experienced, all things being equal. Liquid injection offers heat of vaporization cooling from the fuel to cool the intake air and recover lost volumetric efficiency.

Pressurized systems have been developed to maintain the stored fuel as a subcooled liquid. These systems have specialized fuel tanks with in-tank pumps that boost fuel pressure to compensate for heat input to the fuel system from the engine. This additional pressure increases system sealing issues and safety concerns of fuel under pressure. The other parameter that controls the state of a fluid is temperature.

This work is concerned with utilizing temperature reduction of the saturated fuel to a sub-cooled liquid via a heat exchanger. This is accomplished by sacrificing a portion of the engine fuel requirement to vaporize in the external shell of the heat exchanger. The main fuel line is in the center of the vaporizing shell and acts as a heat source as it cools to a sub-cooled state before injection. The sacrificial fuel is inducted into the intake as a base amount of fuel.

ACKNOWLEDGMENTS

I would like to take the opportunity to thank Kawasaki Motors for providing research funding that has allowed this work to take place. Also, thanks to the University of Missouri-Rolla for providing support and facilities to accomplish this work. Thanks to the administrative assistants, machine shop gentleman, and electronics shop workers for assistance with physical build up of the supporting research facilities. Thanks to the committee members Dr. Flanigan and Dr. Ramsay for taking time to review this thesis document. Thanks to Dr. Drallmeier for taking time to provide guidance and direction during the progression of this work.

TABLE OF CONTENTS

LIST OF ILLUSTRATIONS

Page

LIST OF TABLES

Page

NOMENCLATURE

Symbol	Description
A	Flow area
π	Pi
h	Height of metering valve stem relative to closed position
D_0	Internal valve flow area diameter
α	Angle of taper on the valve stem
$\dot{m}$	Mass flow rate
ρ	Density
P_{up}	Pressure upstream of restriction
P_{sat}	Saturation pressure at upstream temperature
P_f	Pressure at flashing location
σ	Surface tension
K	Boltzmann constant
T_c	Critical temperature
T_r	Reduced temperature
Σ'	Depressurization rate
υ_f	Specific volume of saturated liquid
υ_g	Specifc volume of saturated vapor
z	Axial direction along flow line through the throat
η_V	Volumetric efficiency
V_d	Displacement volume
N	Engine speed
PW	Injector pulse width
St#	Strouhal number

ω	Frequency
D_h	Hydraulic diameter
v_{fluid}	Velocity of fluid

1. INTRODUCTION

This work describes the development of a thermally controlled liquid propane injection system. Propane is a fuel that offers better emissions characteristics for environments with carbon emission restrictions because propane is a lower carbon content fuel than gasoline. Traditionally, propane is used as a vapor because it is normally stored in a space saving saturated state and then vaporized in the fuel system in order to accurately meter the fuel in one phase. A liquid fuel system, as described in this work, offers power gains over vaporized fuel introduction due to the ability to use the heat of vaporization from the vaporizing fuel to cool the intake charge and improve the volumetric efficiency of the engine. This system uses temperature to control the state of the fuel in the fuel system. Temperature is more effective than pressure in controlling the phase of the fluid from a thermodynamic standpoint. Small changes in temperature of a saturated liquid alter the quality by a larger degree than small changes in pressure. Moreover, engine heat is the main culprit for fuel boiling in the injector as fuel approaches the engine through the fuel system. Therefore, thermal control can easily control fuel state and overcome the main cause of fuel boiling at the injector. For this fuel system, small amounts of saturated fuel are sacrificed to cool the bulk of the fuel flow to a liquid. The sacrificial fuel is vaporized in a heat exchanger to absorb heat from the main fuel that is drawn through a fuel line in the center of the heat exchanger. The main fuel line is injected as a liquid cooling the intake charge and the vaporized fuel is inducted into the intake manifold as a base amount of fuel.

1.1. MOTIVATION

Lower carbon-to-carbon bond energy based fuels are driving alternative fuel research. For this work, spark ignition (SI) reciprocating engines are examined for use in confined environments. The essential goal of fuels such as compressed natural gas and liquefied petroleum gas is lower carbon emissions. These alternative fuels inherently reduce other emissions such as sulfur or lead which are not present in the lighter fuels by nature of the heavy elements not following the light fuel through refining (1). The two

fuels mentioned also allow higher compression ratios in reciprocating engines (2). Liquefied petroleum gas (LPG) has an advantage over compressed natural gas however. LPG can be stored in a denser, saturated liquid state at lower tank pressure than compressed natural gas. Additionally, the conversion of liquid LPG to gaseous form presents some charge cooling opportunities due to a phase change from liquid to vapor. Liquid injection allows the fuel to vaporize and absorb heat from the control volume via heat of vaporization. If the control volume is limited to the gas in the intake manifold by insulating the manifold from engine heat, then the intake air supplies the heat absorbed by the vaporizing fuel. Looking at an ideal gas relationship under constant pressure and volume in the intake manifold, a reduction in intake temperature would necessitate a larger mass of intake constituents. Therefore, the volumetric efficiency, an engine performance metric that measures the effectiveness of bringing air into the engine, increases from the density increase that resulted from lower intake temperatures. Therefore, LPG has advantages over conventional fuels in carbon emissions as well as advantages over lighter fuels like methane in fuel density, storage pressure, and charge cooling that are important for mobile applications of spark ignition engines.

Currently systems are available to convert existing spark ignition gasoline engines to LPG as investigated by Smith et al. (3) These systems are rudimentary and have numerous drawbacks. They are evaporative kits that vaporize the fuel and then introduce the LPG as a vapor into the engine. Smith et al. (3) addresses the necessity for spark timing maps to accompany the system as a result of the altered combustion properties of the fuel for maximized efficiency of the fuel system conversion. Additionally, the conversion kits that are available demonstrate a lower brake mean effective pressure (BMEP), on the order of 95% of the peak output compared to the same engine operated on gasoline. This can be attributed to a reduced volumetric efficiency of the engine. The efficiency loss is a result of the increased vapor volume of the LPG over gasoline according to the authors of Smith et al. (3) This increase in fuel vapor volume level reduces the available volume for the voluminous oxidizing component, air. A reduction in air reduces the amount of chemical energy in the form of fuel that can be introduced to maintain a given fuel/air ratio.

Figure 1.1 demonstrates the displaced volume of air as a result of the Propane (LPG) fuel volume versus others fuels like gasoline. Propane is similar to LPG as LPG is a blended fuel intended to have properties similar to propane. Propane is also the primary component of LPG. However, LPG is a cheaper blend as manufacturing, refining, and purifying costs are lower. Utilizing LPG and correlating the fuel properties of LPG to propane, Figure 1.1 demonstrates why the kits are not efficient for power performance criteria compared to gasoline. The metric shown in Figure 1.1, partial pressure, is a measure of how much air is displaced by the fuel in the intake manifold. Partial pressure has a direct correlation with volumetric efficiency, which again is a measure of how efficiently the engine inducts air into the combustion chamber. Higher partial pressure of the air to fuel ratio equates to higher volumetric efficiency which in turn means more air which allows more fuel for a given equivalence ratio. Conversely, more fuel volume in the manifold from lower partial pressure and thus lower volumetric efficiency reduces the volume available for air. Reduced power from the lack of air volume and subsequent restriction of fuel to maintain a desired air to fuel ratio is the drawback of concern when considering a vaporized fuel introduction LPG fuel system. Propane has a lower partial pressure and will therefore occupy more space in the intake manifold effectively reducing the volumetric efficiency of the engine.

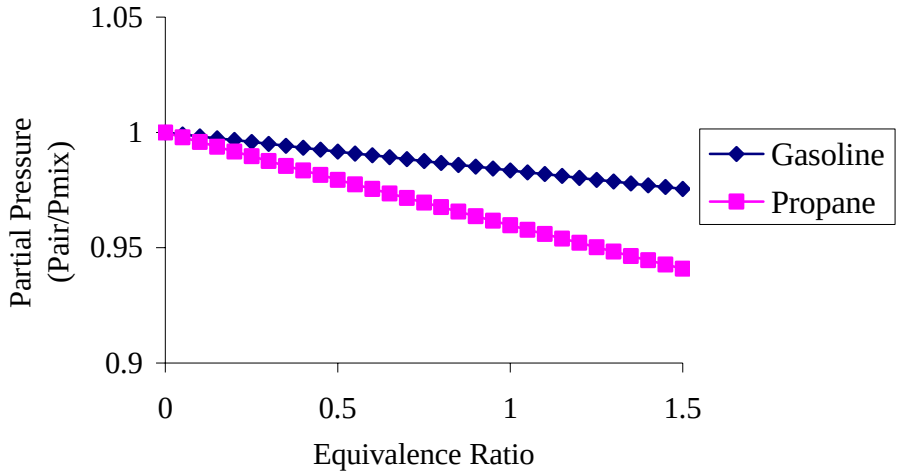

Figure 1.1 Partial pressure comparison of gasoline and propane.

1.2. OUTLINE OF THE WORK

1.2.1. Literature Review. The presentation of work in this thesis will first explore current propane systems to establish a background. Then, the literature review will shift focus to find modeling techniques for the purpose of metering the sacrificial flashing flow. As mentioned previously, metering fuel is traditionally done in a single phase. Two-phase flow presented by a saturated fluid is difficult to meter because of the unpredictable variability in density of the flow relative to time and convective parameters. Therefore, metering the flashing flow must be modeled to aid in predicting the necessary injector pulse widths of liquid flow to maintain the proper air/fuel ratio for the engine.

1.2.2. Apparatus. Following the literature review is a presentation of the experimental setup. This includes the engine and developed fuel system. Additionally, data acquisition, temperature, pressure, and flow measurements are discussed. They are followed by a description of the instrument uncertainty. Following the discussion of the setup, the experimental procedure is then introduced. This entails discussion from locating the injection location and finding injection timing in an iterative test matrix. Then discussion is presented about switching from a traditional fuel like indolene as a base line to liquid propane. After the conversion, the sacrificial vaporizing flow is iteratively tested to determine the optimum cooling flow. Then testing was performed to develop fuel injection maps for the development of the fuel system Electronic Control Module (ECM). Once the injection system was automated, attention is refocused to verifying modeling attempts and more accurately predicting the flashing flow for cooling.

1.2.3. Results/Conclusions. This section of the thesis describes the results from the testing. The results that are provided show the cylinder fuel distribution results from the testing of fuel injection location and injector timing. Then the effectiveness of the heat exchanger is presented with results of the cooling flow testing. Fuel system performance on intake temperature is then discussed. Model performance is evaluated as a comparison of predicted values versus data. Finally, uncertainty in the data is introduced.

The results are then interpreted in terms of the implications and reasons behind the trends. Discussion is given about engine performance that results from the fuel

distribution between the cylinders. Then the heat exchanger results are discussed in the terms of selecting fuel cooling versus maximizing charge cooling and percentage of fuel requirement introduced as a liquid. Modeling results are investigated and anomalies are noted. Finally, uncertainty ramifications are then discussed. After the discussion, conclusions are made about the research and the applicability to immediate engine application. Future recommendations for research sum up the conclusion and the thesis.

2. LITERATURE REVIEW

2.1. LIQUID LPG INJECTION APPROACHES

The first step in the research of this work is to investigate the current attempts to produce a liquid LPG injection system. This will provide insight as to what other researchers have learned and hopefully offer direction to developing a liquid LPG injection system for a small engine application. Moreover, the information contained in this section allows this research to differentiate the experiments to investigate a new approach to solving the two-phase fuel question. Finally, this background information serves as a benchmark for the results of this work.

2.1.1. Review Available Propane Fuel Systems. Propane fuel systems currently exist in industry. They are prevalent in applications such as forklifts and floor buffers. These systems are utilized for applications where carbon dioxide is also an engine emission of concern due to enclosed environments of interior operation. Carbon dioxide can suffocate the people in the building and must be controlled. In addition to reducing carbon dioxide, propane also offers good fuel storage opportunities compared to other low carbon fuels because it is stored in the compact and dense saturated liquid state. This compact state is also at a relatively low pressure of approximately ten atmospheres at room temperature, when compared to methane. Currently propane fuel systems operate on vaporized fuel flow in order to meter fuel delivery to the engine. This is done because two-phase mass flow is difficult to measure due to the large difference in densities of the two phases.

Conversion kits are available to convert existing engines to operate on propane fuel. The conversion kits that are utilized in Smith et al., propane vehicle projects in Caton et al. (4), emission studies of compressed natural gas and LPG conversions of light duty vehicles in Wu et al. (5), and the development of a dual fueled vehicle (gasoline and LPG) in the paper by Nelson (6) all relied on induction of the vapor phase of LPG fuel to reduce fuel system challenges. As stated by Caton et al. (4), some volumetric efficiency and performance is sacrificed to result in fewer complications of increased fuel pressure, satiation of the issue of the fuel saturation condition, and boiling of the fuel before liquid introduction. Vaporized fuel systems allow the fuel to vaporize through a regulator and

are then operational at slightly higher than ambient pressure conditions. The fuel is brought into the intake air through a carbureted induction system that meters the fuel for the engine. As mentioned in the introduction, the vapor form of the fuel displaces air and reduces volumetric efficiency. The amount of air that is brought into a spark-ignited engine determines the amount of power the engine can produce by the restriction of the air fuel ratio requirement for combustion.

For engine operation, an air-to-fuel ratio is selected as ideal for the conditions of the engine. Typically, spark ignited engines (SI) operate at an equivalence ratio of 1 for stability and preservation of the exhaust catalyst. The engine in this research is small enough to not have emissions regulations that are stringent enough to require exhaust catalysts. It is also air-cooled and therefore the engine is operated at an equivalence ratio of 1.1, which is slightly rich. The air-cooled aspect of the engine allows the engine to not require water-cooling and is cheaper. However, the valves can be hot in an air-cooled engine and a rich running engine can have valve cooling from the evaporation of the fuel transitioning from liquid to vapor.

The air-cooled engine arrangement determines the air/fuel ratio in this research. Therefore, if the propane fuel takes up more intake and cylinder volume in the vapor state than does the traditional gasoline, air is restricted and volumetric efficiency is diminished even further by the rich fuel requirement. The restricted airflow and the air-to-fuel ratio constraint effectively determine the quantity of fuel that can be introduced into the cylinder. The fuel limits the amount of energy that is in the cylinder and thus limits the release of energy that is transferred to the crank as power.

2.1.2. Liquid Injection Propane Fuel Systems. In the paper by Cipollone and Villante (7) the questions about maintaining saturated liquid are numerous and formidable, but satisfying the needs of the system can offer power gain from a liquid phase change that ambient temperature vapor introduction lacks. Liquid injection systems offer a method of recovering volume consumed by the fuel volume in the intake system. If propane is inducted as a liquid, the fuel will vaporize in the intake manifold. As the fuel flashes in the intake manifold, the fuel will absorb heat from the surrounding control volume via the heat of vaporization. With a judiciously selected control volume, the heat is drawn from the intake air increasing the density of the intake charge. The

increase in density requires more fuel to be injected to maintain the selected air to fuel ratio. More fuel energy equates to more power output of the engine.

Unfortunately, a liquid system necessitates the high pressure of approximately 10 times atmospheric pressure for saturation of LPG, depending on ambient fuel system temperature. The high pressure is required to maintain the saturated state of the fuel at ambient temperature. As has been suggested previously by Caton et al. (4), there are also parasitic pressure losses involved in liquid injection of the fuel into the intake. This will be discussed later. The losses imply a need for higher than saturation pressure in the fuel system to maintain liquid at ambient temperatures. The other component to the saturation issue is fuel temperature. As the fuel is brought to the warm operating engine in steady state operation, it absorbs heat and the saturated fuel then begins to boil. In a transient case, an engine that is shut off and then restarted after a brief pause allows the heat to boil the fuel with no flow. In either case, fuel has absorbed engine heat, boiled and is now in two phases or in the vapor state. Therefore, the fuel needs to have an elevated pressure above saturation for the ambient temperature or a temperature reduction at an original saturation pressure to counteract the pressure losses of the fuel system and absorbed engine heat.

According to Lutz et al. (8), the authors discovered that the fuel in the system could be pressurized until single-phase liquid is present. The investigated system by Lutz et al. (8) used pressure to control the state of the fuel with regards to the parasitic flow head losses. The system was pressurized over saturation pressure by the addition of fuel pumps. Pumps add large costs to a fuel system and regulators that control the output of the pumps add cost as well. Additionally, sealing the system is a more difficult task as well since higher fuel pressures heighten safety concerns. The absorption of heat is overcome in the Lutz et al. (8) work by a circulation of the fuel, suggesting that a smaller time delay in transient response is incurred by circulating when compared to increasing system pressure further to condense the fuel from a gaseous state.

Pumping the two-phase mixture presents problems as shown from the work by Lutz et al. (8) Increasing fuel pressure is complicated by the saturated fuel condition because the intake pressure drop of the pump can cause boiling in the fluid and difficulty pumping the two-phase flow. Vaporized systems choose the vapor phase because it is the

natural state of the fuel at Standard Temperature and Pressure (STP) conditions that are common for engine intake operating environments. The single phase eliminates issues of pumping a two-phase mixture and the vapor state reduces sealing and pressurized fuel safety concerns. A sacrifice is made in the volumetric efficiency of the engine for fuel system simplicity because the fuel must be in one phase to be metered in the delivery system.

2.1.3. Model Approach to the Liquid Propane Fuel System. In the paper by Cipollone and Villante (7) the pressure losses in pipes, fittings, injectors, filters, and pumps are examined as well as heat transfer to the operating fluid. These effects must be addressed to estimate requisite fuel overpressure or cooling to a sub-cooled liquid state. The paper by Cipollone and Villante (7) presents a model that examines the issues that create boiling in a liquid LPG system. Boiling is a realistic concern, as the fuel cannot be metered as a two-phase flow because of the drastic fuel density difference between liquid and vapor phases. Control of saturated fuel and ensuring that the fuel is indeed a liquid at the fuel metering location is the largest challenge for a liquid phase introduction LPG fuel system. The authors Cipollone and Villante (7) consider higher pressures the solution to maintaining liquid in the fuel system. They essentially treat the heat transfer to the operating fluid as a pressure loss.

2.1.4. Approach of the Present Work. The purpose of this work is to investigate pressure losses and heat transfer as heat additions to the fluid that causes boiling and thus try to control the state of the fuel by lowering the temperature. If the saturation pressure problem is solved with temperature control, then high pressures and expensive devices such as in-tank fuel pumps can be avoided. A heat exchanger can be utilized to control and reduce the fuel temperature before the injector to ensure the liquid phase at fuel metering location. This method reduces system costs and hazards. Also, it is more viable for a small, mobile spark ignited engine application that is investigated in this work. The cooling media can be supplied by the saturated flow. In steady state, a small portion of the fuel can be vaporized in the heat exchanger and used in the manifold as a fraction of introduced fuel. As the sacrificial fuel flashes, the bulk liquid fuel is cooled. This sacrificial fuel induction approach can also lend a solution to warm engine start up issues

for the aforementioned transient fuel system difficulty that is present for any liquid introduction system, as presented by Lutz et al. (8)

The transient conditions of hot start are difficult to predict because the fuel system is traditionally off when the engine is off. This allows the possibility of fuel boiling which results in a two-phase condition or vapor state of the fuel. The quality is difficult to predict and the fuel metering is a larger challenge as a result of the quality issue. Fuel metering is less complicated for a given, stable quality. This is because the quality determines the type of flow regime that exists through the previously mentioned sacrificial vaporizing flow restriction that a portion of the engine fuel flashes through to cool the main fuel line. Also, the lower the quality, the more saturated liquid is available in the sacrificial flashing flow to absorb heat via heat of vaporization. The heat exchanger system can be tuned to operate the engine off of the only the vaporizing flow that is also cooling the injector. Thus the engine can be operated reliably at idle, and the fuel system can realize a rapid response to the warm start.

This research is thus focused on operating a small spark ignition engine on liquid injected propane in emission-controlled environments. Emissions, system cost, and response time of the fuel system are large concerns for this application. Therefore, the heat exchanger approach to fuel phase control is the method used to overcome the saturation problems. Also, this research focuses on the fuel that is cheaper and more readily available to the consumer than propane, which is LPG. LPG is commercially sold as propane but is actually a blend of hydrocarbons that presents variable fuel composition. Lastly, the phase control utilizing the sacrificial fuel flashing provides another aspect to this research. The flashing device has to be investigated as a supportive subsystem to the heat exchanger. This is important to regulate fuel introduction from an air to fuel ratio control standpoint and optimization of utilizing the fuel injector to deliver as much fuel as possible in the liquid state to gain the most increase in volumetric efficiency for this configuration.

2.2. EXISTING MODELS OF TWO-PHASE FLOW THROUGH FLASHING DEVICE

The primary intent of studying the existing models of flashing fluids is to understand the phenomenon that this work hinges upon for success. The present work relies on sacrificial cooling supplied by a small portion of flashing fuel into the outer shell of a counter flow heat exchanger. Understanding this process helps the researcher maximize charge cooling of the fuel system. With an accurate model, the flashing flow can be minimized in the heat exchanger and thus more fuel will be delivered from the injector in the manifold as a liquid. This provides the maximum intake charge cooling possible. The first pass at comparing models is to investigate the most comprehensive models and identify necessary components for modeling the flow of this research. For the necessary components to be determined, however, the needs of this research must be understood first.

2.2.1. Necessary Components to Modeling the Vaporizing Phenomenon. A heat exchanger that utilizes sacrificial cooling for the bulk flow is developed for the fuel system. A schematic is shown in Figure 2.1. A thermodynamic look at attempting to control fuel phase reveals the fact that smaller temperature changes can control the quality of a fluid more effectively than larger pressure adjustments, so the system can be more manageable via temperature control. This allows the bulk of the fuel to be kept as liquid and the vaporized fuel can be introduced into the manifold as a base amount of fuel. However, this approach requires vaporization of a saturated or sub-cooled liquid to cool the bulk of the fuel. This method produces some vapor state fuel induction that will reduce volumetric efficiency. Maximizing charge cooling in the intake manifold requires minimizing the amount of vaporization in the heat exchanger. Charge cooling only takes place if the vaporization of the fuel from the injector absorbs the heat from the control volume of the intake air. If more of the fuel requirement is supplied in a warm vapor because of necessary cooling requirements to cool the liquid in the injector, then there is less cooling available via flashing of liquid introduction for the intake air control volume. Therefore, modeling the vaporization in the heat exchanger becomes essential to maximize the efficiency of this approach. An accurate model can ensure that there exists enough cooling to maintain a liquid state at the injector for steady state and transient

conditions while the cooling from vaporization is minimized in the heat exchanger and thus maximizes charge cooling in the intake manifold.

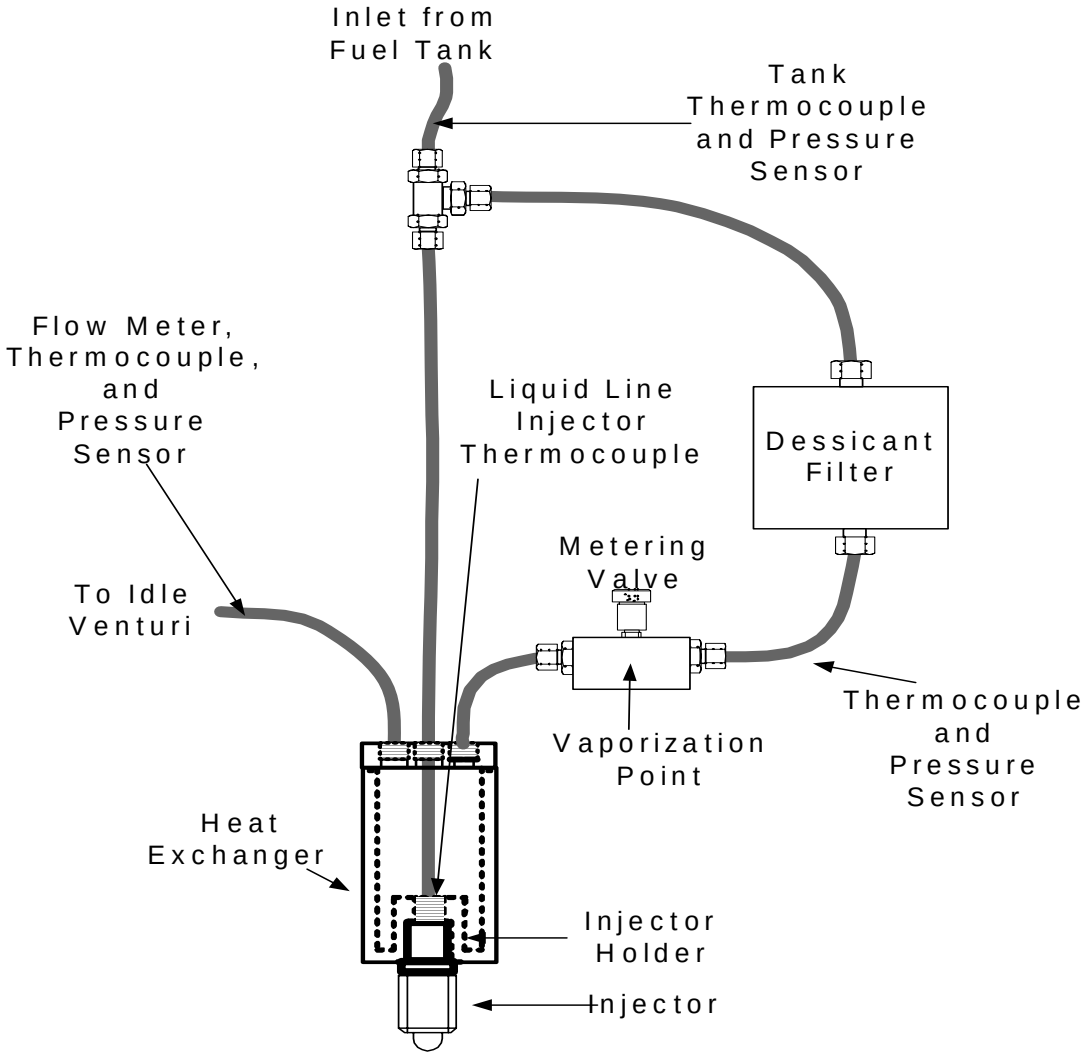

Figure 2.1 Basic Liquid Phase Propane (LPP) injection system components with instrumentation.

A model is required to manage the flow of vaporizing fuel to maximize the charge cooling of liquid injection. The fuel flow is dependent upon the environment of the tank because of the saturated condition of the fuel pressure is dependent upon ambient temperature. The system does not contain fuel pumps or pressure regulators to control

the fuel pressure so a model must account for the pressure changes upstream of the flashing device that is used to vaporize the fuel into the heat exchanger. It is important to regulate the fuel flow across the flashing device for two reasons. The fuel flow should be measured for air-to-fuel ratio control. This is important for developing the fuel map for the injector. The other reason is the fuel flow through the flashing device must be able to be predicted to allow selection of an appropriate cross sectional area for the flashing device. This is required for cooling predictions, which are dependent upon quality and mass flow that reliably ensure liquid in the line to the injector.

For example, a theoretical diagram of model predictions for the fuel flow versus an example flashing device, an orifice, and upstream pressure is presented in Figure 2.2. The orifice diameter is the geometric parameter that can be related to effective cross sectional area of any flashing device. The figure shows the expectations that higher flow rates are achieved with larger orifices. Also, the curves reduce, as upstream pressure increases because a given orifice size at a higher pressure will transition up to a higher flow rate curve.

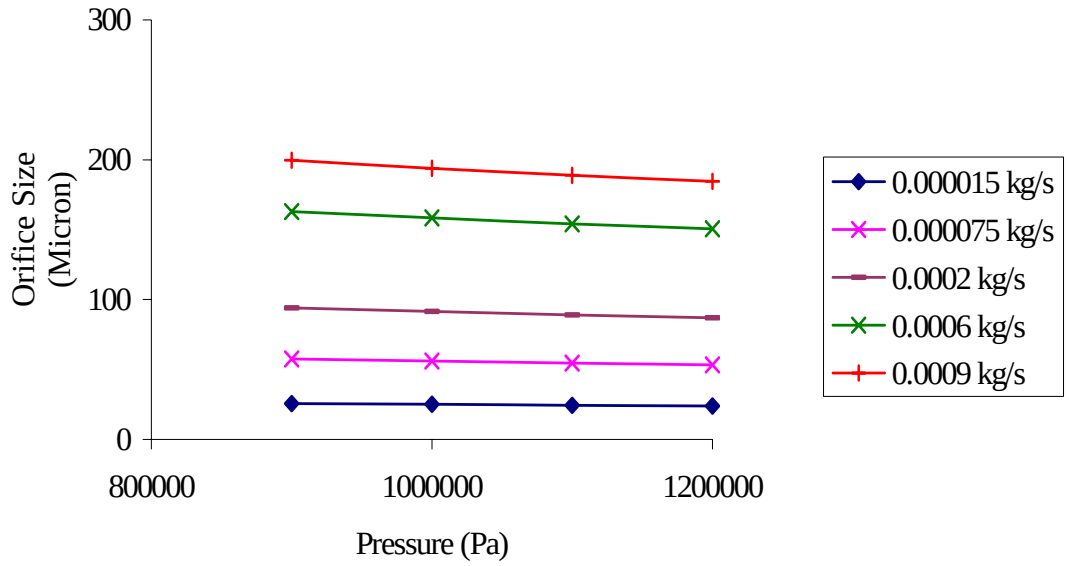

Figure 2.2 Theoretical model prediction of orifice size for a desired flow of fuel and given upstream pressure.

The flashing model should reflect the environment of operation of the fuel system. The devices of interest for this work are interchangeable orifices and a metering valve. It should also confront possible issues of the fuel through the flashing devices such as two-phase flow, choked flow, and other fluid flow parameters. There are no models in existence that can simply and completely predict two-phase flow, so reasonable approximations are sought and investigated for feasibility of measurement verification by experiment. Choked flow is typically a gaseous flow issue and may be neglected if the quality of the upstream fuel is low enough to be approximated as a liquid. The flow parameters should have an upstream pressure that is variable with temperature, as the saturated fuel tank will deliver a different pressure depending on the ambient environment of the tank. Also, the pressure downstream of the flashing device should be slightly above standard atmospheric, as the vapor ultimately vents through the heat exchanger to the intake manifold. Flow friction and fuel surface tension are also considered. Mass flow rate is the desired output parameter of the model for the air-fuel ratio of the engine and heat exchanger cooling calculations. The thermodynamic states upstream and downstream of the flashing device should be known, so temperature at those two locations should be included in the flashing model. Finally, the complexity of the model should be considered so that it can actually be verified via experiments and implemented in a functional role.

The functional role can be as limited as developing a table to decipher what orifice should be installed in the fuel system given the environment. Or it may be as advanced as real-time altering of the fuel injection map in the engine computer to change the pulse width of the injector to reflect different injector supply pressures, but also account for a change in flow rate of the orifice from the tank pressure change given a change in tank temperature. This real time model must be fast however. The injector at wide open throttle (WOT) conditions uses approximately 1/3 of the revolution time at 3600 RPM, the top speed of the research engine. The system state measurements would be taken after injection stops, requiring calculation of next pulse width, and command to the injector to be ready by the start of injection on the next crank revolution. In real time this is on the order of 12 milliseconds.

Utilizing the knowledge of the system needs, several preliminary models for vaporization are investigated. These models attempt to model the saturated flow from the high-pressure side of the flashing device through the restriction to the low-pressure side. To accurately predict mass flow rate, the condition of the fluid must be known in the throat. Pressure and temperature are the state defining thermodynamic parameters that can easily be measured and are the focus of the model selection. These parameters can produce a quality and as previously mentioned, the quality will describe the two-phase flow regime. The last parameter that is necessary to predict mass flow rate through the throat is the velocity of the fluid. This parameter can be used, with a density obtained from the quality, to predict mass flow from a given effective area from the flashing device. Additionally, the scale of the project is a throat on the order of 50 microns, which is roughly the size of the orifice that produced desired mass fuel flow for air-fuel ratio and cooling during preliminary tests on heat exchanger viability. That orifice is a thin disc that is shown in Figure 2.3.

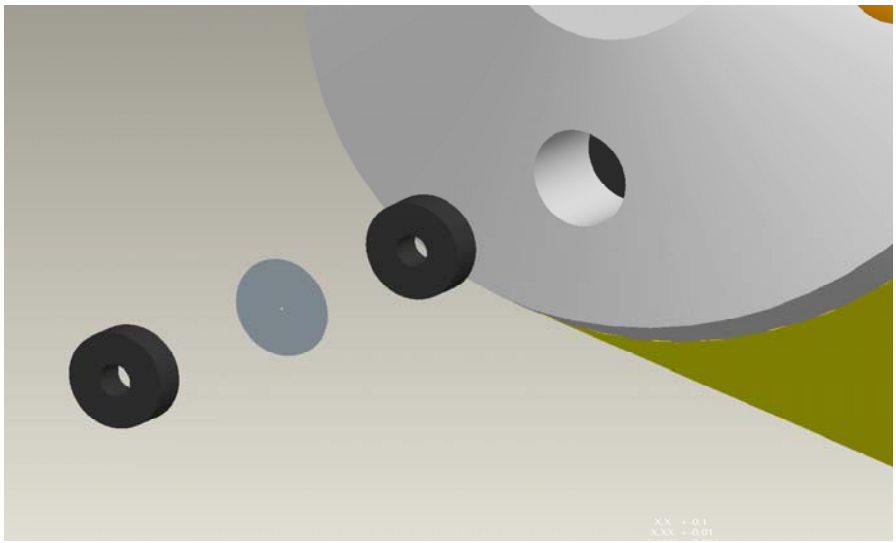

Figure 2.3 Picture of an orifice of minute hole size.

The orifice is a tiny hole in the middle of the thin grey disk in Figure 2.3. The hole size of the orifice in the picture has been enlarged compared to the other components

for visualization purposes. A hole the size of 50 microns in diameter is not visible unless light shows through the disc from behind. Therefore, the scale of the model is a concern that physical similarities between a reference model and the work of this paper must be investigated. Models that address flow in nuclear reactors use plumbing facilities that are many orders of magnitude larger than the plumbing fixtures of this work. As a result, the flow regime through the plumbing of this work may be subject to different relative flow friction coefficients and physical structure of plumbing components. The orifice of this work must resist approximately ten atmospheres of pressure and have a diameter on the order of 50 microns. The orifice essentially becomes a short tube even though the thickness of the orifice is on the order of hundredths of a millimeter.

2.2.2. Vaporizing Model Review. An inherent criterion for the model is that it should maintain simplicity so that a programmable logic controller can be employed for the control of the system if the model employment is aggressive enough to be utilized in the engine computer. The goal of the model search is to find a model that meets the needs of the work that is discussed above with as much detail that can be afforded by the simplicity of the system and desired use. Therefore, intricate models are presented first and discussed. Although they provide useful insight, they are then discarded for stated reasons of superfluous detail for this work. The simpler models are then investigated. With this direction the model review is given below.

The reference by Van der Meer (9) is an extensive model that thoroughly examines the fluid vaporization model in terms of thermodynamic properties. However, the model relies on quantities that are difficult to measure in a flashing device with an effective area equal to a 50 micron orifice, such as velocity. The reference from Miyamoto and Watanabe (10) is another extensive property model. This model is specifically focused on propane and is quite thorough as well as practical in application. It requires a fair amount of computing power and could not feasibly be employed in a computer in the cost scale of the fuel system developed in this work.

There are several other models available that examine two-phase flow through flow restrictions. The models make assumptions about the flow and the conditions to simplify the approach to the complex problem. The assumptions can be as limited as regulating the slip ratio between the phases as the flow progresses through the test section

to assuming the flow is one phase through the measurement section. Resulting from the assumptions that are made, there is a myriad of different complexities that can be applied to the model for two-phase flow with associated levels of reliability, accuracy, or practicality.

The first model that was examined was from Jeong and Choi (11). The main purpose of this paper was to devise a model that could accurately describe fluid movement through an orifice. The approach is a very comprehensive use of the Navier-Stokes equations. However, assumptions still have to be made such as slow, viscous flow that travels axis-symmetrically through the orifice in the pipe as well as assume the fluid is single phase because they wish to implement a CFD code. Also, the assumptions of fluid incompressibility and an infinitesimally thin orifice are used for the authors' paper. These are assumptions that are applicable to the research for this thesis. Unfortunately, the CFD approach is too computationally intensive and is excessive for simplistic flow rate and orifice size prediction in real-time models. Additionally, two-phase flow presents complications for CFD code. Phase interaction between the liquid and vapor states requires assumptions. As a result of making assumptions on phase interactions, it is difficult to predict changes in the flow regime of the fluid that result from a possible quality change of the fluid For this research, flow regime change is important because saturated liquid is considered to flash to vapor. However, it is not necessary to track every streamline in the flow regime and a CFD approach is therefore too intricate for the work of this thesis.

The next model from Zhang and Yang (12) is intended to simulate refrigerant flow through short tubes as an intentional vaporizing process experienced as the expansion process for a refrigerant cycle. The authors rely on a two fluid model to describe the interaction of the phases. The Newton-Rhapson method is used to iteratively evaluate the equations defining the two phases. The results of the model conclude that a pressure drop exists at the entrance of the short tube orifice, as there is a sudden contraction in the flow cross-sectional area. According to the authors, this pressure drop is large enough to convert supercritical fluids to subcritical liquid or two-phase flow quickly. Conversely, after the authors discuss the numerical solution they state that the homogeneous equilibrium model of a single fluid produces acceptable results compared

to the two-fluid model. The two-fluid model and set of assumptions are similar to the flow motivating this work in the concern for two-phase flow as well as the flashing of a refrigerant. However, the six-equation model that is solved iteratively is still too computationally intensive. The statement about homogeneous flow approximating the flow effectively is of interest for the work of this thesis. If a homogeneous model can adequately predict the flow rate of the flashing device, then the Newton-Rhapson iterative method presented by Zhang and Yang (12) is too extensive for the work of this thesis. Additionally, they do not consider an orifice or provide any provisions on how their model can be related to an orifice flow. Therefore, this model is also not feasible for the scope of this research.

The next paper that was investigated is by Lorcher and Mewes (13). The purpose of their model is to investigate the atomization of liquid and vapor mixtures for the purpose of enhancing heat transfer and mass transfer. In this paper the authors examine gas and liquid ratios and relied on the liquid and vapor Reynolds numbers to describe the phases. However, they attribute variations in parameters like droplet size and velocity to liquid properties and not viscous differences as expected by Reynolds number references. The model assumptions include flow characteristics that cover single-phase liquid flow as well as various qualities of two-phase flow. Also, the model assumes that there is frozen flow through the restriction. The authors' model is relevant to the research of this work by way of investigation into the flow of liquid and two-phase fluid through an orifice. The authors' model assumption of frozen flow can simplify the model presented in this work by reducing terms and parameters that involve the slip ratio of the phases and the interaction of the phases based on mass, momentum, and energy. However, the model presented by Lorcher and Mewes (13) assumes a given orifice size and then uses the Reynolds number in the definition equation for each phase to determine other parameters such as fluid velocity across the orifice. To utilize the model of Lorcher and Mewes (13) in the current work would necessitate a fluid velocity measurement and flow rate measurement that is difficult in a 50-micron diameter test section. Additionally, the authors assume compressibility when the flow into the orifice of the model for the work of this thesis is assumed to be a saturated liquid. Therefore, the model from Lorcher and Mewes (13) is not the basis for a vaporizing model for the research of this thesis.

The work by Bahajji et al. (14) focuses on new refrigerants that will replace the CFC and HCFC refrigerants. One fluid that is investigated by the authors is the fluid of interest for the current work, propane (R290), which is similar to LPG. The model is concerned with the expansion process in a metering valve. The metering valve geometry was examined to produce a normalized area for the valve geometry shown in Figure 2.4.

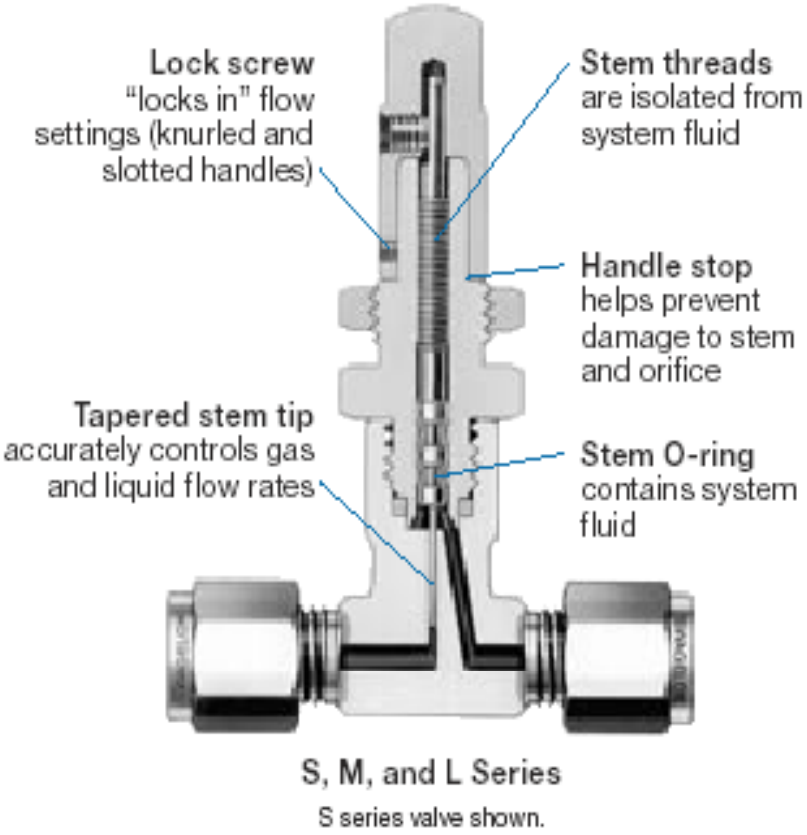

Figure 2.4 Picture of valve geometry.

$$A = \pi h[D_0 \sin(\alpha) - \frac{h \sin^2(2\alpha)}{4\cos(\alpha)}] \quad (1)$$

Equation 1 is the geometric throat area equation for the metering valve in Figure 2.4 (Swagelock documentation: *http://www.swagelok.com/downloads/webcatalogs/EN/MS-01-142.pdf*). It is used to calculate the flow area through the throat of the metering valve.

The effective flow area parameter allows a relation of the metering valve model in the paper by Bahajji et al. (14) to be related to an orifice restriction. The effective area parameter is a number that represents the area a circular orifice requires to flow the same quantity of mass at the same test conditions and is described in Equation 2.

$$A_i = \frac{\dot{m}}{\sqrt{2\rho(P_{up} - P_i)}} \tag{2}$$

Equation 2 is the effective flow area equation for the metering valve in Figure 2.4. This parameter represents the variable donut of flow area around the valve stem and inside the stem housing as a function of valve lift as visualized in Figure 2.4. Valve lift affects the function via the tapered valve stem changing the inside diameter of the donut and thus allowing a change in flow area.

The parameters for the model are measurable conditions such as steady state pressure and flow rate. The authors also examine choke concerns with experiments that vary upstream pressure, upstream sub-cooling, and valve lift. Based on the upstream conditions and the effect they have on the flow rate, the authors develop an effective flow area that is founded on the Bernoulli equation and the assumption that the flow through the orifice can be treated as single-phase liquid. A note is made on the difficulty in measuring a pressure at the throat and a method is derived to circumvent that issue via the saturation pressure and depressurization rate given below.

$$P_{sat} - P_f = 0.253 \frac{\sigma^{\frac{3}{2}}}{\sqrt{KT_c}} \frac{T_R^{13.73}\sqrt{1+14\Sigma'^{0,8}}}{[1-\frac{\upsilon_f}{\upsilon_g}]} \tag{3}$$

Equation 3 is the critical flashing flow equation used by the authors for the metering valve in Figure 2.4. The capital Sigma prime term defined in Equation 3 and

defined in Equation 4 represents the depressurization rate across the vena contracta for the metering valve in Figure 2.4.

$$\Sigma' = \frac{\dot{m}^3}{\rho^2 A_f^4}\frac{dA}{dz} \tag{4}$$

$$\frac{dA}{dz} = \frac{dA}{dh}\frac{dh}{dz} = [D_0 \sin(\alpha) - \frac{h\sin^2(2\alpha)}{2\cos(\alpha)}]\frac{\pi}{\cos(\alpha)} \tag{5}$$

Equation 5 is the change in area along the streamlines of the flow for the metering valve in Figure 2.4. The primary assumption is that the flow is an incompressible single-phase liquid flowing through the orifice and flashes upon the exit of the restriction. Also, no heat transfer or transport phenomena between phases are assumed as the single-phase assumption negates the possibility of interfacial interaction. This simplifies the model but allows some uncertainty into the analysis. No viscous forces are mentioned and are therefore assumed neglected. This assumption can also add uncertainty to the analysis as viscous forces could cause pressure gradients in the flow that cause local vaporization in the restriction.

For the use in this research, the model was used in an explicit code to predict the orifice area given temperature and pressure at both upstream and downstream of the flow restriction. The pressure and temperature parameters are required to satiate the model equations. Physically, the conditions are measured for use in the thermodynamic quality transfer from 0 to 1 after the orifice in the flashing process. Additionally, the input parameters are required to calculate the velocity through the orifice via the stated Bernoulli origin of the model. The implementation of the model in the program code is discussed later. The intent of using the model is to develop a relationship between orifice diameters at different ambient temperatures for the saturated pressure in the fuel tank as shown in Figure 2.2. This allows the environmentally susceptible saturated fuel system to be configured to operate in variable conditions efficiently.

2.3. MODEL SIMPLIFICATION

The testing of the Bahajji et al. (14) model from the above discussion revealed a possible simplification of the flashing flow model that can be beneficial to the application for a relatively small-scale engine. The Bahajji et al. (14) model did not produce reasonable flow rate predictions compared to experimental data for this fuel system. Investigation into the extreme cases of flow to bracket the flow rate prompted with the consideration of simply using the Bernoulli equation. The Bernoulli equation was acceptable at predicting the flow rate compared to the data. This simplification is beneficial in numerous ways. First and foremost, it ensures that an effective area of a flashing device can be predicted for a desired flow rate using only measurable parameters of pressure and area upstream of the throat in the flashing device. Moreover, the simplicity implies that this model can be implemented for real time control of the flashing flow as well as the injector. Therefore the cooling can be adjusted to maintain the desired liquid temperature at the injector for all engine set points. In theory, this adjustable flow restriction area can further increase charge cooling at lower fuel demand set points of engine operation by further reducing flashing flow to the heat exchanger thus requiring more injection to cool the low load charge. Then the flow area of the flow restriction can be increased to satiate the high cooling demand on the heat exchanger brought on by high fuel demand engine operation. However, this assumption of real time flashing flow adjustment in the effective flow area of the flow restriction must be validated with testing.

2.3.1. Revised Modeling Approach. During the testing and cooperative modeling stage, the model from Bahajji et al. (14) experienced under prediction of the flow rate that was measured in experiment. The Bernoulli equation was implemented to use as a baseline to verify the data, as the authors' made reference to their model being based on a Bernoulli analysis. The existing experimental work agreed with Bernoulli's on an average flow rate basis. This is not unfounded as the authors Zhang and Yang (12) had alluded to a homogenous model adequately predicting the flow in their experiment. Also, the paper by Lorcher and Mewes (13) suggested that frozen flow exists across the throat. This prompted more literature research to investigate flashing flow and determine

if a more simple approach like Bernoulli's equation could realistically be applied to flashing flow.

A model by M. W. Benjamin and J.G. Miller (15) investigates the flow features of various levels of quality of saturated water through throttling orifices. The intent is to model the possibility of throttling orifices being utilized for the drainage of condensate from feed-water heaters. They note that a supply of fluid that overwhelms the flow rate of the orifice will stagnate and build a pressure head in front of the orifice. This creates a pressure on the centerline of the orifice that is equal to the upstream pressure. This suggests that the saturated fluid will not flash in the restriction. Moreover, the authors state that no critical pressure was found in their data to suggest choking of the orifice relative to variations in pressure conditions. From observation of the results the authors state that saturated water passing through an orifice will not flash until after the orifice. They also state that cold water can be used to approximate the flow of low quality saturated water through an orifice. This model supports the use of the Bernoulli equation to predict flashing flow through an orifice by the statement that the pressure in the orifice throat is the same as the upstream pressure and the comparison of low quality two-phase flow through the orifice to sub-cooled liquid.

The model by McNeil (16) addresses the flow within the restriction device. The model is extremely thorough as it examines inter-phase transfers of heat, mass, momentum and even addresses flow orientation with respect to vertical or horizontal flows. The results from the paper indicate that the pressure in the restriction is similar to the upstream pressure. Moreover, the Mach number for incompressible orifice flow only reached 0.36 indicating that compressibility effects are negligible in abrupt expansions under the conditions considered. The model is based on stagnation conditions that are easy to measure. The model also uses an averaged specific volume across the flow restriction, which supports the model by Lorcher and Mewes (13) of a frozen composition through the restriction. The study supports previous models on the premise that a two phase-fluid will not alter composition through the restriction. Most importantly, the model has an explicit equation via mass continuity to calculate an area for a given mass flow rate. Unfortunately, this model is heavily focused on choking of the flow and not on finding an effective orifice area. The more comprehensive

examination of flow area deals with Mach numbers and the speed of sound in the fluid. The speed of sound in propane can be established if the phase or quality is know, but the Mach number entails obtaining an average velocity term at the throat to predict a mass flow rate and thus an orifice area. This extensive and detailed model is not applicable to the intent of this research because of the throat velocity requirement, but it does support the use of the Bernoulli equation via the frozen flow assumption and the upstream pressure to throat pressure correlation.

The work of Perry, Jr. (17) investigates critical flow of a compressible fluid through a sharp-edged orifice that supplements the existing critical flow data. The focus of the model is a relationship between pressure, temperature, and orifice area in an explicit equation. The intent is to predict a flow rate from a given orifice area. One of the experimental assumptions is that the fluid before the orifice is stagnant. This allows the author to neglect the velocity of the approaching fluid to the orifice and can be justified by a simple pipe diameter ratio and conservation of mass. The first assumption is extended so that the orifice is sufficiently small relative to the pipe to treat the pipe as a pressure vessel. The model meets the objective of this research in having an explicit equation to relate orifice area to measurable flow parameters such as pressure and flow rate. However, the author's model is for single-phase compressible gaseous flow and is therefore not used as the model for this thesis. However, the paper did support the use of the Bernoulli equation with the statement of stagnant conditions before the flow restriction.

The model by Robert E. Henry and Hans K. Fauske (18) has the purpose of modeling two-phase flow to allow more accurate safety predictions for pressurized systems, nuclear reactors, and refrigeration systems. This extensive model allows the phases to interact through the flow restriction devices. The model is applicable to this case as the quality goes to zero. However, a flow that has a quality below 0.14 is treated as frozen flow across the throat according to the model and they state that the homogeneous equilibrium model actually underestimates the flow rate. Therefore, saturated and sub-cooled flow will not have vapor in the flow until the throat exit. However, the derivation of the flow rate, that will ultimately be used to provide orifice or effective valve cross-sectional area, is based upon velocities in the throat that need to be

measured. It requires input velocities at the throat that are not practically measurable in this application. Therefore the model is not used, but does support the use of the Bernoulli equation for low quality two-phase flow through a flow restriction by the frozen flow statement.

A model from Uchida and Nariai (19) entails flashing saturated water through short pipes and orifices. The orifice produces similar flow rates for saturated water at low quality as it does for the sub-cooled water. The authors state the pressure remains constant through the pipe or orifice that is represented as a very short pipe. The pressure in the fluid does not reach ambient pressure until a short distance after the pipe exit in their experiment. This statement is important to determining the flow regardless of the scale of the authors experiment. The pressure will not be reduced to the down stream pressure condition until after the orifice exit. This leads to frozen flow across the restriction. Moreover, the author's employed a high-speed camera in the experiment for two-phase flows and no difference was noted in the velocities of the two phases upon exit of the tube. The fluid was ejected as a homogeneous froth. This further supports the frozen fluid conclusion.

2.3.2. Final Vaporization Model. The models presented above support the use of the Bernoulli equation in predicting the mass flow through the vaporizing orifice. The papers treat the pressure in the throat as the same pressure upstream of the flashing device. This means that the quality of the fluid will not change across the contraction and thus lead to a frozen flow assumption. These models therefore validate the assumption of frozen flow across the throat of the flashing device. Therefore, the final approach chosen to model the vaporizing flow uses the Bernoulli equation to approximate the flashing flow mass flow rate. The results obtained using this approach are discussed in the results section.

3. EXPERIMENTAL SETUP

3.1. APPARATUS

The research is conducted on a 4-stroke air-cooled 500 cc unbalanced V-twin engine. The engine is unbalanced because the two cylinders of the engine are not fired completely out of phase with each other. A balanced two-cylinder engine would have one cylinder fire and provide power through an evenly spaced, with reference to crank angle degrees, power stroke for every revolution of the engine crank. For the standard 4-stroke internal combustion engine, there are 2 crank revolutions for every 4-stroke piston cycle. The two-cylinder arrangement allows for one power stroke initiation every 360-degree rotation of the crank after the other cylinder power stroke initiation. Figure 3.1 shows the cylinder events for cylinders 1 and 2 versus crank position for the unbalanced engine of this research. Figure 3.1 shows that the cylinders are out of phase. A balanced 2 cylinder engine would have cylinder one and two volumes equal to each other though one is in compression to power while the other is in exhaust to intake.

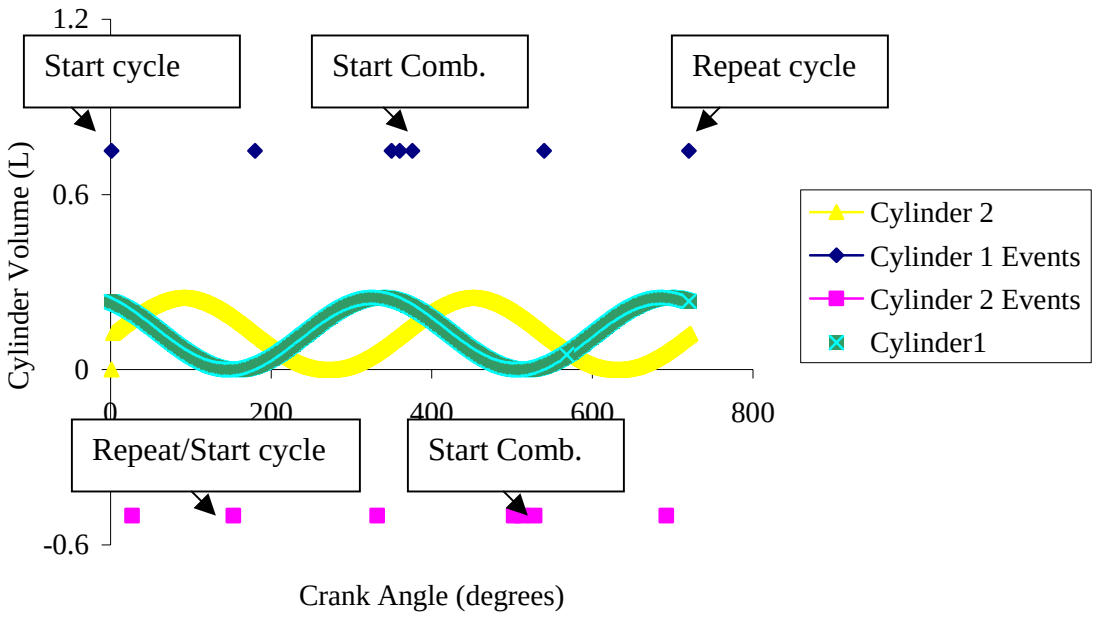

Figure 3.1 Figure that shows the cylinder volume for cylinder 1 relative to cylinder 2.

Figure 3.1 shows cylinder 1 events marked above the x-axis in blue and cylinder 2 events below the x-axis in pink. The events have no barring relative to the y-axis. They are simply moved away from the cylinder volume trace for visual clarity. There function is to simply highlight points relative to the x-axis in support of the following discussion. Each single point shows important cylinder events. The point at x = 0 shows top dead center (TDC) on cylinder one. The initial configuration begins with the piston moving down for the intake stroke. The next point traveling along the x-axis away from the origin is for cylinder 2. This point denotes the power stroke change to the exhaust stroke. It is phased 90 degrees behind where a balanced engine would place this event relative to the cylinder 1 event at the origin. The next point is the change over from intake to compression for cylinder 1. Following that point cylinder 2 begins the intake stroke at 270 degrees after cylinder 1. This is the phase difference between the two cylinders. The engine is unbalanced because the phase difference is not 360 degrees or one complete crankshaft revolution. As a result, cylinder 2 will always have notable flow differences upon air and fuel mixture induction than cylinder 1. This is especially notable when considering the power pulses to the crankshaft. The three-point cluster for each valve denotes major combustion events. The preceding point is spark plug spark and the trailing point is the peak cylinder pressure point. The middle point denotes the stroke change from compression to power. These three point clusters are representative of the power pulses and a balanced engine would have pulses equally spaced. A balanced two-cylinder engine would have a pulse every crank revolution or every half cycle or every 360 degrees.

The original fuel delivery system is a carbureted induction of gasoline. This introduction point creates issues in fuel distribution that is evident in cylinder exhaust temperatures. Because the flow of air into the engine is dependent upon the vacuum created by the cylinders during the intake stroke, the flow is unsteady. More importantly, the variable flow is not consistent between the cylinders. Cylinder one leads cylinder two and therefore must initiate flow in the intake manifold. However, cylinder one also experiences a higher manifold pressure because the full crank revolution has allowed time to equalize the manifold vacuum created by the two pistons. Since cylinder two fires after cylinder one, the pressure in the intake manifold is reduced from the vacuum

created by the filling of cylinder one when the cylinder two intake valve opens. Cylinder two experiences a lower manifold pressure than cylinder one, but also has a ram effect created by the flow of air in the intake manifold created by cylinder one. As a result, the charge from cylinder two has a different density and fuel energy content than cylinder one. This is evident in the exhaust temperature distribution of the two cylinders that is presented in the results section. Exhaust temperature from the cylinder is a good indicator of the energy released in the cylinder.

Two fuel introduction sites at each intake valve can alleviate fuel distribution issues. A more stable fuel distribution platform could have simplified controls testing and produced a more robust engine operation from which a liquid propane system could be applied and subsequently tested. That fuel system could then have also used two injectors and heat exchangers at the intake valves. Unfortunately, the dual fuel introduction system would have greatly increased the relative cost for the system via a second injector and heat exchanger. The scope of this research is the applicability of a fuel system for a 500 cc engine. The fuel system is a replacement for an effective and inexpensive carbureted system. In light of the cost concern, single point injection was a design requirement from the beginning and presented serious fluid dynamic issues that required extensive tuning of the injection timing. The tuning to find the most advantageous injection timing and location is discussed later in the Experimental Procedure section.

Another issue that affects the timing issue is the fact that the simplicity of the original engine configuration had no on-board control computer. Fuel injection timing requires an indication from the engine to determine start of injection. The most cost effective location to gain a signal for injection is the crankshaft flywheel. A simple hall effect sensor can be used to sense the passing of an indicator that is rigidly affixed to the flywheel and thus output a reference signal for every crank revolution. This sensor can be oriented, at discretion of the designer, anywhere that is geometrically advantageous with respect to the engine. Then a delay clock can be used to sense the signal, count the requisite time, and then open the injector. The issue that affects timing for this arrangement is that the injector must fire every crank revolution and the cylinders do not fire every crank revolution due to the unbalanced arrangement of the engine. Timing

would be simpler if the engine was balanced and the injector could fire a few crank angle degrees before an intake valve opening that occurs at the same crank degree every revolution and simply alternates between cylinders. The issues of injection timing further increases the fuel distribution issue due to the fact that an injection cannot be designated to a particular cylinder. This arrangement effectively forces sharing of the metered fuel between the two cylinders in which the distribution is ultimately decided by the unsteady flow dynamics as described earlier. This is the elected approach by submission to the primary design criteria of cost effective operation.

The fuel system that is proposed for this liquid propane injection system is designed with the constraints of cost and simplicity. The system begins with a standard, commercially available fuel tank. The tank contains the fuel in the volumetrically economical state of a saturated liquid. The pressure inside the tank is roughly ten times atmospheric depending on the ambient temperature environment. The tank therefore drives the fuel through the fuel system with the saturation pressure at ambient temperature as the fuel system pressure. This eliminates some of the specialized fuel tank and pump combinations described in references like that of Lutz et al (8). A fuel pump is an expensive addition to a fuel system, especially if the fuel pump may be required to encounter a two-phase fluid. Also, there is no need for a pressure regulator in the fuel system. A regulator operates off of differential pressure and the upstream side of the regulator must be higher than the downstream operational pressure. Without a pump, the upstream pressure is a maximum of saturation pressure from the tank and any pressure reduction in the system would boil the fuel. The elimination of these two components complicate fuel flow and pressure control because fuel pressure is thus dependent upon the tank saturation conditions. Therefore, if the environment around the fuel tank changes temperature, the pressure in the fuel system changes pressure as the pressure in the fuel tank adjusts to maintain saturation. This means that injector pulse widths and flashing flow rates through fuel flashing devices change with temperature of the tank. However, this allows the fuel system to be inexpensive as an OEM installed fuel system and a plausible retrofit kit for current engine systems since the most expensive piece of equipment is the injector with heat exchanger and the fuel tank can be any standard propane storage tank.

The rest of the liquid injection system including sub-cooling with a temperature reduction system is shown in Figure 3.2.

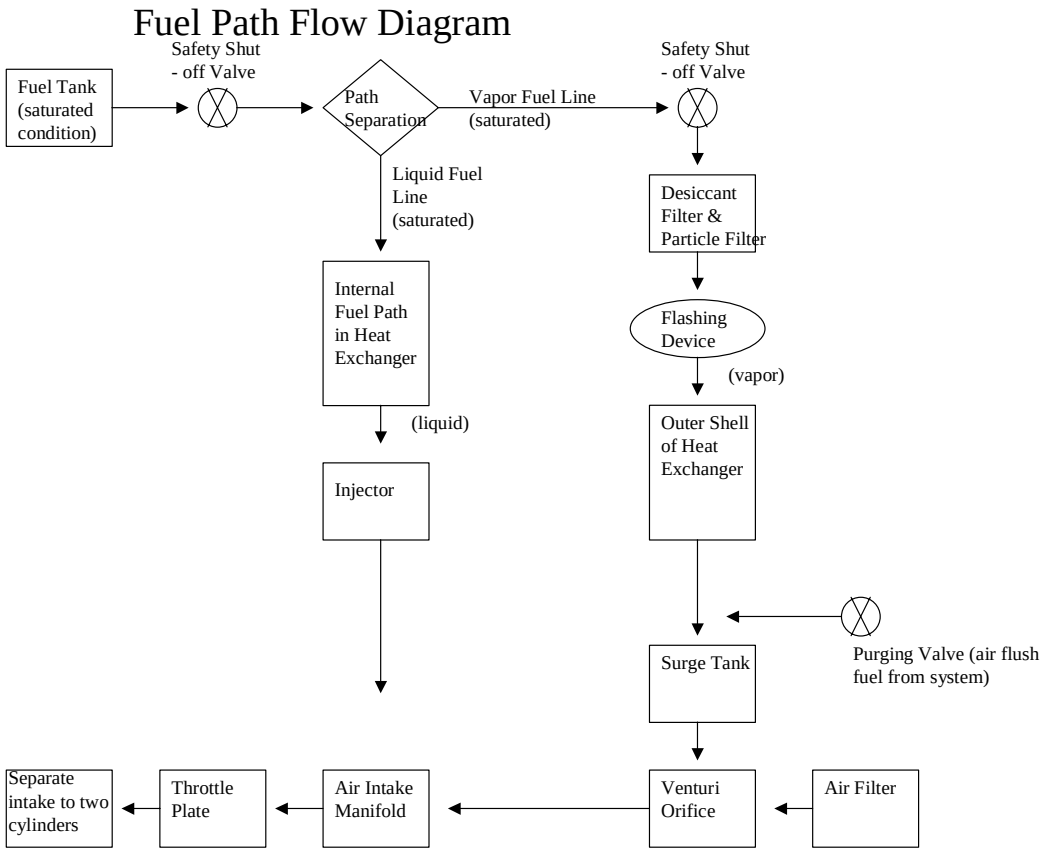

Figure 3.2 Figure depicting the fuel pathways in the proposed fuel system.

The fuel is supplied by the commercially available and easily interchangeable fuel tank. The single fuel line to the tank is the supply line for the fuel system. The fuel starts from the tank and transfers into a safety shut off valve. This valve is energized to open and allow fuel flow. It ensures that fuel can be shut off in emergencies as the ground state of the valve is closed. After the safety valve the fuel supply line is then split into two supply lines. The first line is the liquid line. It immediately tracks into the center tube of a counter flow heat exchanger. The details of the heat exchanger are presented later in this section. At the end of the heat exchanger, the liquid fuel immediately enters

the fuel injector. The injector is mounted to the intake manifold of the test engine. Through testing, the most advantageous location for fuel injection was determined to be in front of the throttle plate furnished in the original carburetor assembly. A fixture developed during this project is upstream of this throttle plate and the purpose is to provide a location to inject fuel. The details of this fixture are discussed later in this section. The fixture is shown in Figure 3.3.

The second fuel supply line, the vapor line, continues from the separation point to a second fuel shut-off valve that is identical to the first safety valve that was discussed previously. From the second safety valve, the vapor line passes through a desiccant filter that removes water from the fuel. As commercial propane fuel is a blend and may contain a fraction of water, there is a possibility of the water from the fuel freezing in any flashing device and thus closing the restriction or at least restricting the cross-section available for flow. This is a requirement for this fuel line because the constant vaporizing of fuel will produce sub-freezing temperatures for water at the flashing device. Ice can build up over time during operation. After the desiccant filter a particulate filter of 2-micron size is in place. This is to ensure that particles cannot coagulate around the vaporizing device throat and eventually clog the flow.

The fuel is then delivered to the flashing device after the filter. The device is discussed later in this section. The flashing device vaporizes the fuel into the outer shell of the counter flow heat exchanger. On the vapor outlet side of the heat exchanger, the vaporized fuel continues to a tee junction. One branch continues to a surge tank. The surge tank helps separate the engine intake pressure fluctuations that are created by the intake strokes of the pistons from the vaporizing operation of the flashing device. The other branch of the tee connects to a valve that can be opened to draw in air through the surge tank and purge the tank of any remaining fuel at the end of testing. During testing this branch is dormant. After the surge tank, the vapor fuel is introduced to the intake airflow via the throat of a venturi orifice that is placed coaxially inline with the inlet airflow. This orifice is upstream of the injection site, and the location is presented later in this section. The venturi orifice allows the vaporized fuel to be consumed as part of the engine fuel requirements and is shown in Figure 3.3. The orifice accelerates the intake

airflow and reduces the pressure on the downstream side of the throat. The reduced pressure and faster fluid velocity aids in inducting the vapor fuel into the intake flow.

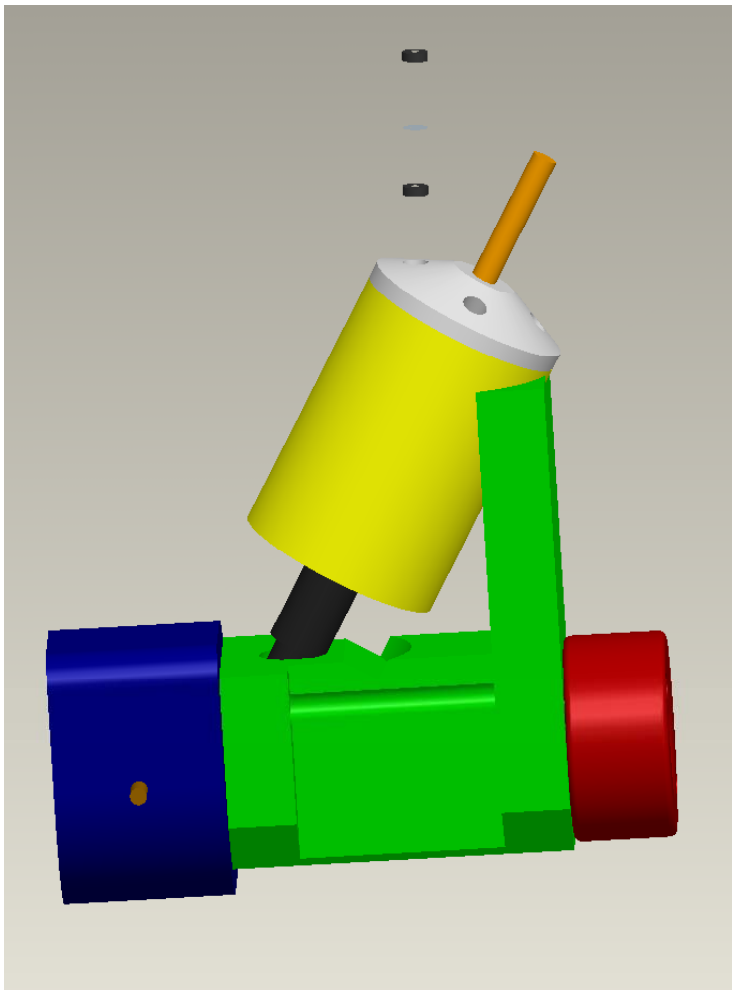

Figure 3.3 This is the solid model of the injector mount in green and the venturi orifice in red.

Through the implementation of this fuel system research some alterations to the air system of the engine have been made. The air intake system remains in the original configuration from the intake valves to the throttle plate in the original carburetor assembly. The air cleaner was originally affixed to the upstream side of the carburetor.

However, the carburetor is where some additions to the air system are made. Immediately upstream of the carburetor is the location of injector mount that provides a place for the injector to introduce fuel into the manifold. The discussion about why this location is preferred is given with the heat exchanger presentation and the experimental procedures. On this fixture, the injector is positioned to inject the fuel along the intake air path to ensure the fuel travels to the cylinders. This is an important consideration considering the injection timing arrangement that requires the injector to fire during a crank revolution that does not have an intake valve-opening event to create flow towards the engine in the air system.

Upstream of the injector mount is the venturi orifice. It is placed before the injector mount in the flow stream because this allows a base amount of fuel the maximum time to mix with the intake air. The fuel mixing issue and the ramifications of the fuel mix on the fuel distribution between the cylinders is discussed in the Experimental Procedure section. Also, the vaporized fuel is considered warm and can benefit the charge cooling efforts to be mixed with the intake air as the liquid injection flashes as opposed to warming the intake charge by introducing the vapor flow after liquid injection has vaporized. The air cleaner is then attached to the upstream side of the venture orifice.

The major fuel system component is the counter-flow heat exchanger. As stated previously the liquid line enters the heat exchanger and travels through the center. The liquid fuel line enters from the top of the heat exchanger to the bottom at the injector. The central liquid fuel line is brass and has brass fins brazed onto the surface for enhanced heat transfer. The fins also aid in directing the flow of the flashing flow from the flashing device. The liquid fuel line flows into the fitting that houses the injector. The pressure that is experienced by this fuel line in the heat exchanger is the tank saturation pressure for the given ambient tank temperature. This is important because the drop in fuel temperature in the heat exchanger does not induce a drop in pressure to maintain saturation because the pressure is externally driven from the tank. Therefore, the thermodynamic process dictates that the saturated liquid fuel becomes a sub-cooled liquid.

Fuel enters the exchanger shell as it vaporizes through the flashing device, which is discussed later. The shell of the heat exchanger is aluminum and experiences slightly higher than atmospheric pressure as a result of the flow restriction vaporization originating from saturation pressure of the fuel. The pressure drop from saturation is enabled by the connection to the slightly less than ambient pressure offered by the venture orifice. The flow of the vaporizing flow out of the flashing device travels down from the top of the heat exchanger to the bottom and back up on the other side of the cooling fins. Then the vaporized fuel exits the heat exchanger canister at the top of the canister on the opposing side of the fins from the flashing device. The fuel routing is depicted in Figure 3.2. During testing, this shell is insulated from the engine heat and surrounding environment. This helps isolate the cooling control volume in the heat exchanger where the only source of heat for the vaporizing flow is the liquid line.

The location of the heat exchanger is critical. The most important parameter is the proximity of the heat exchanger to the injector. Ideally the injector is inside the heat exchanger to ensure liquid phase propane at the injector. In less than ideal cases, the injector should be located as close to the heat exchanger as possible. For this research, the injector is partially fit into the heat exchanger. Therefore, the heat exchanger is now location dependent upon the ideal injection location for the cylinder-to-cylinder fuel distribution issues and charge cooling maximization. The injector/heat exchanger should be located as close to the cylinders as possible to allow the charge cooling benefits to be maximized by limiting the time available for heat transfer to warm the charge. However, the fuel must mix with the air before the manifold separates for the two cylinders. If mixing is insufficient, the fuel distribution issue is aggravated further. Mixing requires time, which translates to an injection location further away from the cylinders. Due to the converse nature of these aspects, the location of injection had to be optimized iteratively with injection timing as fuel travel time to the cylinder changes with a location change. For engine operation stability, the injector and heat exchanger are located before the throttle plate of the original air system arrangement. Discussion of the testing for these issues is discussed in the Experimental Procedures section. The location is shown in Figure 3.3. Finally, the heat exchanger is insulated during testing.

The essential fixture to the heat exchanger is the flow restriction that reduces the pressure and creates the condition suitable for fuel vaporization. Examples of the restriction devices are shown in Figure 3.3 as the thin grey disk between two black orifice mounting disks. The flashing is the result of a simple reduction in the cross-sectional area of the flow from pipe to orifice and then exhausting to a large volume of the heat exchanger shell that vents to the manifold vacuum.

Initially, a metering valve was used to flash the propane. The metering valve shown in Figure 2.4, which is a Swagelock s-series valve was investigated to gain insight into tank conditions and allow variation of the effective cross-sectional area. The valve allows variable flow control without the need to stop the engine to change the flashing device. This feature is important for quickly validating the heat exchanger concept and finding flow rates between the orifice sizes that were tested. The metering valve is simple to install and reduces the time for tuning of the injector pulse width relative to the vaporizing flow and desired equivalence ratio for the engine. The drawback to the valve arrangement is further complication of flow measurement due to the relative complex geometry of the internal valve flow compared to an orifice plate. Additionally, the valve is not efficient as the valve body has more surface area and allows more heat to transfer to the flashing media from sources other than the control volume of the heat exchanger. It is therefore not as efficient as an orifice placed in the wall of the heat exchanger.

The simplest way to create a flow restriction is with an orifice. The orifice flow is the least complex because the geometry is a simple pipe diameter change. The diameters of the orifices that are used in this work are 35, 50, 75,100, 150, and 200 microns. Additionally, the flow area of the orifice is repeatable. The orifice is also a very efficient method of flashing because it is small enough to mount in the control volume of the heat exchanger and therefore does not transfer heat to the flashing fuel that does not originate with in the control volume. This allows more of the engine fuel requirement to be introduced from the injector and promote charge cooling. However, the orifice does not offer the ease of installation and dexterity of the continually variable metering valve.

The orifice is difficult to install and align and is a set flow restriction for varying tank conditions. An image of the alignment is shown in Figure 2.3. It is not tunable. The orifice is 0.026 mm thick metal disc with a circular hole of diameter on the order of

50 microns. It is mounted in between two plastic discs 9 mm in diameter and 3 mm internal diameter. Special concern must be given to coaxially align the orifice with the mounting discs. This alignment is critical because if the alignment is not achieved, the tiny orifice will be covered and no vaporizing flow will occur. Also the lid of the heat exchanger has a 3 mm hole drilled into the bottom of the threaded vaporized line fitting so the orifice mount can be seated in the lid. Again, Figure 3.4 (Edmund Optic Documentation:*http://www.edmundoptics.com/onlinecatalog/displayproduct.cfm?productID=1794&search=1*) shows the orifice restrictions and Figure 2.4. is an illustration of the metering valve.

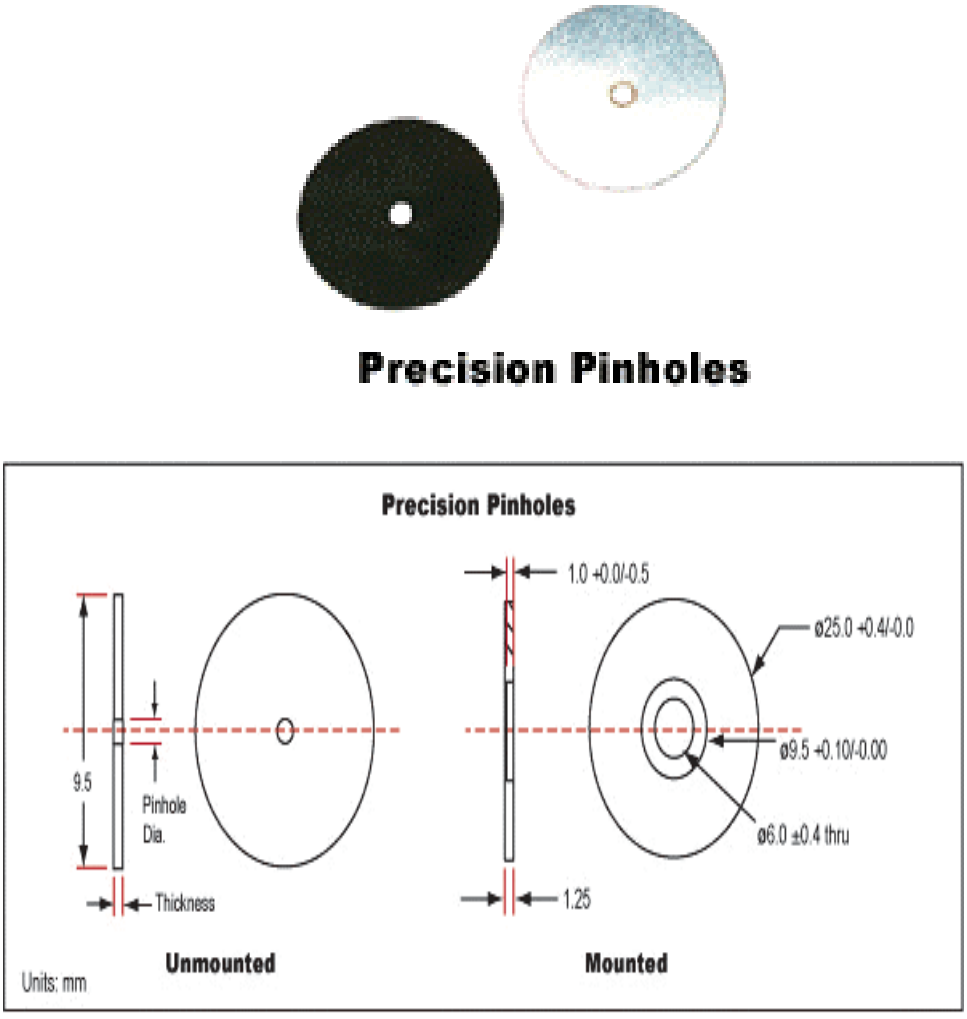

Figure 3.4 Picture of flow restriction devices (orifice).

Alignment of the hole in the lid with the disc mounts and orifice is also critical as demonstrated in Figure 2.3 and the alignment view of Figure 2.3 is magnified for Figure 3.5. The size of the orifice is exaggerated in both figures for visualization. This is the complication of installation not realized with a metering valve.

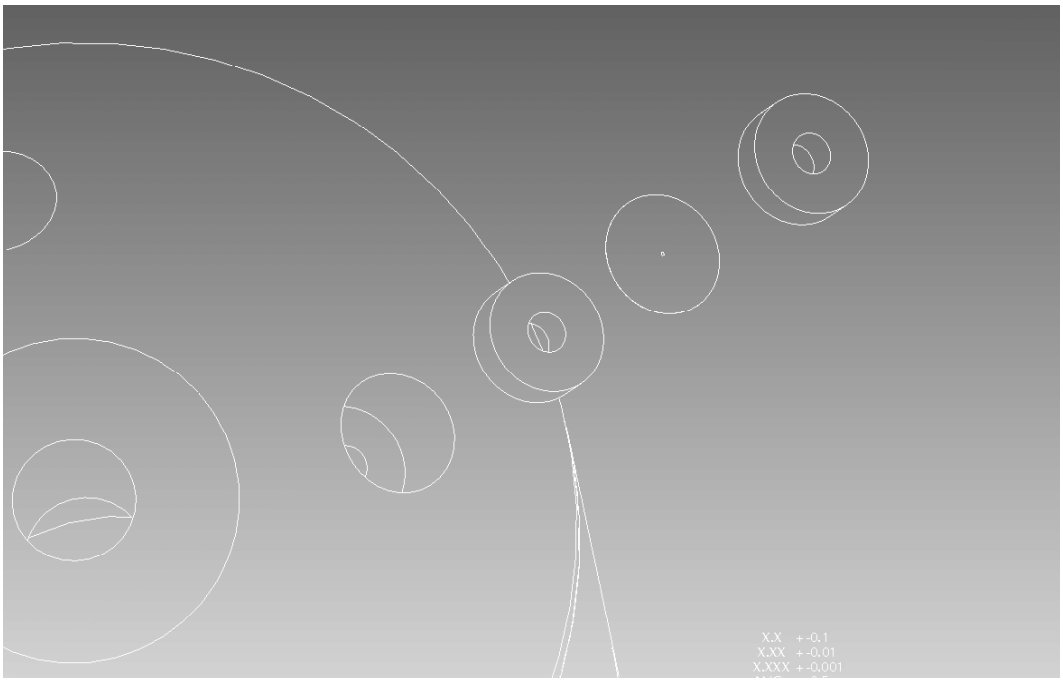

Figure 3.5 Schematic of hole alignment.

The orifice size for a given test condition changes with varying tank conditions. This creates problems with experimental repeatability. The fuel system temperature should be controlled to provide controlled pressure tests for a given orifice size. Controlling the tank temperature is not sufficient as the fuel could boil in the liquid lines to a vapor from a lower tank temperature than the fuel system environment. This is discussed in the Experimental Procedure section. The metering valve offers an ease of use benefit that allows minor adjustments in the valve setting to reproduce a vaporizing flow rate or a cooling rate for the heat exchanger.

As mentioned previously, the orifices that were tested are on the order of 50 microns in diameter and the discs with the orifice hole were 0.026 millimeters thick. Thus the orifice hole is 0.026 millimeters long. Strictly speaking the length versus diameter (L/D) for the orifices qualify them as short tube orifices, but a thinner orifice disc will not sustain the saturation pressure of propane at room temperature. A table of L/D is presented for the orifices for the respective diameters and lengths. However, the length is not considered an issue in the flow model. This information is displayed in Table 3.1.

Table 3.1 Table of length to diameter ratio of the orifices.

Orifice Diameter (micron)	Disc Thickness (mm)	Disc Thickness (micron)	L/D
30	0.0254	25.4	0.846667
35	0.0254	25.4	0.725714
50	0.0254	25.4	0.508
75	0.0254	25.4	0.338667
100	0.0254	25.4	0.254
150	0.0254	25.4	0.169333
200	0.0254	25.4	0.127

3.2. INSTRUMENTATION

The instrumentation employed in testing the fuel system is demonstrated in Figure 3.6. The experiment used an electronically controlled fuel injection system that was developed for a carbureted 680 cc v-twin engine (20). From that work, this research then uses a MAP (manifold air pressure) sensor, Motorolla MPX4115AP, to measure intake manifold pressure and a thermistor to measure intake temperature for the computer. However, this signal was not used as a measurement channel. The Motorolla MAP sensor is the same sensor that is used in the downstream section of the vaporization model testing. It has an uncertainty of 1.5%. These two manifold signals are used as inputs in a two-dimensional fuel map that output a pulse width. This fuel map handles the change in fuel demand from a change in load on the engine that is altered by throttling the engine that subsequently changes the manifold pressure. The temperature is necessary to scale

the pulse width for a given manifold pressure to a reference density so the mass of the intake air is known and an appropriate fuel mass can be delivered to produce the desired equivalence ratio for that mass of air. This is a discrete calculation and the map assumes that the air in the manifold for one crank revolution is the total amount of air. The map is developed for resolution to one crank revolution and not an engine cycle because of the simple hall-effect trigger mentioned in the Apparatus section.

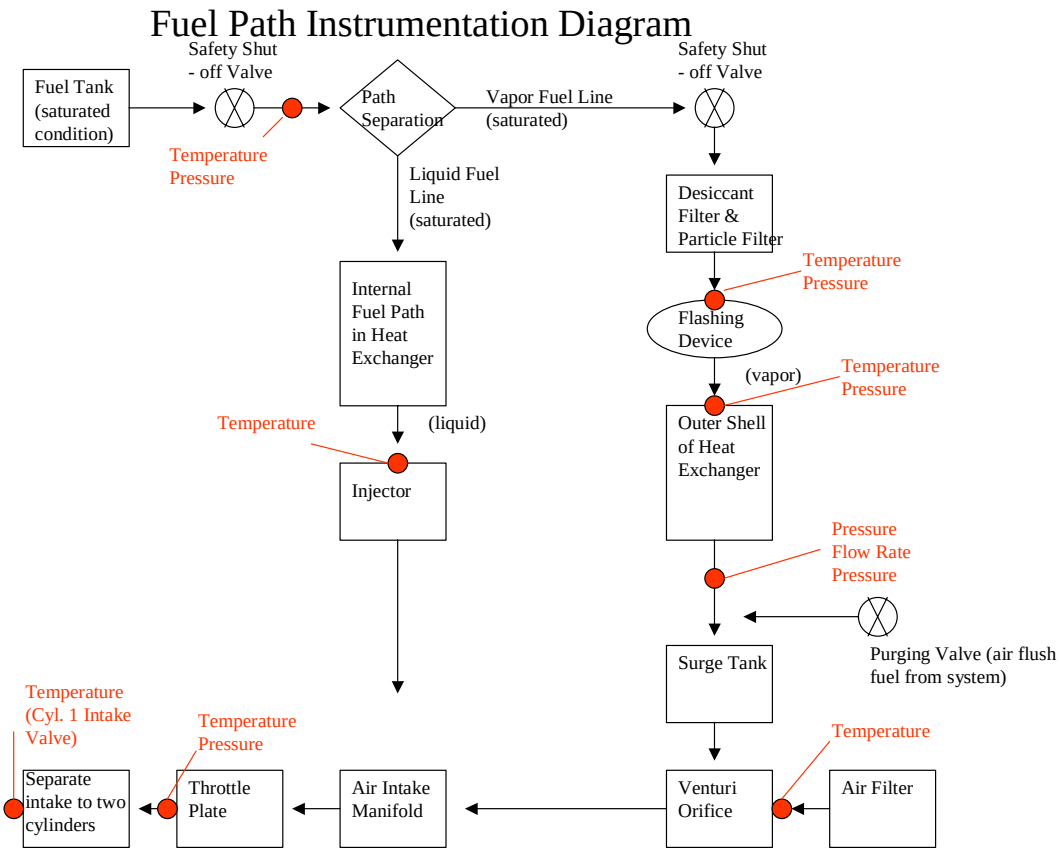

Figure 3.6 Figure showing the instrumentation points in the fuel system.

The repetition of injections is triggered by this hall effect trigger. The computer that processes this data is a microcontroller pic chip programmed with the iteratively tuned fuel map in this research. This computer has the load control in the fuel map and

the speed control in the hall signal to accurately meter fuel for the engine and allow testing of the fuel system to commence with autonomous engine control.

This system is tuned for the 500 v-twin engine in this research using DAVID, a Delphi Automotive Virtual Injector Driver. This injector driver allows the researcher to experimentally develop a fuel map to suit the purposes of the research engine. The driver aided in the development of fuel maps for Indolene, a fuel that is representative of commercially available pump gas. This map is a baseline reference for the fuel map that is developed with the LPG fuel. The details are discussed in the Experimental Procedure section. The injector that was controlled by this driver and the computer injection system that is developed for the liquid LPG injection system is a Delphi Multitec 3 injector.

The tuning of the injector map also required sensors that monitored the engine processes. The pressure sensor that is implemented for this process is the MAP sensor that provided the manifold pressure signal to the computer. The temperature readings are taken by type K–type thermocouples from Omega and have an error of 0.75 % above 0 degrees Celsius and 1.5 % below 0 degrees Celsius. They are displayed on an omega thermocouple reader. These thermocouples are used to track intake temperatures, oil temperature, exhaust temperatures, and cylinder wall temperatures. The exhaust determination of the air-fuel ratio control utilizes a UEGO sensor. This aids in determining the accuracy of the injection system in maintaining the desired equivalence ratio. The procedure of tuning the fuel map and results are discussed later.

In Figure 3.6, the fuel system test instrumentation is shown. Tank pressure is measured up-stream of the first safety shut-off valve by an Omega PX 302 pressure transducer connected to a data acquisition (DAQ) system. The high pressure measurement has an error of 0.25% BFSL for the pressure transducer from Omega. Then, downstream of the first shut-off valve, the tank temperature is acquired by the DAQ system using a Type-T thermocouple from Omega. These two measurements allow the state of the fuel system and tank to be tracked as an initial state before the heat exchanger and flashing device. Then the fuel line splits into the vapor and liquid lines.

The only instrumentation in the liquid line is a temperature measurement of the fuel at the inlet to the fuel injector. The pressure here can be assumed to be the same as the upstream tank pressure measurement. The temperature is measured to verify that the

design criteria of –5 degrees Celsius temperature reduction from the tank temperature exists at the injector and therefore ensure that the fuel is a sub-cooled liquid. The measurement error for this device is the same as the temperature measurement from the tank line temperature measurement as the Omega type T thermocouple was used and recorded in the DAQ system.

The vaporization line is given more attention to validate the flashing model. Temperature and pressure measurements are acquired immediately before and after the flow restriction. The flow is dependant upon the upstream and downstream quality condition of the vaporizing fuel. Therefore, the temperature and pressure measurements are required upstream and downstream of the flashing device to determine the changing thermodynamic state of the fuel through the flashing device. Upstream pressure and temperature measurements are obtained from fittings in the fuel flow line. The pressure and temperature of the downstream measurement are actually taken from the heat exchanger canister. They are close to the vaporizing flow entry into the canister. After the heat exchanger there is a pressure sensor followed by a flow meter and another pressure sensor after the flow meter. This arrangement of acquired pressure data after the heat exchanger is implemented to determine the cause of the pressure fluctuations downstream of the flow restriction. The determination of whether the pressure fluctuations occur from the flashing phenomenon or the fluid dynamics created by the unbalanced V-twin engine pulses is required to establish the stability of the fuel system.

Larger pressure pulses from the pressure transducer from the engine side of the array would imply that the intake pulses from the engine is the culprit while larger amplitudes on the flashing device side indicates that the flashing process is fluctuating. The same pressure transducer that is in the tank line acquires the pressure measurement taken upstream of the flashing device. The pressure transducer that provides these measurements is an Omega PX302 that has a measurement error of +/- 1 mV on a 100 mV output scale. All three pressure measurements made downstream of the flashing device are made with Motorolla MAP sensors and are recorded by the DAQ system. The temperature measurements upstream and downstream of the flashing device have the same details on operational characteristics as the thermocouple used in the tank line. The flow meter that is used is a FL 111 rotameter from Omega. It has a measurement error of

+/- 2 %. Additionally, the flow from the rotatmeter must be manually recorded, as there is no connection for a DAQ system. This aspect is very important in the discussion of pressure fluctuations because the rotatmeter bead bounces and is therefore not easily read in real-time. The discussion of the vapor flow rate variability demonstrated in testing is presented in the Results section. A more sophisticated flow rate measurement technique was infeasible from a cost standpoint.

The DAQ system is a standard desktop PC that included a PCI DAQ card 6024E from National Instruments with measurement and Recording Specs 16.504 mV error for the 10V pressure transducer signal. The low pressure signal measurement error for the PCI card is 5.263 mV on a 5 V scale. The pressure measurements are introduced directly into the card from the DAQ board supplied with the DAQ card. The temperature measurements had to be logged by a 4 channel USB DAQ system, cRIO-9211 coupled with a USB-9162 interface from National Instruments. The measurement specs of this system are 0.05% at 25 degrees Celsius. Both of the signals from the two acquisition systems are conditioned, displayed on the computer screen real-time, and written to files via Lab View code developed for this application.

4. FUEL SYSTEM CONFIGURATION

The development of the liquid injection LPG fuel system is complex. Many interrelated aspects of the fuel system must be tested iteratively like nested loops in computer code. The testing matrix is therefore, also complex and interdependent. These tests include fuel injection location in the intake manifold, injector pulse width and injection delay, as well as cooling flow provided by the vaporizing device. An example of the threefold complexity is that a certain flashing flow set point is tested for the entire fuel map at all injection locations. The process is time consuming and each test is discussed individually below. This issue is further exasperated by the fact that any change in the tank temperature will cause the fuel system pressure to change due to the saturated state of the fuel.

4.1. LOCATING AN INJECTION POINT FOR THE PROPANE SYSTEM

The first task in the development of the liquid injection system described in this work is to locate an injection point. This is necessary to allow the testing to begin without the carbureted induction of fuel. Utilizing the overall goal of cooling the charge in the cylinder, the first injection location is chosen as close to the two cylinders as one injector allows. The location is in the tee junction of the intake manifold. With this configuration a baseline test is run with Indolene. Indolene is a research fuel that represents standard pump gas from automotive fueling stations. Originally, the carbureted system of the development engine is designed to operate on pump gas. The Indolene baseline is developed to provide a reference for fuel system performance for a conventional fuel versus the developing system of liquid LPG. The liquid LPG system is tested at this location as well. Indolene and LPG injection realize a cylinder exhaust temperature disparity, which indicates a biasing of the fuel distribution to each cylinder. The solution from the injection location standpoint is to move the fuel injection location further upstream to allow more fuel mixing at the expense of charge cooling. Originally the carbureted fuel is mixed at the throttle plate and the flow disturbance created by the throttle promotes mixing. The alternative injection location is therefore in front of the

throttle plate to promote mixing and minimize the cylinder exhaust temperature distribution disparity. Figure 4.1 shows the change in position of the injection location.

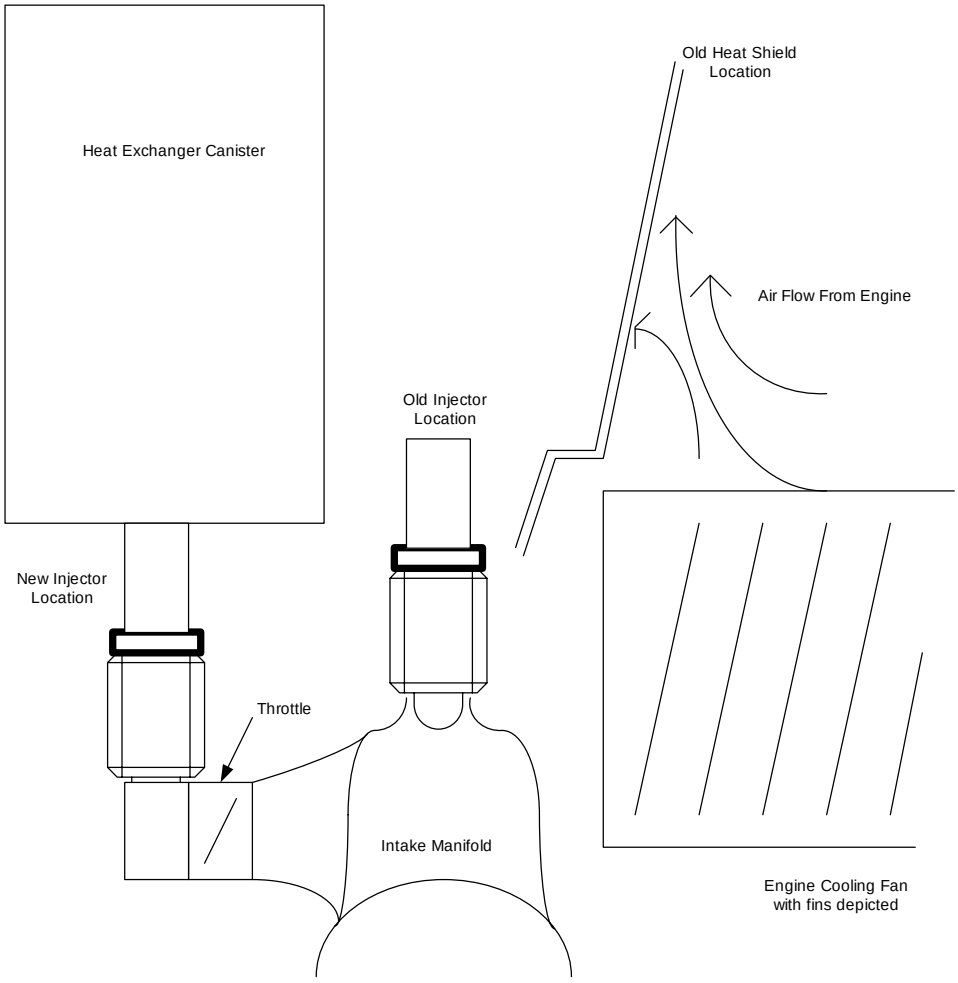

Figure 4.1 Figure showing changes to the injection location to increase robustness of the fuel system design.

The additional mixing should bring the temperature disparity closer to the results of using completely vaporized fuel flow that is discussed later. This vaporized fuel most closely represents the original carbureted system. In order to relocate the injector and heat exchanger, an injector mount is designed and shown in Figure 3.2. This mount holds the injector and canister as described in the Experimental Setup. The location of the

injector mount is upstream of the stock throttle plate and down stream of the vapor introduction venture orifice. This allows more time for mixing the injected fuel with the air and provides a flow disturbance to aid in the mixing process. The throttle plate from the stock carburetor serves in this capacity. The results are discussed later, but the new location resulted in a closer exhaust temperature distribution. Therefore this injection location is determined to be the injection site for the fuel system because cylinder-to-cylinder temperature distribution is important to stable engine operation. Equal fuel distribution allows the torque pulse on the crankshaft to equalize shaft torque.

An additional benefit of moving the injector location is that the heat exchanger can be moved away from the engine heat and insulated from the bottom side. As discussed previously, the heat exchanger is placed immediately above the injector. At the intake plenum separation point, the flywheel engine fan does not allow significant insulation of the injector or heat exchanger as the heat exchanger is in close proximity with the engine-cooling fan. The engine-cooling fan is designed to draw air into the fan cowling along the air-cooling fins. The fan then exhausts the heated air upwards off of the engine. The location of the injector at the intake plenum places the heat exchanger canister in the warm airflow.

4.2. INJECTION TIMING

The baseline fuel map test is run with the aid of the DAVID injector driver. This controller allowed the real time alteration of injection timing during the test. The goal of the test is to develop a fuel pulse width map and injection timing map for Indolene injection. The map includes injection delay from the hall effect signal at a set engine speed and a pulse width that delivers the amount of fuel required to maintain the desired equivalence ratio for a given manifold pressure. The manifold pressure is systematically altered from low manifold pressure or load to high load in order to vary the load at a constant engine speed. This provides a fuel map of required pulse widths and injection delays for every load at this engine speed. This fuel map is limited to the idle speed case of 1550 RPM because the selected injector could not deliver enough fuel at the shorter cycle times of higher engine speeds and maintain the desired equivalence ratio. The

injector is not replaced because the propane fuel does not have this flow rate problem due to the higher injection pressure supplied by the saturated fuel in the fuel tank. The smaller injector offers more resolution to the liquid LPG injection system and provides the complete speed and load range flow rates required for the development of the fuel system on the 500 cc engine.

During the map development of the baseline fuel map with indolene, the two parameters of pulse-width and injection delay are determined experimentally. They are also iteratively determined for each load at the idle engine speed. The iteration occurs because a change in injection timing alters the distribution of the fuel between the cylinders and therefore the equivalence ratio for the two cylinders is altered. The distribution disparity is evident in the exhaust temperatures from each of the cylinders. Equal fuel distribution generally produces equal exhaust temperatures and as a result exhaust temperatures are an indicator of fuel distribution. When the fuel distribution is not optimized, the equivalence ratio that is tracked by the UEGO sensor is subject to lean and rich pulses that make selection of the appropriate fuel pulse width difficult. However, the timing is dependent upon the pulse width because the length of time the injector is open can affect fuel distribution. Preliminary estimates of pulse widths are produced from calculating the air flow into the engine at the engine speed and current manifold temperature for each manifold pressure setting and volumetric efficiency numbers that come from a previous flow bench test of the engine with a laminar flow element in previous work. The volumetric fuel equation is shown here as Equation 6.

$$\eta_V = \frac{m_A}{\rho_{air,i} V_d} \tag{6}$$

The fuel demand can then be calculated using the mass of air for the intake manifold pressure at the desired speed and the tabulated volumetric efficiency values along with the desired air fuel ratio to produce fuel mass demand. This is shown in Equation 7.

$$\dot{m}_{fuel} = \left(\frac{N}{2}\right) V_d \eta_V \left(\frac{\dot{m}_{fuel}}{\dot{m}_{air}}\right) \tag{7}$$

The fuel demand rate must still be broken into fuel demand shots per engine revolution due to the simple engine arrangement discussion earlier that described the need to inject fuel every crank revolution. Equation 8 shown below is the product of the fuel rate times the cycle time, which is the engine speed over 2 for cycles per unit time. Then cycles per unit time is inverted for cycle time. This product is multiplied by 2 cylinders for the fuel demand and then divided by 60 to convert cycle time in terms of minutes to seconds. This is done to align with the flow rate units in terms of seconds.

$$m_{fuel} = \dot{m}_{fuel} \left(\frac{2}{N}\right)\left(\frac{2}{60}\right) \tag{8}$$

The pulse width is calculated by using the flow rate of the injector and the fuel demand per revolution to convert to a pure time dependent pulse width for the injector as shown in Equation 9.

$$PW = m_{fuel} / \dot{m}_{inj} \tag{9}$$

These estimates provide a reasonable pulse width value given the flow rate of the injector. However, they are only guesses and must be tuned for the engine and fuel system. This tuning is required because of the approximations made in the aforementioned calculations such as volumetric efficiency and the rate shape of the opening injector is not perfectly digital. Never the less, a pulse width that is close to the pulse width required by the set point of the engine allows the injection timing to be

adjusted until the cylinder exhaust temperatures are equalized. The pulse width is trimmed and the timing readjusted. This process is repeated until the pulse width and timing are set with roughly equal exhaust temperatures and the desired equivalence ratio is met.

Unfortunately, the initial baseline test was unable to equalize exhaust temperatures at either injection location. However, a fuel map is developed with the desired equivalence at the closest exhaust temperatures that could be produced for this configuration. The results are provided later in section 5.1. Two possible causes for distribution are fuel pooling under the injection location site of fuel that did not vaporize out of the injector and inadequate mixing of the fuel and air. The mixing issue was addressed by testing a new injection location upstream of the throttle plate as previously discussed. Fuel pooling, seen in Figure 4.2, can cause uneven distribution of fuel because there is no timing control over when and how fast the fuel from the pool vaporizes. A solution to this issue could be to switch over to the LPG system, which injects more volatile fuel that vaporizes faster out of the injector.

Switching to the propane fuel system was the first alternative tried to investigate the distribution issue. This system was tried at both injection locations. The motivating factor for switching to the propane fuel system was maintaining proximity to the cylinders for charge cooling if the difference in fuel volatility allows the injector to be placed at the intake runner separation point. The test was performed with the new fuel system and for two additional test speeds; 2200 and 3600RPM. A metering valve was used for the vaporizing flow that allows the vaporized flow to be increased if additional cooling is required at the high speed case of 3600 RPM and high load. However, this adds another iteration dimension to the process of determining pulse widths and timing. This is discussed in detail later. For the preliminary experiment, the high speed wide open throttle (WOT), case was run first to ensure that required cooling is provided and the rest of the test was run with that vaporizing flow setting to minimize iterations. This flow was introduced into the intake manifold before the throttle plate. Therefore the pulse width calculation has to be reduced to account for the additional vapor fuel that can be found from the valve flow coefficient at the test conditions.

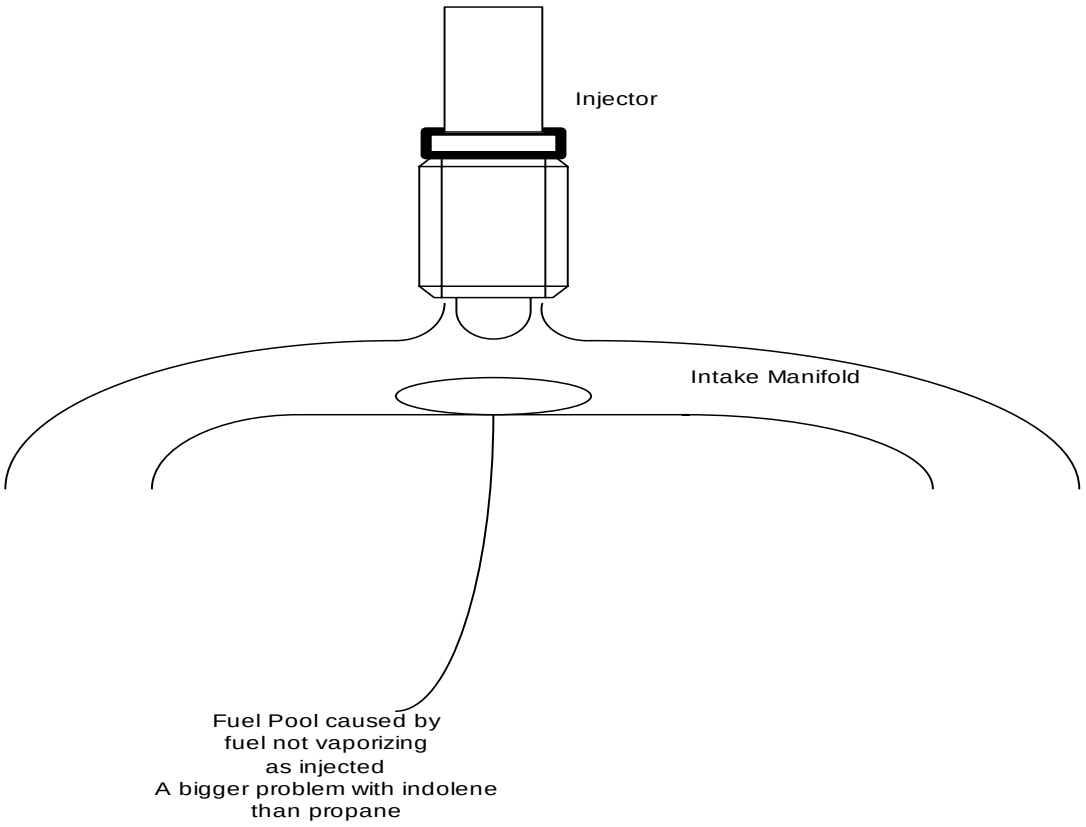

Figure 4.2 Fuel pool figure showing how the fuel may pool under the injector during injection before the fuel can vaporize.

Figure 4.3 (www.swagelock.com) shows the flow coefficient for the metering valve used in this research. Additionally, the fuel timing was affected because there now exists a fuel content in the incoming charge at the injector location. With these considerations, the iterative process discussed for the Indolene baseline was conducted with the prototype liquid injection propane fuel system.

The test of the propane system yielded the same cylinder temperature disparity that is evident for the Indolene baseline at both injection locations. The fuel map sweep for this test was completed for the desired equivalence ratio and the most equal exhaust temperatures that could be achieved. Either the fuel pooling was not the cause or the propane does not flash out of the injector fast enough to resolve the problem. During the

test, the idle condition of 1550 RPM and manifold pressure of 70 kPa was operated purely on vaporized flow from the vaporizing flow rate set for the WOT case.

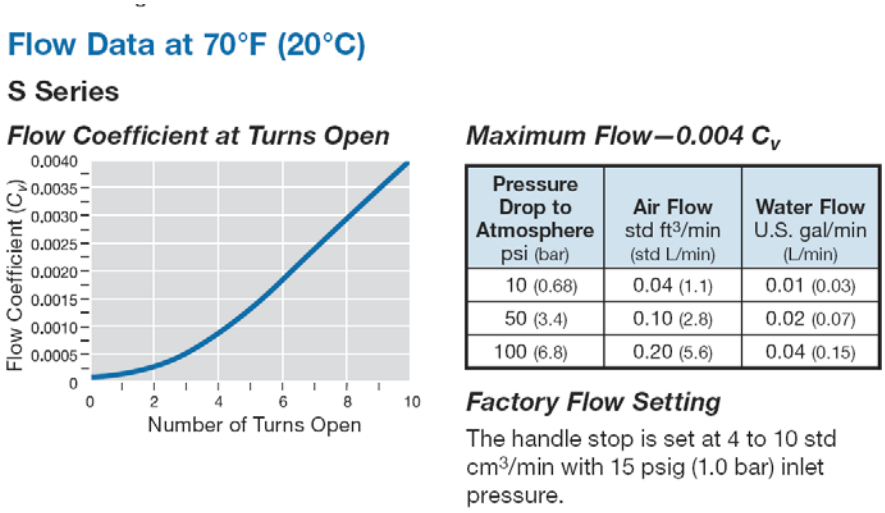

Figure 4.3 Figure showing the flow coefficient for the Swagelock valve used to meter the vaporizing flow.

This case had no fuel injection to cause fuel pooling and the introduction of the gaseous propane occurred before the throttle plate of the intake. Mixing was maximized at this arrangement. This means that both fuel system concerns of mixing and pooling were minimized at this point. The cylinder-to-cylinder exhaust temperature disparity that exists for this case is apparently a result of the stock engine intake arrangement.

4.3. PRESSURE EFFECTS FROM TEMPERATURE CHANGES OF THE SATURATED FUEL

All of the injector timing and pulsewidths are also dependent upon the temperature of the fuel tank. The fuel is in a saturated state and therefore a change in tank temperature changes tank pressure, which is the pressure for the fuel system in this study. Therefore, the fuel flow can be set by the previous tests. However, the effective cross sectional area of a flashing device mentioned for the LPG system is not determined

because the environment of the tank affects the absolute pressure of the liquid injection. The results are seen in the pressure drop across the flashing device, the injector pulse widths, and timing. Consequently a given orifice, metering valve setting, or injector pulse width will produce different flow rates as the temperature of the fuel system changes. The temperature change of the saturated fuel changes the pressure in the fuel system and by a simple application of the Bernoulli equation; higher pressure will produce a higher flow rate with all other variables equal.

Initially testing began to bracket the fuel flow from the flow device that will satiate the fuel requirements described above for different temperature ranges. Testing occurred at room temperatures to obtain data for the valve setting and orifice flows at that saturation pressure at that temperature. The testing included an ice bath test. This provided another temperature point for which to gain flow data for the vaporizing flow. However, attempting to put the fuel tank in the ice bath produced unacceptable results. The fuel pressure reduces to the saturation pressure at 0 degrees Celsius. When the fuel reaches room temperature in the fuel system. The fuel boils out of the tank and into the fuel system. Therefore, there is no saturated liquid in the fuel system to flash across the vaporizing device and cool the liquid line. In order to perform the test, the environment of the entire system should be adjusted to the same low temperature. The scope of this research does not allow for an environmental chamber for testing. Therefore, testing of fuel system at temperature variations larger than typical room temperature fluctuations was not conducted.

4.4. VALIDATE HEAT EXCHANGER

In order to minimize the disparity of fuel distribution to the two cylinders, the injection location was selected upstream of the manifold for further testing. With an injection location selected and a fuel map for the fuel injector at the location developed, the focus turned to validating the heat exchanger. The fuel must be a liquid at the injector to be metered accurately. An initial guess for the heat exchanger performance goal was that the fuel temperature at the injector should be at least 5 degrees Celsius below the temperature of the fuel tank. This allows the fuel pressure that is provided by the fuel

tank to be higher than saturation pressure of the fuel at the injector. Therefore, the fuel is cooler than saturation temperature for the tank pressure provided and is thus, a sub-cooled liquid.

The heat exchanger was tested using the fuel injector timing and vaporizing flow settings that were determined for the injection location selected before the throttle plate. Through testing of the heat exchanger performance, the same speed and load test matrix that was used to build an injector fuel map is utilized to validate the heat exchanger. This was conducted to validate the heat exchanger at all selected engine set points. The results of verifying this assumption are provided later.

The reason that testing the heat exchanger is important is that more fuel injected from the injector and flashes in the manifold further cools the intake charge. This provides further improvement to volumetric efficiency. However, the heat exchanger must provide enough cooling to maintain the 5 degree Celsius drop from the tank temperature or the fuel system becomes unstable. Therefore, the cooling flow must be reduced to the minimum flow rate that still satiates cooling the liquid line. Additionally, insulation on the heat exchanger is beneficial. At standard atmospheric pressure, the saturated liquid temperature is –42 degrees Celsius. This means that the temperature of the heat exchanger can reach sub-freezing temperatures for water in a test facility that is approximately 23 degrees Celsius, room temperature. As the sacrificial fuel flashes to cool the liquid line, the temperatures in the heat exchanger can drop to the saturated temperature level. This is especially true for low injected fuel demand cases like idle. Therefore, maintaining the temperature of the control volume of the heat exchanger canister requires insulation to maintain efficiency with temperature differences around 50 degrees Celsius. Additionally, heat from the engine should be diverted from the heat exchanger via the insulation. Other insulation should be installed on the intake manifold downstream of the injection point. This maximizes charge cooling and protects the reduced temperature benefits from engine heat as the charge moves into the cylinders.

A side benefit for an air-cooled engine, as the one used in this research, is that the typical reason for running the engine rich is evaporative cooling occurs from the fuel and keeps the valve head cool. Charge cooling thus has beneficial side effects in this application.

4.5. BRACKETING VAPORIZING FLOW FOR THE HEAT EXCHANGER COOLING

The flow from the vaporizing device serves two functions. The primary function is to cool the liquid line fuel for injection. An additional use of the fuel stemmed from the use of the fuel in the intake manifold as a test for cylinder exhaust temperature distribution. The vaporizing flow can provide enough flow for idle operation of the engine. This provides an opportunity to operate the engine during transient conditions of the fuel system such as start up or hot-soak delay where the liquid state of the fuel at the injector is not assured. Idle flow must not be so large that charge cooling from injection at WOT is adversely affected. Volumetric efficiency can be improved for all engine-operating conditions via opening the throttle plate to reduce the efficiency loss across that restriction. However, the WOT condition can not improve volumetric efficiency by opening the throttle plate further and this condition is where charge cooling is most critical.

The primary function of the cooling flow is to cool the injector flow through all operating conditions. The most coolant demand is during the operating conditions of highest fuel flow. WOT is the case that demands the largest amount of fuel flow. The assumption is made that all the fuel for the WOT demand is supplied by the injector to produce a conservative cooling demand requirement. This calculation is performed without regard to ambient environmental conditions that typically affect this fuel system because the only temperature difference of interest is the relative temperature drop from tank temperature to injector temperature. The temperature drop is a minimum in addition to the minimum amount of fuel flow required for cooling. The secondary purpose of the vaporized fuel system is to provide enough fuel flow to operate the engine at idle which sets a minimum required fuel flow.

The fuel system requirements are determined by the fuel demands of the engine. By design, the vaporized flow should operate the test engine at 1550 RPM and a manifold pressure of 54.8 kPa. This is the base idle operation that should be fully operated by the vaporized flow.

The result for idle fuel flow rate requirement is compared with the minimum amount of fuel flow that is required for cooling. The flow rates are on the same order of magnitude and are comparable given the inherent variability of an unbalanced v-twin

engine. Therefore, the larger requirement will determine the flow rate for the flashing device. This ensures that there is enough cooling for the injector and enough fuel from the vapor flow to idle the engine. If there is extra fuel required for cooling then the engine idle speed or load will be higher than if the fuel flow was set purely for the purpose of idle. If idle requires more fuel than cooling, then the injector will run colder and some charge cooling is sacrificed. However, the simplicity of the system is enhanced with the ability to idle the engine on vapor flow. This determination is the minimum amount of fuel flow that can be allowed for the temperature difference desired in the liquid fuel line at WOT and idle

4.6. DEVELOPMENT OF THE ECM

With the data that has been acquired for the fuel map matrix at the established injection location and fuel timing that is referenced to crank angle degrees, the ECM is produced. The two dimensional fuel map is input into the chip as a range of pulse widths for a given first dimension of manifold pressure. The second dimension is manifold temperature. The temperature is used to scale the pulse width to account for variable density in the manifold air resultant from temperature changes. The pulse width is calculated for the intake pressure, scaled for temperature, and then triggered by the hall effect sensor that marks every revolution of the crankshaft. This automates the fuel system via computer control as a typical fuel injection system operates with constant fuel pressure. For the system in this research, temperature correction for the environment should be considered. The pulse width should be scaled for varying tank temperatures. Higher tank temperatures from the environment produce higher fuel saturation pressures. Variable pressure on the fuel during operation changes the mass flow of the fuel. Therefore, the ECM map requires a temperature correction for variable tank temperatures to account for the variable fuel pressure that is supplied by the tank in response to variable environmental temperatures. This can be implemented as another dimension of the fuel map that adjusts the pulse width provided by the previous two dimensions based on tank temperature

Another adjustment can be made to an ECM program. The metering valve for fuel vaporization can be actuated by a servomotor and controlled by the ECM. This requires a one-dimensional fuel map that has an input of tank temperature. Then a valve set point is output to adjust the effective flow area of the flashing device in response to variations in the changing saturation pressure. However, testing the valve map requires changing the operating environment of the engine in a climate controlled test cell. This requires a degree of sophistication that is outside of the scope of this research.

4.7. SCOPE OF THE EXPERIMENTS

The complexity that is produced by variable fuel pressure necessitates different orifice areas for changing fuel tank environment temperatures. The saturation condition of the propane fuel in the fuel system alters the pressure in the fuel as a result of a temperature change. The scope of the research does not allow reliable testing of the fuel system at different ambient conditions to produce brackets of tank temperature that a certain effective flashing device effective area should be used to allow the desired vaporizing flow rate. Therefore, a model is required to predict operational temperature bands for orifice sizes or valve settings. Therefore, a review of current flashing model literature was conducted as described in the Literature Review.

The preference for the model is one that is practical for implementation on this research. This includes measurable parameters. Temperature and pressure before and after the orifice are measurable. However, the scale of this research does not allow any parameters to be measured at the throat. Additionally, flow rate is difficult to measure at the minute scale of flow that occurs through orifice sizes on the order of 50 microns. Also, the model should make explicit predictions on required effective flow area.

A simple Bernoulli analysis proved to produce accurate predictions of flow rate compared to the measured flow rate. This implies that the fluid before the flashing device is low quality or a liquid before the vena contracta. The assumption is verified by the temperature and pressure parameter information before the flashing device discussed in the results section. These data are also used to verify the saturated liquid condition through the exit of the vena contracta as in Uchida and Nariai. (19). This verification

step ensures that the application of a single-phase incompressible flow equation can be reasonable for a low quality flashing two-phase flow regime. This approach will err on the maximum flow rate side as only the dense liquid is considered through the throat and thus choking is not an issue. Assuming a liquid through the throat, the Bernoulli equation is implemented into a computer code that outputs an effective orifice diameter given inputs of temperature and pressure.

The ECM that is developed for the injector operation is implemented to control the engine and allow focus on the flow rate of the vaporizing device. The basis of this testing is to compare data with the model that is implemented for flow area prediction of a given flow rate with variable pressure and temperature conditions. Also this is where the DAQ system is implemented to log the channels of temperature and pressure for the fuel system. Through this testing, the model predictions for the input conditions of the test accurately predict the average flow rate in the data. The results are discussed later.

However, the flow prediction of the Bernoulli equation is only comparable to the average flow rate of the system. As shown in the results section, the flashing flow appears to have a pressure fluctuation that affects the engine operation. The pressure fluctuation is experienced by the downstream rotameter and then the air fuel ratio of the engine oscillates around the desired equivalence ratio. This is the point where the large surge tank in the vapor flow line between the heat exchanger canister and the intake manifold is employed, as mentioned in the Experimental Procedure section. The tank is utilized to provide pressure fluctuation isolation from the engine to the heat exchanger. As discussed previously, the engine intake strokes create erratic flow dynamics in the intake manifold. The purpose of the surge tank is to isolate the flashing process from the erratic flow dynamics in the intake manifold. Figure 3.5 demonstrates measurement points in the instrumentation arrangement to track the source of the pressure pulses.

The results presented, show the flashing flow exhibits the same pressure oscillations with the surge tank in place. Therefore, testing is performed to definitively determine where the source of the pressure fluctuations. The upstream of the flashing device fuel system is already instrumented with a pressure transducer, however a second pressure transducer immediately out of the tank is used as a method of capturing pressure history upstream of the flashing device. The downstream side is fitted with three

pressure sensors. One is immediately after the flashing device, the second is before the rotameter, and the third is immediately before the surge tank. In addition to logging the fuel flashing data for this pressure phenomenon, dry gaseous nitrogen is passed through the system from a high-pressure tank that has a regulated output similar to the propane pressure. This is a baseline of what the pressure characteristics of the fuel system are with a single-phase gaseous fluid.

5. RESULTS/DISCUSSION

5.1. FUEL DISTRIBUTION RESULTS DEMONSTRATED IN EXHAUST GAS TEMPERATURES

The first set of results is combined for the iterative efforts of injection location, fuel injector timing, and tuning of the vaporizing flow. These results demonstrate engine stability as equal exhaust temperatures imply the cylinders are pushing equal power into the crankshaft. The results in Figure 5.1 show the initial indolene injected temperature distribution results. These results give an average exhaust temperature disparity of 240 degrees Celsius. Also, cylinder 2 is higher in temperature than cylinder 1. Thus the higher energy density is going to cylinder 2. This is a result that is not responsive to changes in injection timing as discussed in the Experimental Procedure section. Fuel pooling is suspected and evaporation delay favors cylinder 2.

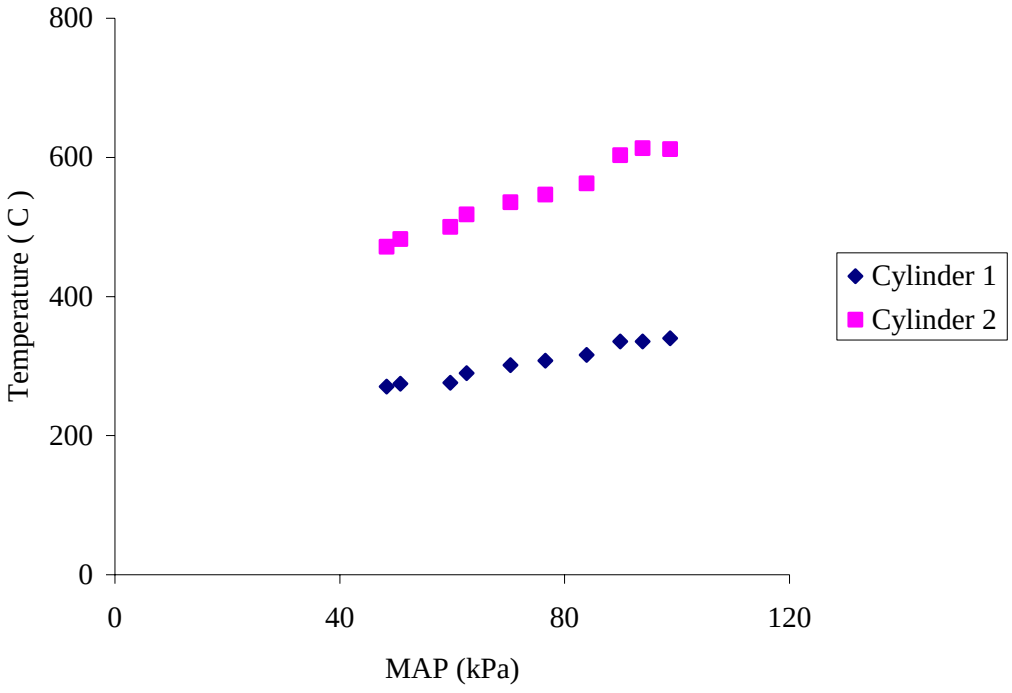

Figure 5.1 Cylinder exhaust temperature distribution for injected indolene at 1550 revolutions per minute.

The first test to enhance injection timing response and reduce fuel pooling is a switch to the fuel of interest for this research. The results for the more volatile propane at the intake separation point are shown in the Figure 5.2. This figure represents vapor flow and injected liquid, as injection is required by the engine fuel demand.

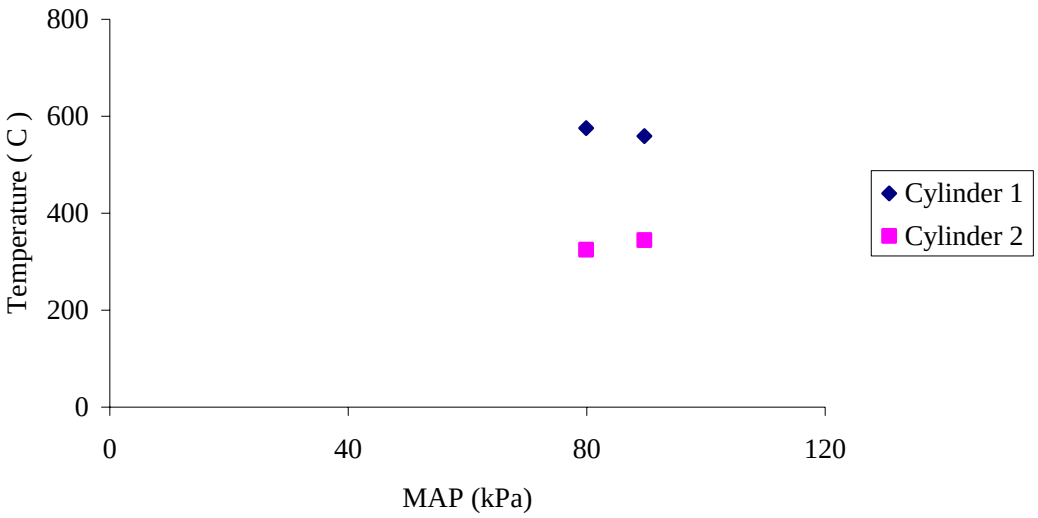

Figure 5.2 Cylinder-to-cylinder exhaust temperature disparity with propane as the injected fuel at 1550 revolutions per minute.

The results are a mix of vaporized introduction of the sacrificial cooling flow and the injected flow by design of the system. There are only two data points because lower loads at 1550 RPM do not require any fuel injection to reach the desired equivalence ratio of 1.1 and are omitted from the mixed fuel phase introduction figure. The magnitude of the average temperature disparity for Figure 5.2 is 232 degrees Celsius. The difference is smaller, but not much change in the magnitude of the distribution has occurred. However, in this plot cylinder 1 is the hotter cylinder. This is a result of having more fuel vaporize immediately from the injector than pools in reserve for cylinder two. As a result of the exhaust temperature disparity, the investigation into the ideal case of gaseous

introduction of propane before the throttle plate, i.e. idle conditions, is examined in Figure 5.3.

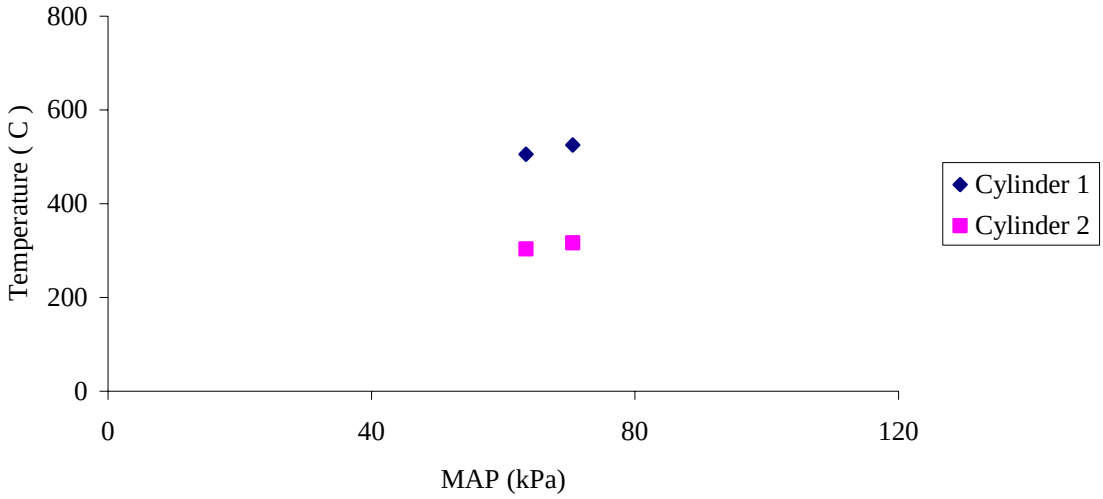

Figure 5.3 Cylinder exhaust temperature distribution utilizing gaseous propane introduction before the throttle plate at 1550 revolutions per minute.

Figure 5.3 shows the final exhaust temperatures for the two cylinders of the engine with vaporized propane introduced before the throttle plate. There are only two set points because higher engine loads at 1550 RPM require some injection. This is the most ideal distribution of fuel the engine arrangement will allow. There is an average 205 degree Celsius disparity between the cylinder exhaust temperatures. Additionally, cylinder 1 is hotter than cylinder 2 in this ideal case as in Figure 5.2. Another injection site is attempted that puts the injector and the venturi orifice that is used to deliver gaseous propane further upstream to best emulate the ideal case. The intent is to produce more even exhaust temperatures for the two cylinders. The gaseous propane results are very favorable with a reduction in the average difference of the exhaust temperatures to 188 degrees Celsius. However, the vapor flow augmented with liquid propane injection at the intake manifold separation point has little change in the magnitude of the temperature difference and actually increases to 234 degrees Celsius. More mixing time

is required to mimic the vapor flow, however, more mixing time reduces the charge density by allowing more time for the fuel to absorb heat from the engine. Results for reducing the fuel disparity by increasing mixing time is shown by the reduction of temperature difference in the vapor flow exhaust gas temperature difference resulting from the additional mixing time granted by the injector move.

Figure 5.4 reflects results for variable load at 3600RPM. The temperature difference in this data is on average 306 degrees Celsius. It is not as close as the temperature difference experienced at 1550 RPM. This difference is caused by larger relative exhaust temperatures and the reduced distribution mixing time of the higher engine speed reduces the cycle time for the fuel system.

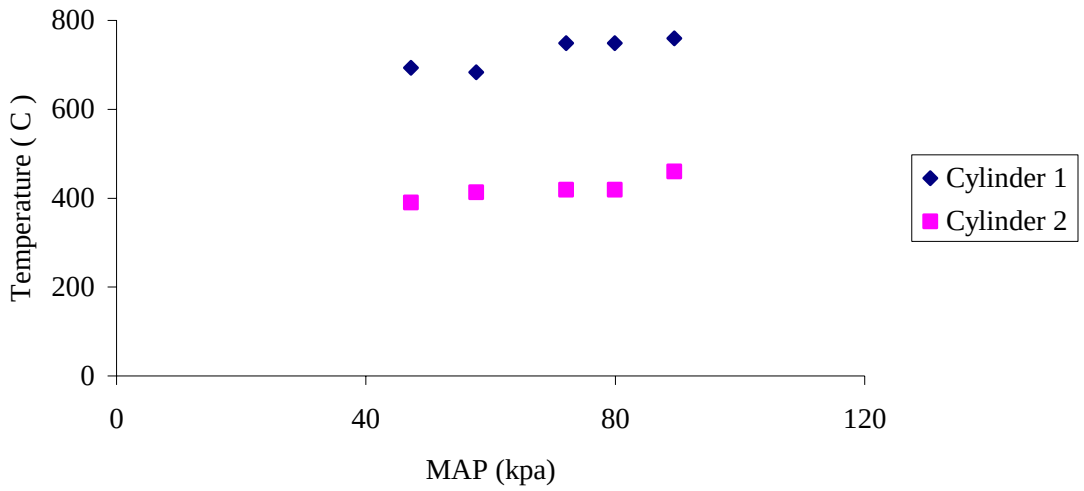

Figure 5.4 Cylinder-to-cylinder exhaust temperature distribution for injected fuel data at 3600 revolutions per minute.

Essentially, the maximized charge cooling for the engine would be realized as close to the intake valves as one injector will allow. This is because the fuel has less time to absorb heat from the engine. However, the engine becomes more stable in application of torque on the crank if the pistons via the rod apply equal torque to the crank during the cycle. This is accomplished by moving the injection point away from the cylinders to

increase mixing time and allow for more even fuel distribution. While completely equal fuel distribution is not possible in this arrangement due to the unbalanced v-twin engine and existing manifold, higher stability is needed for stable engine operation. As a result the injection location before the throttle plate is selected as the prime injection location for the fuel system.

5.2. INJECTOR TEMPERATURE

The injection location move did not effectively reduce the exhaust temperature difference as assumed. However, the move did allow effective application of insulation to the heat exchanger and injector. The initial injection location at the intake manifold separation point, produced a fuel temperature in the injector for engine set points in the test matrix as shown in Figure 5.5. The figure shows injector fuel temperature versus increasing load utilizing three different speeds.

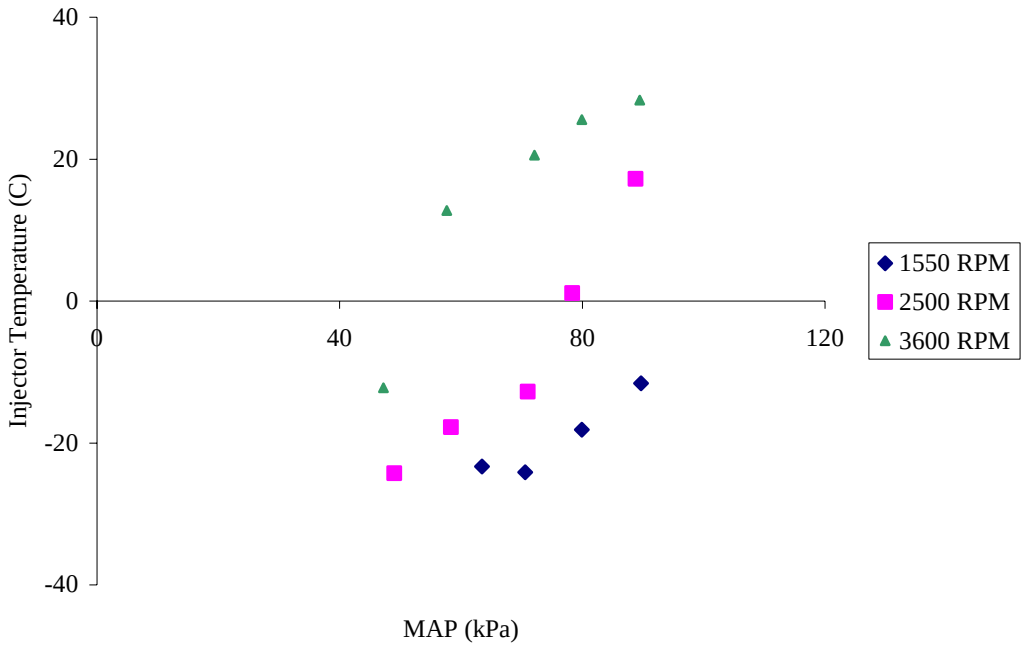

Figure 5.5 Injector temperatures versus increasing engine load for the injection location at the intake manifold separation point.

The new injection location that is located upstream of the throttle plate produces liquid fuel temperatures shown in Figure 5.6. Again, the injector temperature is shown versus increasing load for three different speeds.

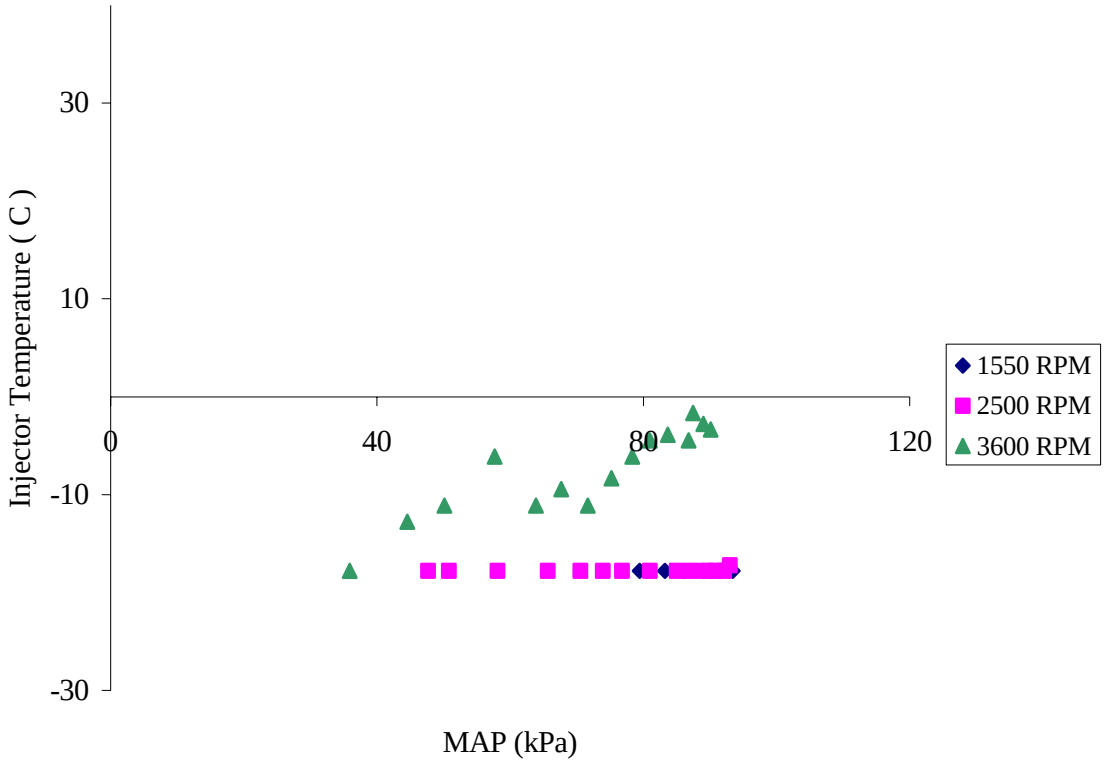

Figure 5.6 Injector temperature for the fuel map at injection location upstream of the throttle plate.

The new injection location shows a reduction in liquid fuel temperature at every engine set point in the test matrix. In order to attribute the temperature reduction to the injector relocation and increased insulation, the flow rates of the flashing flow should be compared. Equal flow rates of the cooling flow imply the move in injection location is the largest driver behind the injector temperature reduction. The flashing flow rate change from Figure 5.5 for the separation point location to the pre-throttle location does not show a discernable change in flow rate to cause the cooling improvement for the pre-throttle location. The cooling is a result of the pre-throttle location allowing adequate

insulation to be applied to the heat exchanger. The insulation allows a lower cooling demand and thus the injector delivers a higher proportion of the required engine fuel. Thus, the sacrifice in charge cooling from the increased travel distance of the flashing injected fuel as the fuel travels from injection point to the cylinder can be recovered by an increase in the injection flow rate that provides additional charge cooling. However, determining a flow rate change is difficult given the variability in the flow data discussed later.

Utilizing the pre-throttle plate injection location and the insulation that can be implemented, the performance of the heat exchanger is investigated. The first qualifying test for the heat exchanger is to investigate the fuel temperature at the injector and verify the 5 degree Celsius temperature reduction is satisfied at all engine set points as previously discussed. This data shows the injector temperature is below 0 degrees Celsius for all of the engine set points while the ambient temperature the tank experiences is 27 degrees Centigrade. Therefore, the injector fuel is approximately 30 degrees Celsius lower than the saturation temperature for the pressure supplied by the fuel tank during the highest fuel demand case of 3600 RPM and a MAP of 90 kPa. The state of the fuel at the injector can be reliably assumed to be liquid and a fuel injection map can thus be made to operate the injector. The two speeds of 2200 RPM and 1550 RPM show flat response temperatures at -18 degrees Celsius. This is a measuring limitation of the employed instrumentation. This is not a concern as the purpose of the test is to verify that the injector temperature was below 22 degrees Celsius for a tank temperature of 27 degrees Celsius. The heat exchanger of the fuel system performs as required.

The change in injection location has not only allowed for more engine stability via additional mixing time, but via additional insulation the pre-throttle location has allowed more fuel to be injected as a liquid. The heat exchanger is more effective with the insulation and therefore less cooling is required. Lower cooling requirement for the same fuel demand for the engine dictates that the fuel be delivered by the injector for increased charge cooling.

5.3. CHARGE COOLING

The second test to validate the productivity of the LPG system is to examine the system impact on the engine performance. The metric for the fuel system impact is the post injector location temperature of the airflow. Liquid injection should vaporize in the manifold and absorb energy from the intake air by heat of vaporization. The liquid injection system should lower the air temperature to increase the density of the intake charge. Increasing the air density and thus the quantity of combustion reactants is the advantage of a liquid LPG system over the conventional ambient temperature vapor method. The system must reduce the temperature of the intake manifold as more fuel is introduced to offset the volume of the vapor fuel. Figure 5.7 shows the results of increasing pulse width of liquid fuel from the injector in response to higher engine fuel demands and the resulting manifold temperature downstream of the injection location.

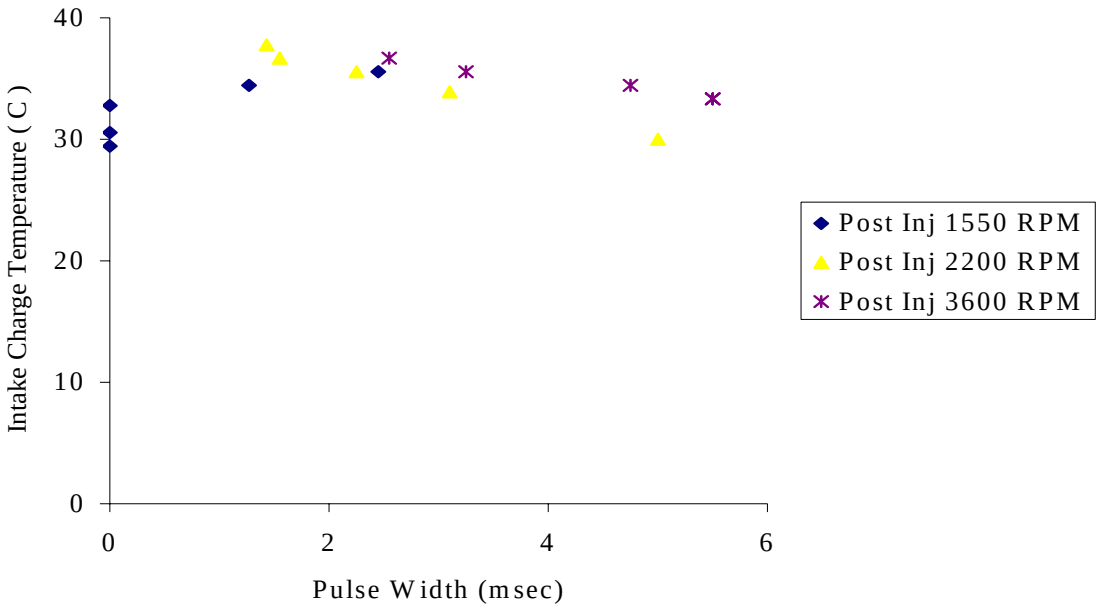

Figure 5.7 Pulse-width versus post-injection manifold temperature.

This figure shows that the temperature in the manifold after the injection is reducing for 3600 RPM and 2200 RPM cases as fuel flow rate and airflow rate are

increasing. The 1550 RPM case must begin injection before charge cooling is realized and that is why the post injection temperature initially increases when there is no injected fuel. This is what is expected considering the heat of vaporization should absorb heat from the intake air. Figure 5.7 is more impressive when Figure 5.8 is considered showing the effect of the additional fuel has on the manifold in the form of latent engine heat. The additional fuel causes the exhaust temperatures and thus the engine to run at an elevated temperature. Figure 5.8 also demonstrates that the pulse width cooling comes from the injector, as the intake air temperature is relatively constant. The manifold temperature reduces as a result of the vaporizing fuel even considering exposure to increasing engine heat from the engine as larger amounts of fuel energy are released in the engine. This test is performed without an insulated manifold that would have protected the manifold gases from engine heat. Figure 5.8 demonstrates the ambient environment of the exhaust located by the intake manifold.

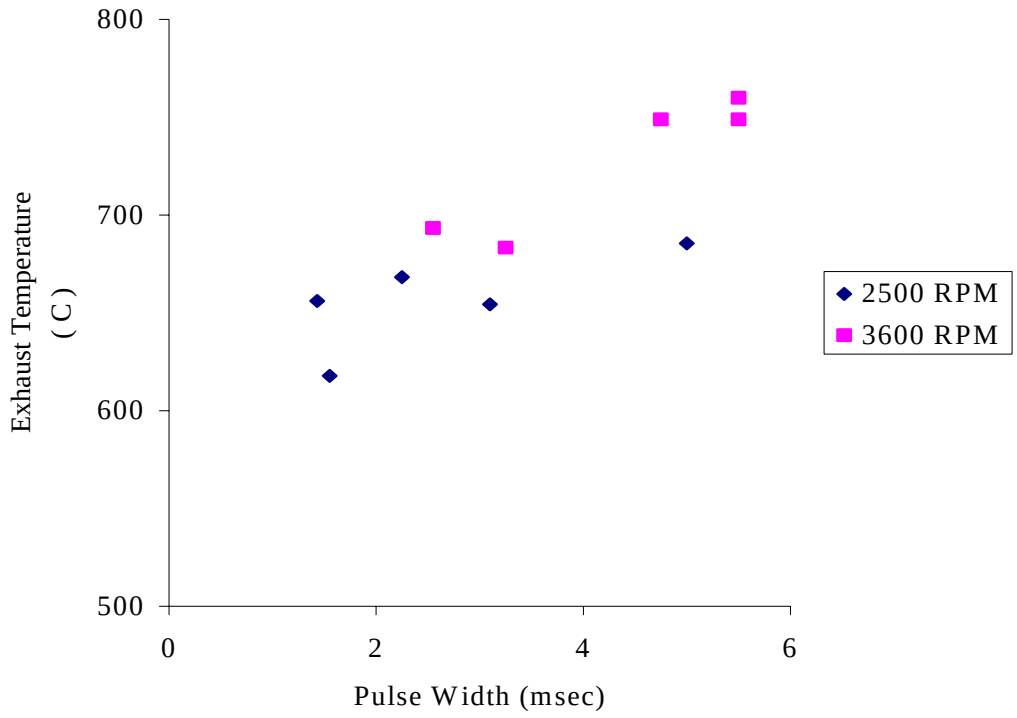

Figure 5.8 Exhaust temperature of cylinder 1 versus an increase in pulse width.

As would be expected for higher fuel delivery, the exhaust gas temperatures increase with increasing chemical energy release in the engine. The point is that the environment around the intake manifold is increasing in temperature with higher fuel consumption and the intake manifold reduces in temperature with higher fuel consumption as a result of the flashing fuel from the liquid injector.

However, it can be further optimized with a reduction in the required cooling flow to a level that achieves 5 degree sub-cooling so that a larger percentage can be injected as a liquid from the injector at all engine conditions. This change could save the fuel system about 25 degrees of cooling the liquid fuel which equates to approximately 0.0293 kJ/s cooling fuel flow that could be utilized in the manifold. This could produce an additional 3-degree Celsius drop in temperature at high load. Moreover, lower idle speed and load conditions can be achieved for smaller fuel flow requirements in the cooling system.

These results are supported by engine performance papers that have been conducted with extensive measurement of the engine response to liquid injection versus vapor induction and gasoline performance as in the paper by J. A. Caton et al. (4) Simply achieving liquid injection and measuring reduction in manifold temperatures ensures improved volumetric efficiency. Additionally in the paper by Sierens (1), liquid LPG injection systems were shown to recover much of the power loss that is experienced with pre-vaporized LPG introduction systems. The research for the project of the reference paper utilizes complete liquid injection. Therefore, the system in this research suffers from a diminished power recovery, especially at lower loads and speeds where a smaller percentage of the fuel introduction is in liquid state. This is acceptable as long as the WOT engine condition shows notable improvement because WOT power is where volumetric efficiency is most important. At this condition, the injector fuels more than 70% of the fuel requirement at faster engine speeds and larger engine loads.

The reduction of temperature noticed in the manifold gases is a result of a larger percentage of fuel being introduced into the intake manifold as a liquid as the load is increased. This is shown in Figure 5.9. Figure 5.9 shows three engine speed conditions. The percent of fuel that is larger than 100 percent is a result of operating conditions that are richer than the design goal.

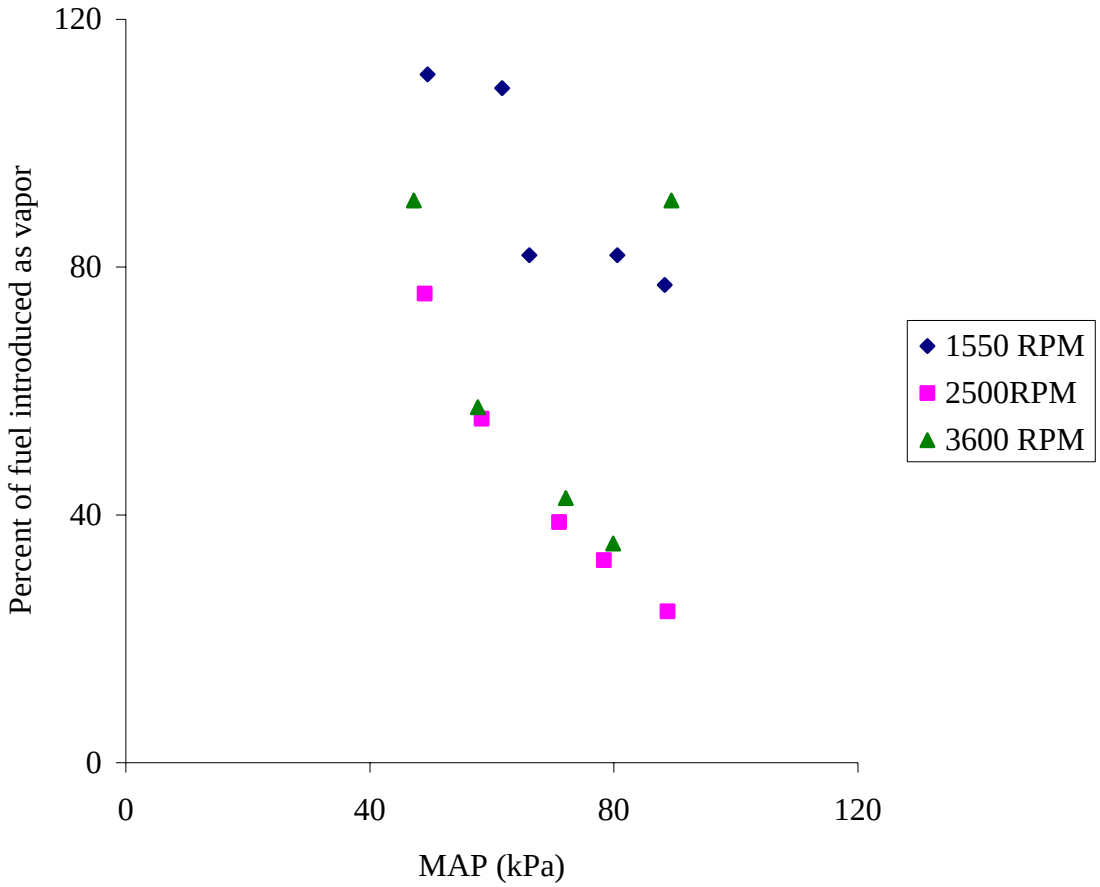

Figure 5.9 Percent of vapor phase introduction of fuel compared to engine load.

The richness is due to fixed vapor flow of an orifice that must be large enough to cool WOT injector flow. Note that only the 1550 RPM cases at low MAP are above 100 percent. All of the speed conditions reduce the percent of fuel introduction via vapor-phase as load increases. Again, charge cooling exists at high load where volumetric efficiency is a concern. The vaporized fuel flow rate is effectively fixed by the metering valve or orifice. Therefore, an increased engine load is satiated by increased liquid injection. As engine load increases the percentage of fuel supplied by the liquid injection increases. This is how the manifold temperature reduces as opposed to increases with additional engine heat of combustion if the percent of liquid fuel flow rate is held constant over the span of fuel requirements for the engine. Figure 5.10 shows the total fuel requirement and the respective components of liquid and vapor introduction.

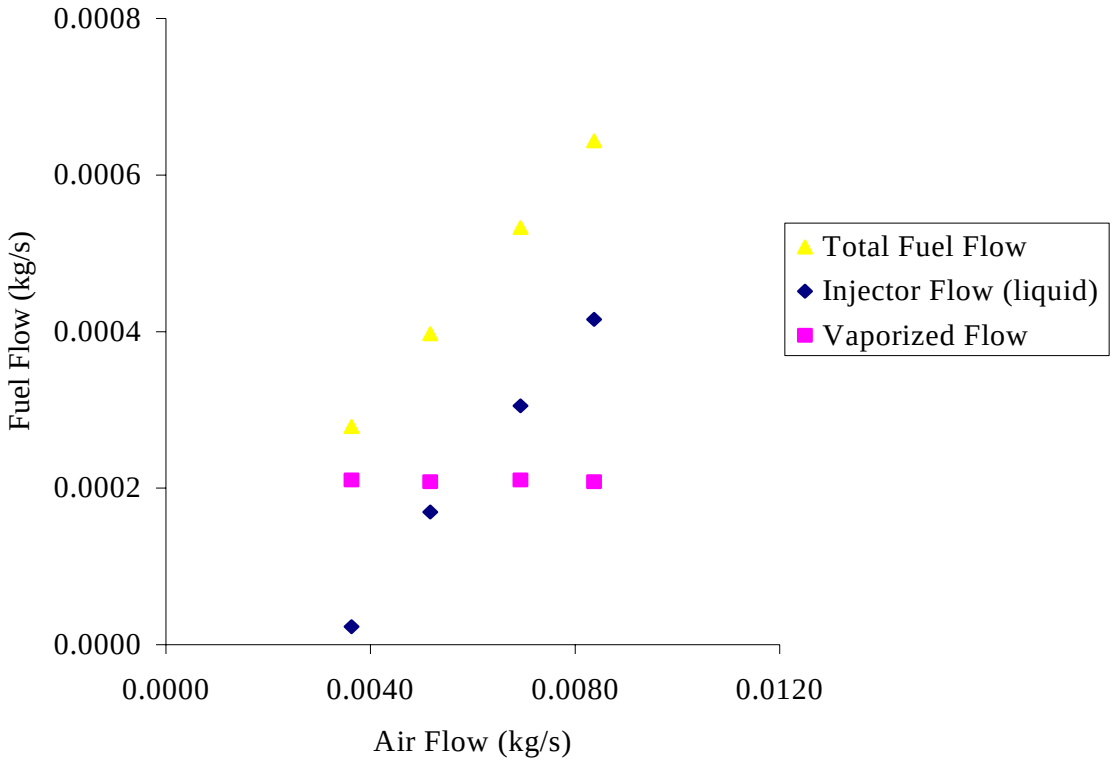

Figure 5.10 Fuel flow vs. vapor flow for various fuel map requirements.

The vaporized flow is relatively constant for the load range of a given engine speed. Therefore, the increase in fuel demands from a higher load on the engine is satisfied by liquid injection as shown. The liquid injection curve matches the slope of the total fuel requirement curve and the injection curve is simply shifted down by the amount of vaporized fuel required to maintain liquid in the injector fuel line. This is how the system supplies charge cooling at higher engine loads where volumetric efficiency is a concern. The percentage of fuel that is supplied as a vapor reduces where the load increases. This is shown in Figure 5.9 and 5.10.

As the percentage of fuel introduced as a liquid increases, the intake charge should be experiencing a cooling effect and thus reduce in temperature. Figure 5.11 below is supplied to demonstrate that the cooling rate actually affects the air temperature of the intake charge. Utilizing the constant specific heat of air, the temperature difference between the intake manifold temperature before injection and after injection, and the air

mass flow rate for that set-point, the cooling was calculated as a rate of kilo-Joules per second via the actual manifold temperatures. This is the actual cooling from calculations based on data. This plot is compared to a theoretical cooling plot. The theoretical plot is based on the resulting injected liquid fuel mass that was delivered to produce the temperature difference in the intake air and the heat of vaporization of propane. As anticipated the actual cooling is lower than theoretical because the theoretical cooling does not account for losses to the environment.

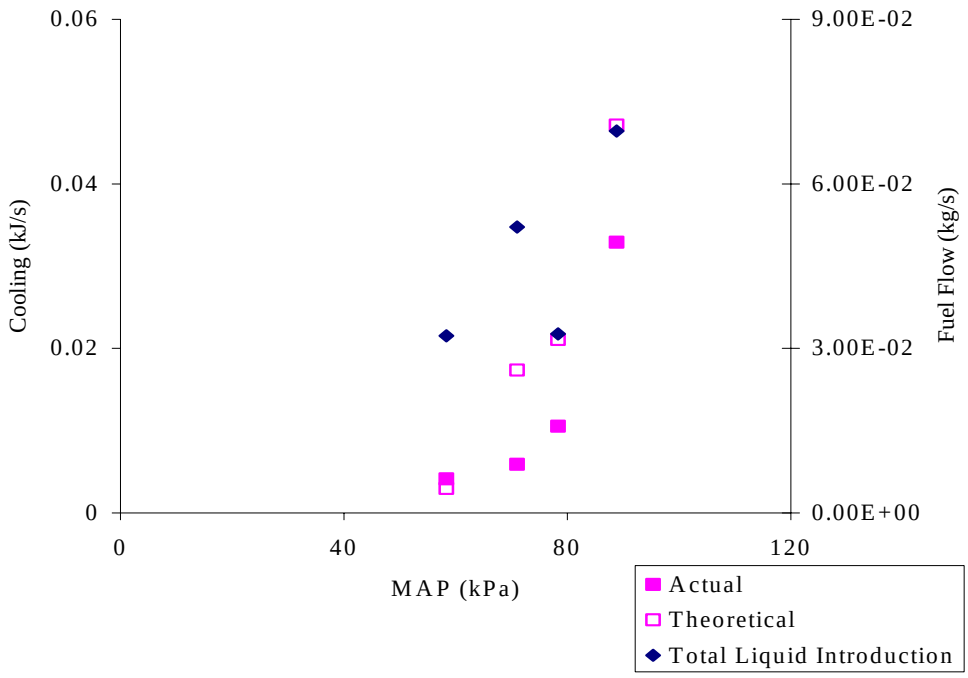

Figure 5.11 Actual cooling at 2200 RPM calculated from data vs. theoretical cooling of intake air versus load on the engine.

Additionally, the actual cooling for the gases in the intake manifold is increasing as load demand for the engine is increased as shown by the Total Liquid Introduction plot in Figure 5.11. Total liquid injection simply shows the relationship between increased liquid introduction and increased charge cooling. This increase in fuel introduction as a

liquid allows the intake manifold to reduce in temperature against rising exhaust temperatures and increasing intake air flow rate required of higher engine load as shown in Figures 5.7 and 5.8. In comparison to the paper by Sierens, (1), the theoretical calculation was extended to the complete fuel flow for the engine as liquid introduction for the high-pressure system. The additional cooling available from supplying the complete fuel requirement as a liquid is small at high load where charge cooling is most necessary. Any cooling that takes place is subject to the difference in the theoretical calculation to the actual cooling showed in Figure 5.11. The third point in the total fuel introduction curve seems low and this is a result of the small change in fuel flow rate from one set-point to another because the calculated fuel flow for the cooling is a difference in flow rate calculation between set-points. This anomaly highlights the variability issue within the flowrate data that is discussed in the uncertainty section.

Figure 5.12 shows the cooling that is supplied as in Figure 5.11 versus the cooling required for injection. This is a measure of how much cooling is required to maintain liquid at the injector for an engine set point.

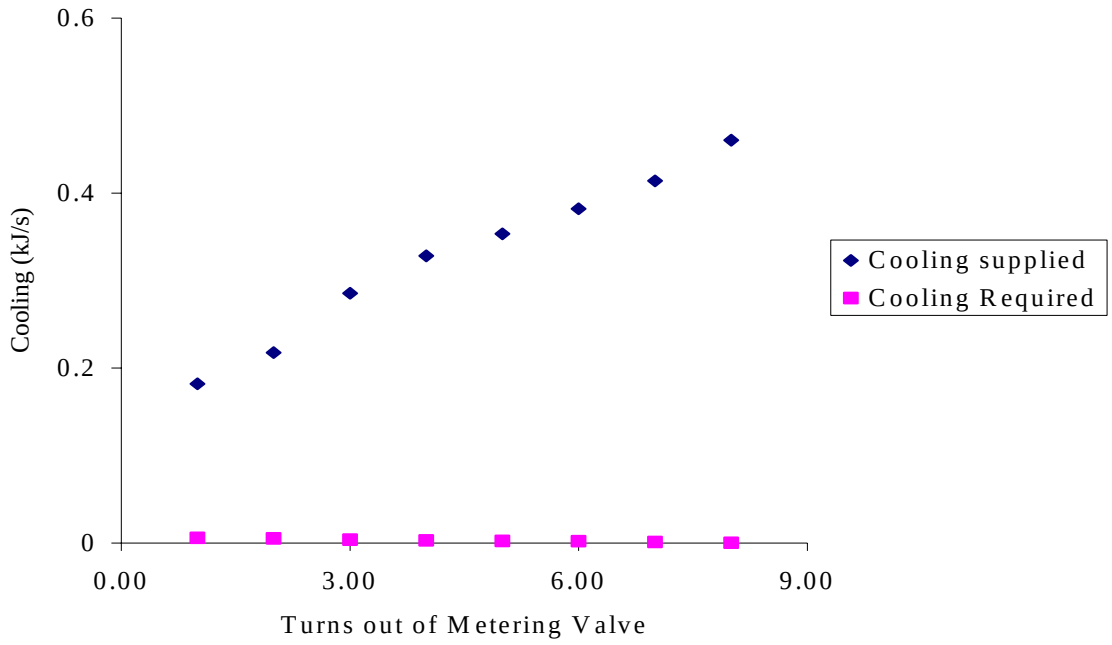

Figure 5.12 Cooling supplied by the metering valve via flow rate calculation versus the cooling required via average injector flow rate calculated by pulse width.

As expected, the provided cooling in Figure 5.12 increases as the metering valve is opened to allow more fuel to be vaporized. This figure is referenced for a single engine setpoint to show the possible vaporizing flow combinations. The figure shows how those flow possibilities translate to the distribution of cooling and fuel flow between the injector flow cooling the manifold or the metering valve cooling the heat exchanger. It is interesting to note that the cooling required drops as the metering valve opens. This is because the vaporizing flow from the metering valve increases as a percentage of the fuel requirement for the engine setpoint. As a result, the fuel requirement on the injector to meet the fuel demand of the engine is reduced. Thus, less cooling is required to cool the diminishing liquid flow.

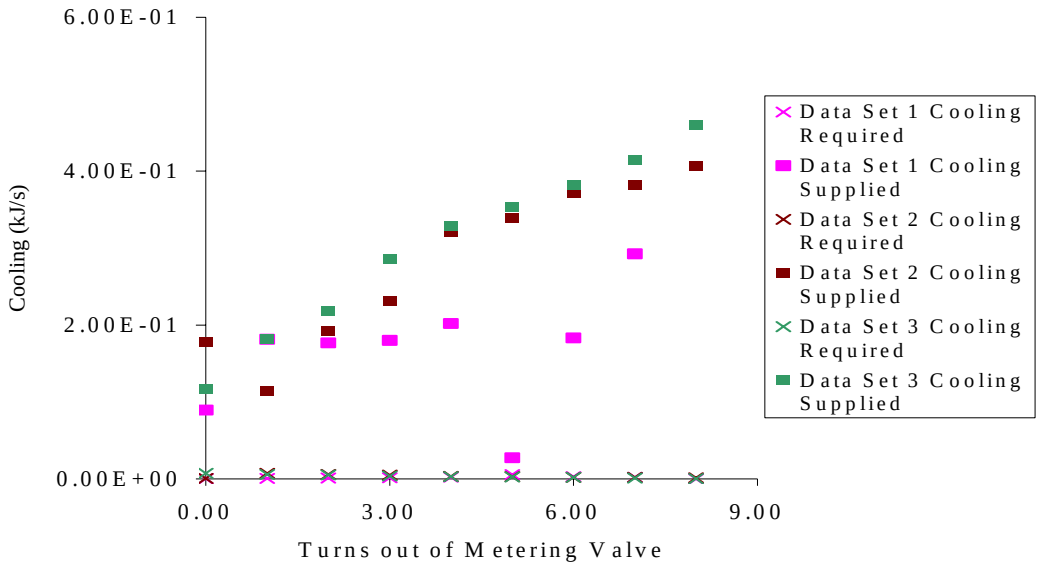

Figure 5.13 Figure depicting calculated cooling given valve flow data and heat of vaporization for propane.

As shown in Figure 5.12, Figure 5.13 shows increase in cooling from the vaporizing flow versus the opening of the metering valve. This shows calculated results for repeated tests on opening the metering valve. These figures show that charge cooling is realized in the intake manifold from the liquid fuel supplied by the injector. Also, the

injector cooling exists from the flashing flow in the heat exchanger. The relationship between the manifold cooling versus the cooling of the liquid fuel is explored.

5.4. VAPORIZING FLOW RESULTS

Vaporizing flow results encompasses the work both with the metering valve and the orifice flow. Figure 5.14 shows how the flow rate of the valve relates to the turns out from the closed setting. The metering valve allows more real-time control over the flow rate than an orifice.

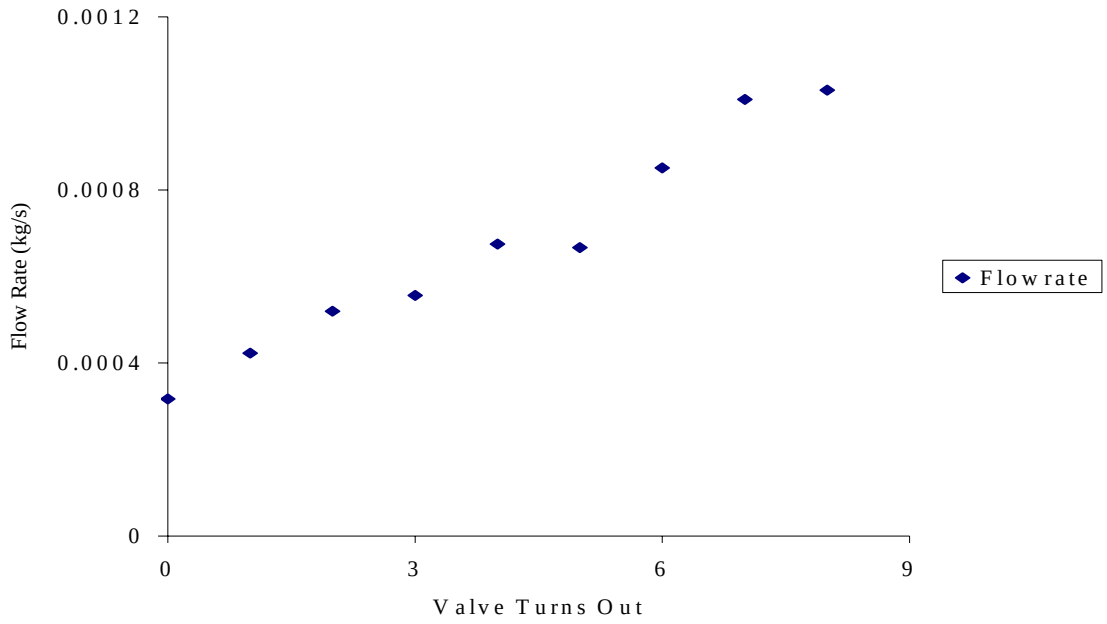

Figure 5.14 Valve flow rates versus turns out of the metering valve.

However, the results of the model are the final concern in this paper. For simplicity in geometric parameters, the model focused on the orifice. The Figure 5.15 presents the theoretical predictions for orifice size versus desired flow rate and upstream pressure as calculated by the Bernoulli equation discussed previously.

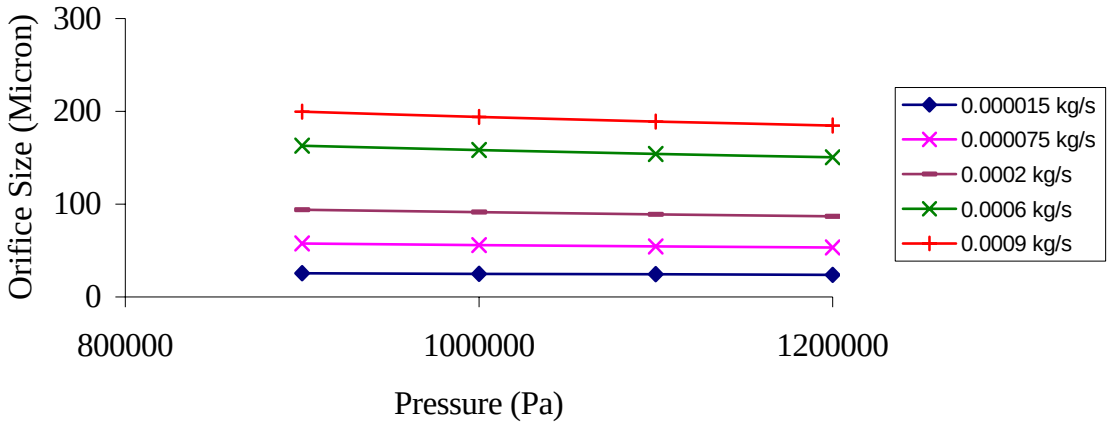

Figure 5.15 Theoretical predictions of orifice size.

Figure 5.16 shows the actual flow through a 75 micron orifice versus upstream pressure variations on the x-axis. The data points on Figure 5.16 are test data that are the result of measuring upstream pressure and vaporized flow rate. The lines on the plot are the result of the use of the Bernoulli equation. These lines produce a flow rate through a given orifice size of 75 microns as used in the test. The only input variable that was changed in the Bernoulli equation was the upstream pressure as the downstream was assumed to be ambient in all cases and other parameters like gravity are neglected.

The plots in Figure 5.16 represent different points of testing for different engine operation conditions and no trend is intended. An investigation of the clustering of model prediction vs. the actual measured flow rate is the aspect of interest in Figure 5.16. Notable variability in the instantaneous flow rate is recorded and discussed in the subsequent downstream pressure fluctuation topic. However, the average flow predictions are not dismissible. The average flow rates are on the same order of magnitude at the 10^{-5} kg/s level of the theoretical prediction. Unfortunately, DAQ flow meters are difficult to find and expensive for the studied flow rates of this work and therefore out of the reach of this research. However, the Bernoulli approach is reasonable from a standpoint of average flow rate.

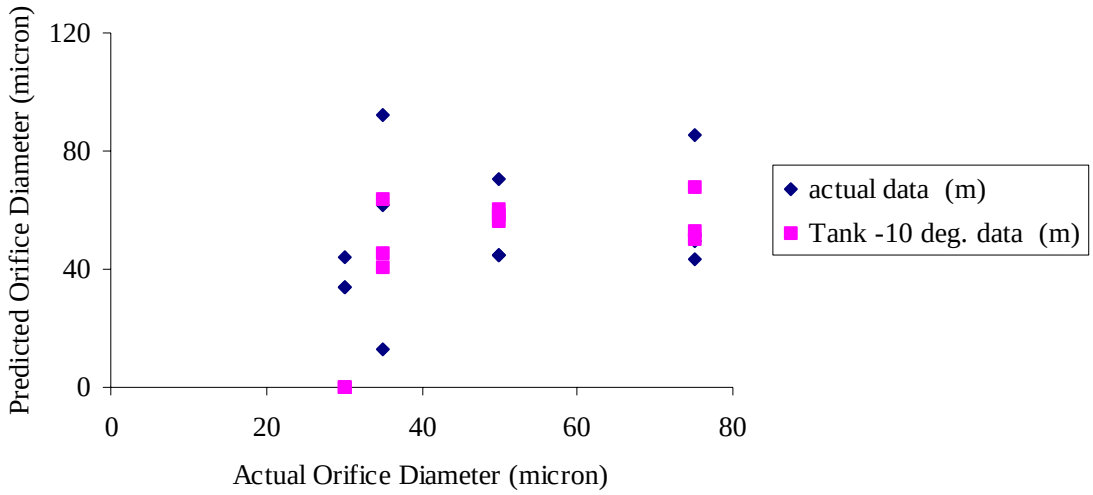

Figure 5.16 This figure shows the orifice diameter relative to the theoretical orifice diameter resulted from a Bernoulli calculation using the flow rate data.

Moving downstream of the flow restriction to look at the temperatures with regard to their position in the flow stream demonstrates that the temperature downstream reduces as the flow leaves the heat exchanger for higher vapor flow rates as shown in Figure 5.17. This figure is from a wide-open metering valve. Part of the fuel is vaporizing after the heat exchanger for the case shown that is from a fully opened metering valve. Actually, on a humid day this data point eventually froze the venturi orifice in the air stream, that is used to induct the vapor fuel into the intake air, shut. The engine lost manifold pressure as no air could be brought into the system.

A picture of the frozen venture orifice is shown in Figure 5.18. The bottom picture shows the frost that formed from condensate of the humidity in the air on to the cold venturi orifice. The orifice was especially cold because of the high vaporizing flow rate that was being tested when the intake froze over. This high flow rate was still flashing after the heat exchanger and very cold upon induction to the intake manifold. This means that all of the cooling potential stored in the liquid state of the saturated liquid that flashes into the heat exchanger is not utilized in the heat exchanger canister, at least at higher flashing flow rates.

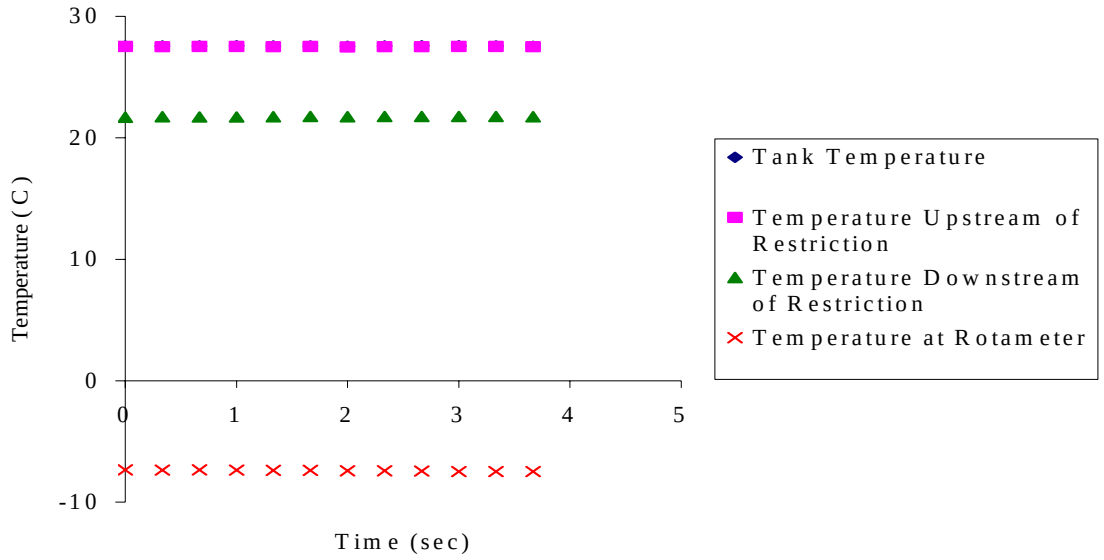

Figure 5.17 Downstream temperatures that reduce as vapor flow moves away from heat exchanger.

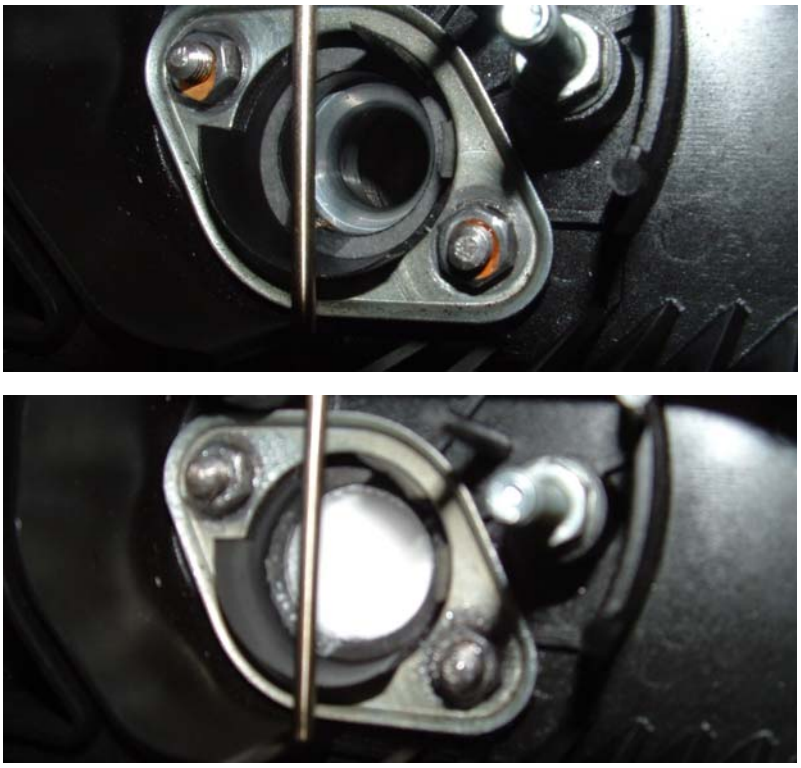

Figure 5.18 This figure shows the result of excessive flashing flow freezing the venturi orifice shown at top shut as shown at the bottom.

Therefore, the heat exchanger could be further optimized and tuned to meet the needs of liquid cooling and completely flash the sacrificial fuel in the heat exchanger. The heat exchanger vapor flow path can be extended to allow the fuel to finish vaporizing before exiting the heat exchanger canister. Also, more fins can be added to the liquid line for increased surface area. This optimization can reduce the required flashing flow rate and allow more charge cooling. This additional optimization is limited by the temperature that is experienced at the WOT condition. This condition must remain sub-cooled by 5 degrees Celsius.

5.5. VALIDATION OF MODEL ASSUMPTIONS

Figure 5.19 shows the temperatures taken during the data acquisition testing to validate the model with an orifice restriction. The flow restriction shown in this figure is the result of a 100 micron orifice.

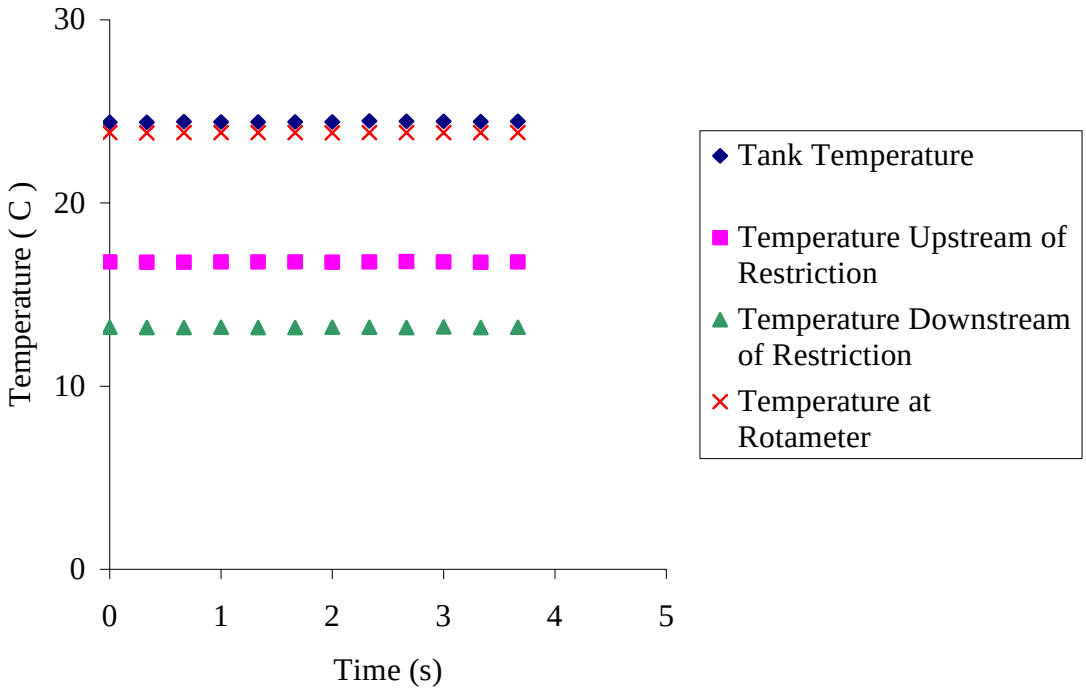

Figure 5.19 Plot depicting the temperature measurements for the fuel system upstream and downstream of the flow restriction.

The temperature immediately upstream of the flow restriction is 2.5 degrees Celsius lower than the temperature of the fuel that is released from the tank as a saturated liquid. Therefore, the reduction in temperature of the saturated liquid allows a sub-cooled liquid assumption at the orifice. This supports the use of Bernoulli equation for a saturated single component liquid flashing flow. The temperature reduction is from the conduction from the cold control volume transferring upstream to the relatively stagnant upstream fuel and pipe fittings. This phenomenon is not noticed until steady state has been achieved in the heat exchanger and the liquid injection line.

The metering valve shows little temperature change between the tank temperature and upstream of the flow restriction temperature because the valve is not within the confines of the heat exchanger control volume. In fact, the upstream temperature of the metering valve can be higher than the tank temperature due to engine heat as shown in Figure 5.20.

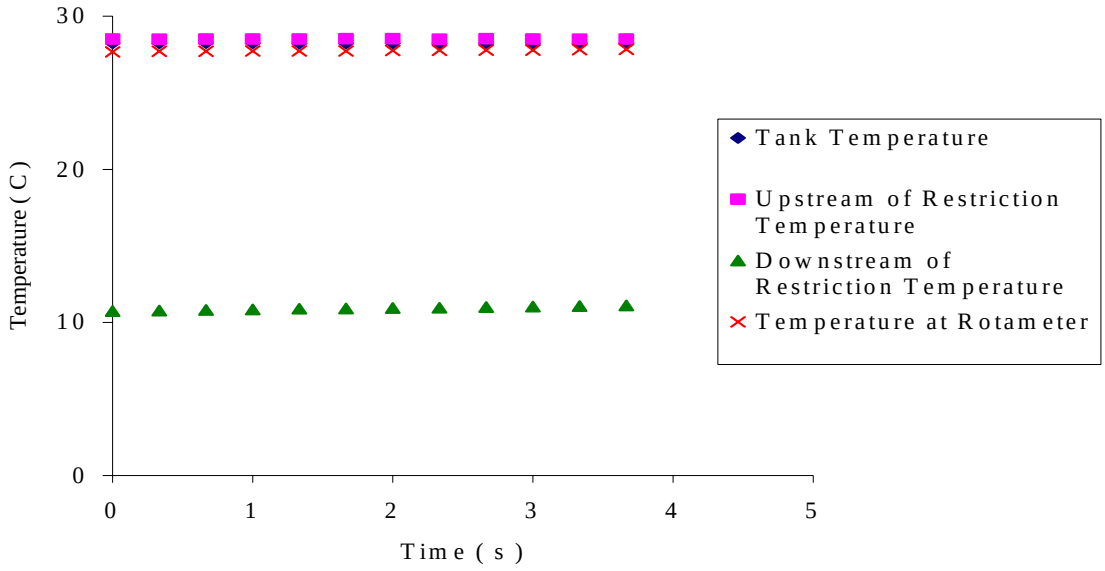

Figure 5.20 Vaporizing fuel temperatures using the metering valve.

As a result of this data the orifice adheres to the Bernoulli assumption well and the metering valve is suspect. No sub-cooling and increased fuel temperature, relative to the tank temperature, ensures that two-phase flow exists in the valve.

Even with the utilization of an orifice, the frozen flow assumption until throat exit for the Bernoulli analysis is suspect, however, with the previously mentioned variability in instantaneous vaporized fuel flow rate. The orifice provides a few degrees of upstream sub cooling, but still may be subject to two-phase flashing flow in the throat. In the case of flashing flow, the first consideration in the fuel system is the pressure fluctuations that are characteristic of flashing flow. Therefore, investigation in the downstream pressure fluctuations for the orifice is considered as shown in Figure 5.21. This plot is utilizing the orifice as a restriction device and testing the Bernoulli assumption in conjunction with the upstream sub cooling offered by the orifice arrangement.

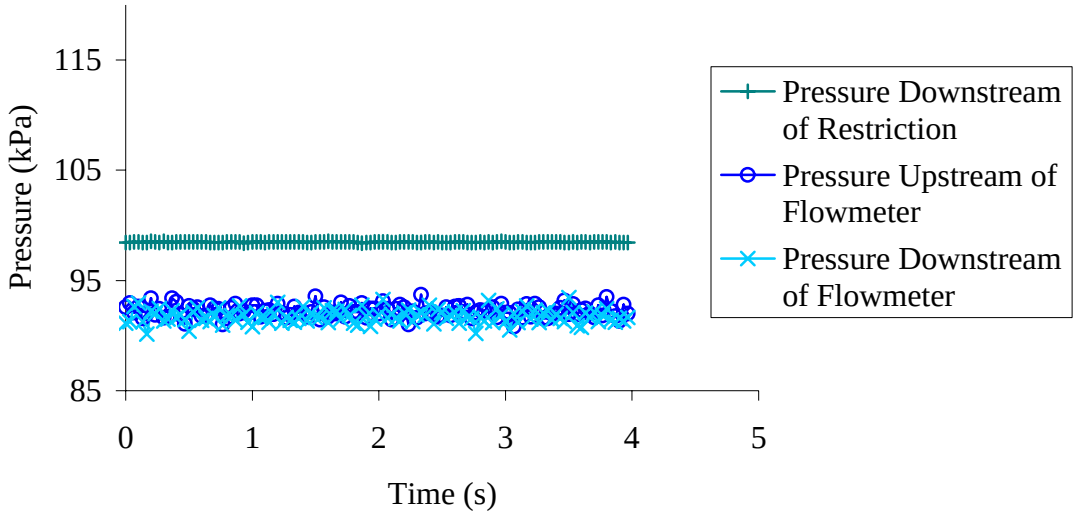

Figure 5.21 Downstream pressure traces depicted to find the cause of pressure variation and flow rate fluctuations.

As expected the pressure immediately following the orifice is the largest pressure in the remaining fuel system until the entrance of the intake manifold. The higher pressure drives the fuel flow from the orifice to the intake manifold. However, the connection to the intake manifold allows the pressure pulsations of the intake valve events to travel up the fuel system path to the orifice. This is depicted in Figure 5.21 by

the orifice, which seems to emphasize the effect of the engine pulsations more than the metering valve. The accentuation is because the orifice adheres to the Bernoulli assumption more closely than the metering valve due to the upstream sub cooling and the simpler geometry. For the orifice, the larger pressure fluctuations are noticed as the fuel approaches the engine. Thus, engine fluctuations are obviously influential in the fuel system. These engine fluctuations can be minimized with a large surge tank between the pressure sensors and the intake manifold. The surge tank employed in the experiment is over 10 cm in diameter and about 50 cm long. The diameter increase is a factor of 16 times larger for the surge tank as a fuel line that is over half a centimeter in diameter. Some of the pressure variations are shown in Figure 5.22 for the metering valve. It is evident that the dominant pressure variations resulting from the metering valve have larger amplitudes than employment of an orifice.

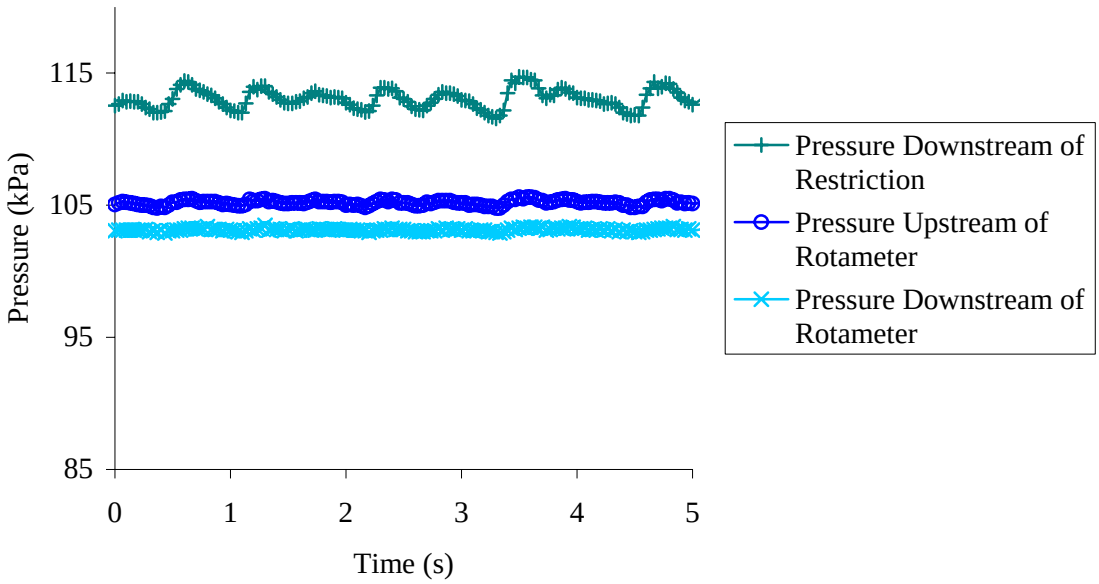

Figure 5.22 Downstream of the metering valve pressures.

The surge tank minimizes the intake pressure fluctuations of the engine. However, there are still fluctuations that appear to exist and originate upstream of the

sensors. To reiterate, these variations are more pronounced with the metering valve than the orifice. The metering valve does not fit into the confines of the heat exchanger control volume like the orifice. As a result, the metering valve has upstream fuel that is warmer than the fuel immediately out of the tank when the orifice has a temperature reduction immediately upstream of the restriction compared to the tank. Also the orifice does not have the complex geometry for the fuel to flow through as the metering valve. Regardless of the orifice or metering valve selection for flow restriction, there are pressure fluctuations that occur upstream of the flow restriction.

As shown in Figure 5.23, pressure fluctuations are noted upstream of the flow restriction and immediately out of the fuel tank. Upstream pressure affects the fuel flow through the orifice and thus the operation of the fuel system and engine. The orifice upstream pressure variation is on the order of 20 kPa.

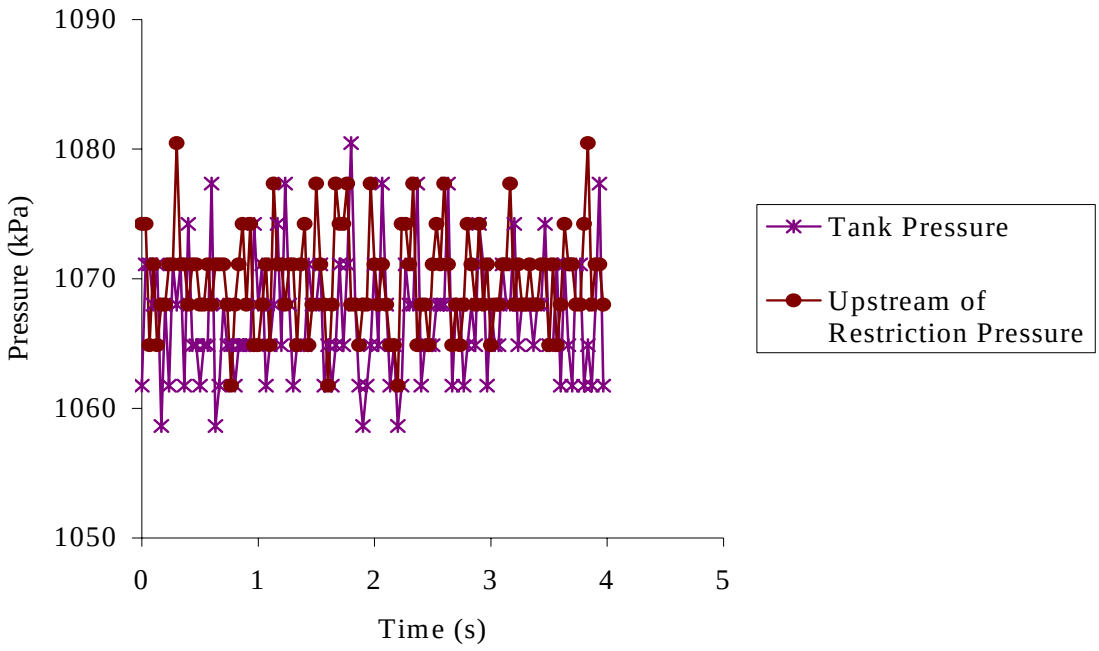

Figure 5.23 Upstream of orifice pressure.

Figure 5.24 shows the pressure fluctuations that are upstream of the metering valve. These fluctuations are on the order of 10 kPa.

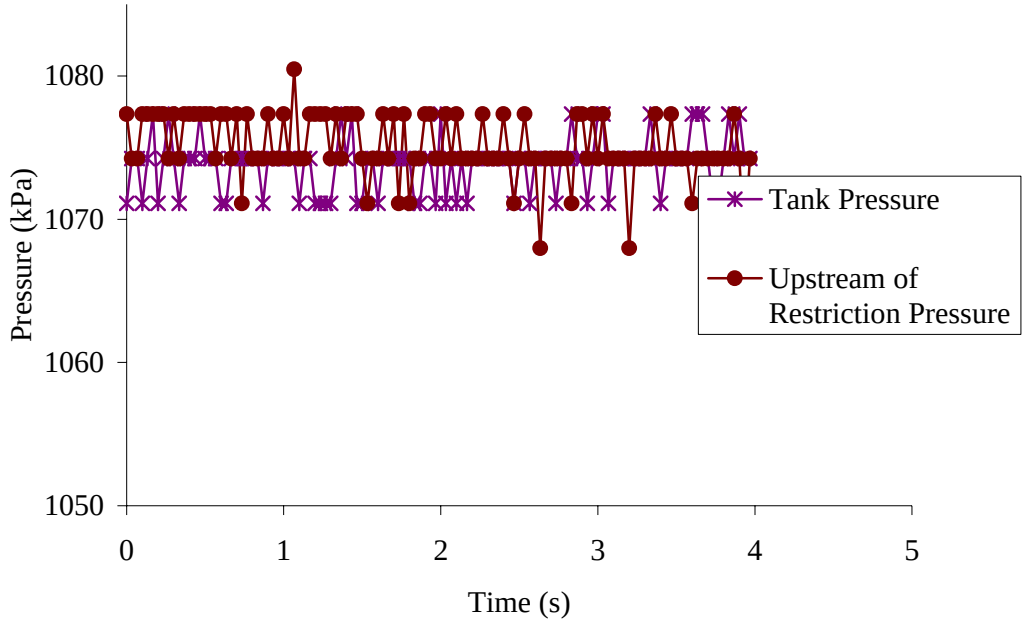

Figure 5.24 Upstream of metering valve pressure.

Like downstream, upstream of the flow restriction pressure variability is different depending on whether the orifice or metering valve is employed. The metering valve has less variability upstream and more down stream when compared to the orifice. It is imperative that these pressure fluctuations for either restriction device be traced to the source.

5.6. PRESSURE FLUCTUATION INVESTIGATION

The pressure fluctuations discussed in Section 5.5 can have multiple sources. This section investigates the probable causes for the fluctuations. One possible source is water that is in solution in the fuel freezes and passes through the restriction causing pressure irregularities. Additionally, other impurities in the fuel can form an oily build up in the throat of the flashing device. Another cause could be the fuel system causes pressure fluctuations. This can be from unstable pressure of the fuel out of the fuel tank or the bends and restrictions in the fuel system cause flow variations that cause pressure

pulsations. The final possible cause is the operation of flashing a two-phase fluid is unstable and unpredictable.

These pressure fluctuations are not the result of freezing and thawing of water in the fuel as a desiccant filter is used in the vaporizing fuel line before the flow restriction. It could be a fuel issue with variations in the blend of the commercially purchased LPG. Commercially available LPG is a blend of hydrocarbons that can fluctuate tank to tank. During testing some instances of flow loss through the orifice are noted. The investigation of these losses revealed an oily film on the down stream side of the orifice. A change in the fuel tank produced no flow loss across the flashing device. A dependable fuel flow allows reliable and repeatable testing. However, the blend of the fuel can also affect the pressure fluctuations through the orifice. The same effect that creates the blocked flow condition as a result of the heavier hydrocarbons can cause intermittent flow variations across the restriction. Variations in the flow restriction can cause pressure fluctuations.

In an attempt to investigate the relationship of the fuel to the pressure fluctuations, dry nitrogen gaseous flow is studied in the fuel system. This reduces the complexity of the fuel system by maintaining a single-phase homogenous flow at constant temperature in the fuel system. Also, the injector can be eliminated to further simplify pressure sinks in the fuel system. Figure 5.25 shows pressure fluctuations that are present with dry nitrogen vapor flowing through the fuel system. This case is for the fuel system with no engine operation. The highest variability is in the measurement that follows the pressure restriction. This is reasonable considering a flow restriction of the orifice would affect the flow more than flow obstruction caused by connection fittings or instrumentation. Without engine operation or vaporization of two-phase flow, the question of how pressure pulses precipitate must be answered. There are two essential causes of the variation in the data. The instrumentation could experience resolution issues. However, the error of the sensors is smaller than the 1 to 4 kPa fluctuations in the data. The instrumentation is discussed in the uncertainty section. An additional possible source is the fittings and instrumentation causes the pressure fluctuations. The rotameter measures flow by lifting a weight against gravity via the force of the flow. However, if the flow creates recirculation zones the weight bobs up and down in the flow. These variable

recirculation zones around the weight could cause pressure variations. The fittings to connect instrumentation and fuel lines can also cause vortices and thus pressure variations.

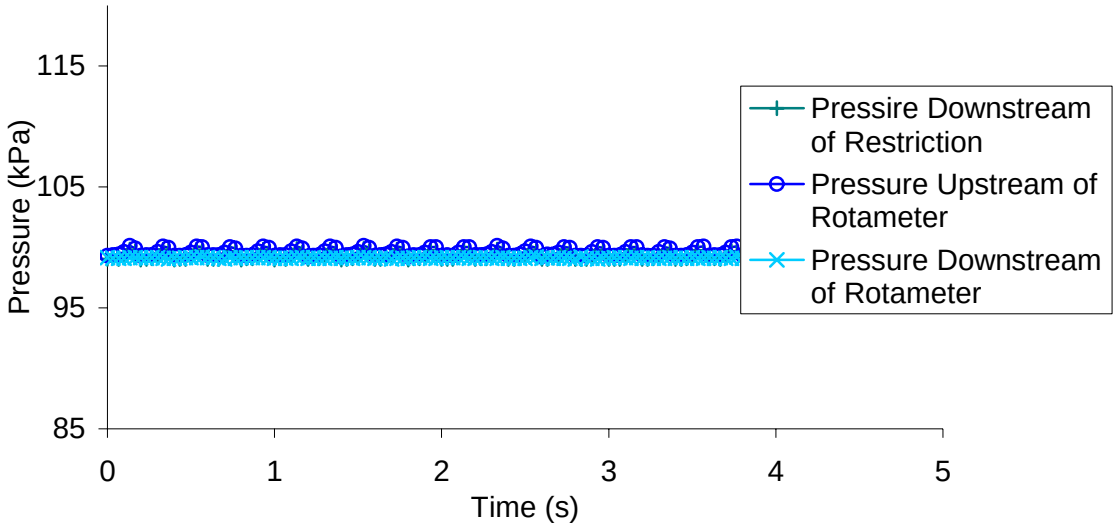

Figure 5.25 Downstream pressure fluctuations with dry nitrogen.

As is evident by investigation of Figure 5.25, the system has inherent flow fluctuations. The variation amplitude for dry nitrogen is only on the order of 1 kPa compared to the 2-5 kPa fluctuations in operational flow of the vaporizing fuel flow. The frequency is on the order of 5 Hz for dry nitrogen flow through a 50 micron orifice with no engine operation. A 1550 RPM engine speed has a cycle frequency of approximately 13 Hz. Therefore, pressure pulses shown in the figure of the 50 micron orifice nitrogen flow, Figure 5.25, would then occur approximately every second engine cycle at the slowest engine speed and every fourth injection as injections occur every engine revolution on a frequency of approximately 26 Hz. Therefore, the engine intake pulses and injection pulses may affect the fuel system, but the dominant frequency in the plot is not the same as these engine events.

After further investigation into the data obtained with the DAQ system, the frequency of the pressure variations is not constant. A Fast Fourier Transform (FFT) is done for the data to investigate the constituent make up of frequencies that produce the variations seen in the data. The flow of dry nitrogen through a 50 micron orifice produces two peak frequencies below the half sampling frequency of 15 hz. Those frequencies are 5 and 10 hz. Flashing flow through the same 50 micron orifice produces frequencies of 4, 8, and 12 hz. Even though the same orifice is used, the flow is not the same because the density of the fuel flow is greater than the density of dry nitrogen flow. The flashing flow also has 3 dominant frequencies. The flashing pressure data for the 50 micron orifice is shown in Figure 5.26.

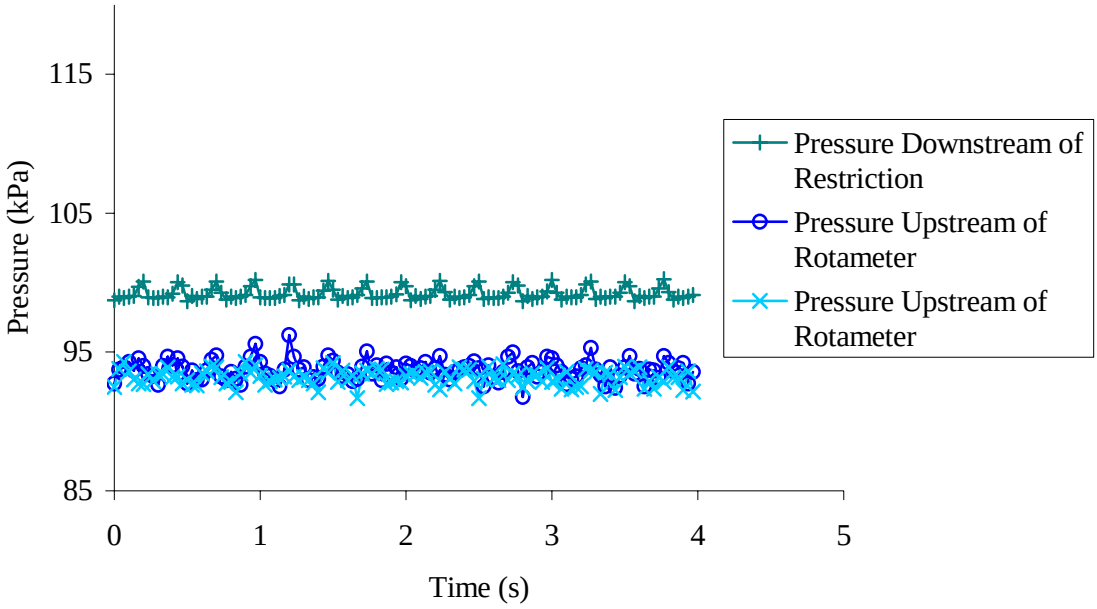

Figure 5.26 Plot of downstream pressure variations using a 50 micron orifice and flashing fuel.

Orifice sizes that are smaller than 50 microns have smaller frequencies. The 30 micron orifice produces frequencies at 3.5, 7.5, and 11.5 Hz in the downstream pressure data as shown in Figure 5.27.

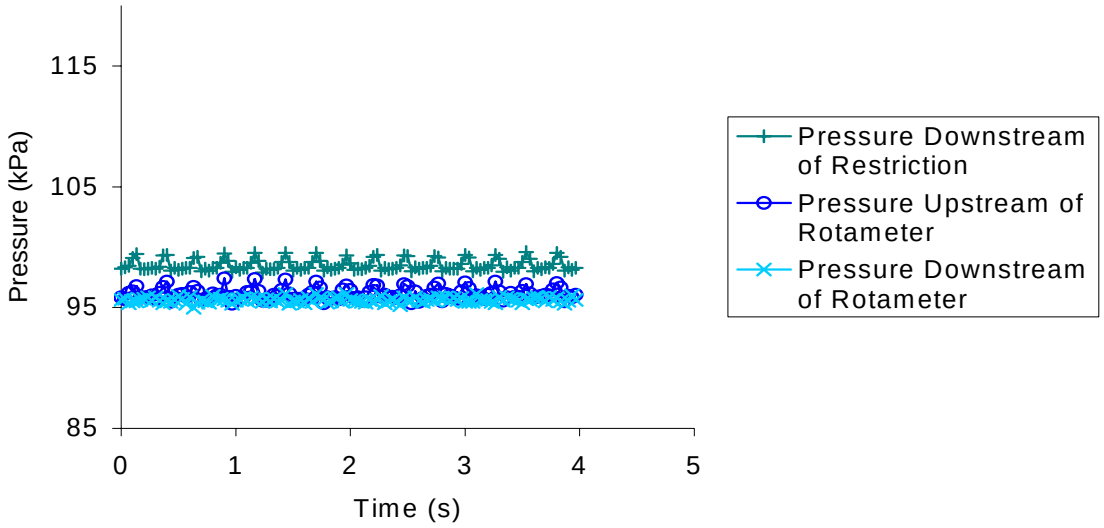

Figure 5.27 Plot of downstream pressure variations using a 30 micron orifice and flashing fuel.

In contrast the orifices that have a larger diameter than 50 microns have larger frequencies. The 100 micron orifice has only one dominant frequency with in the usable FFT domain. This frequency is 9.5 hz. Looking at the pattern of the 30 micron and 50 micron orifice flashing data, the frequency peaks are twice the frequency of the next lower frequency peak. The 100 micron orifice data is shown in Figure 5.28.

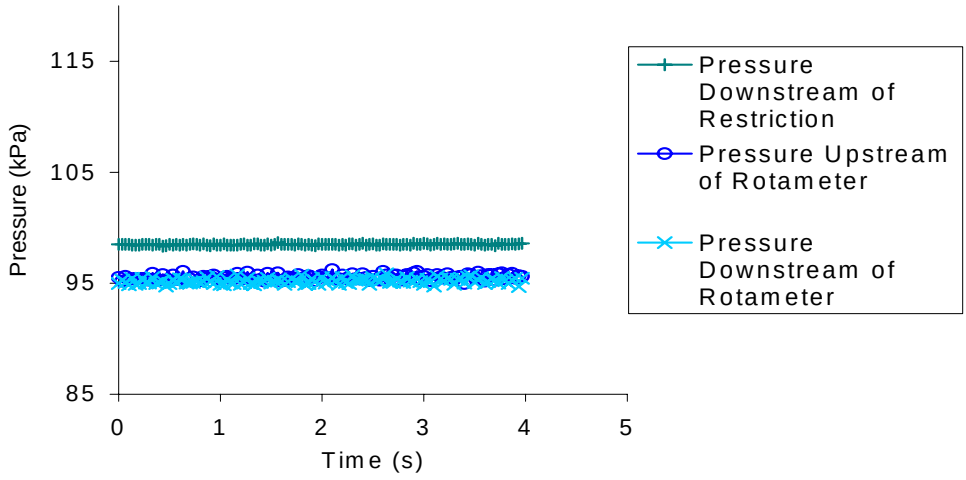

Figure 5.28 Plot of downstream pressure variations using a 100 micron orifice and flashing fuel.

All of the orifices flashing flows seem to have a periodic interruption in the predominant pulsation frequency and a 3 frequency peaks for the two smaller orifices. This characteristic does not exist in the nitrogen flow. The most likely candidates for this phenomenon are the engine operation and the flashing of the fuel as these are the two events that are absent in the nitrogen data. This frequency phenomenon is more complex in the metering valve as shown in Figure 5.29.

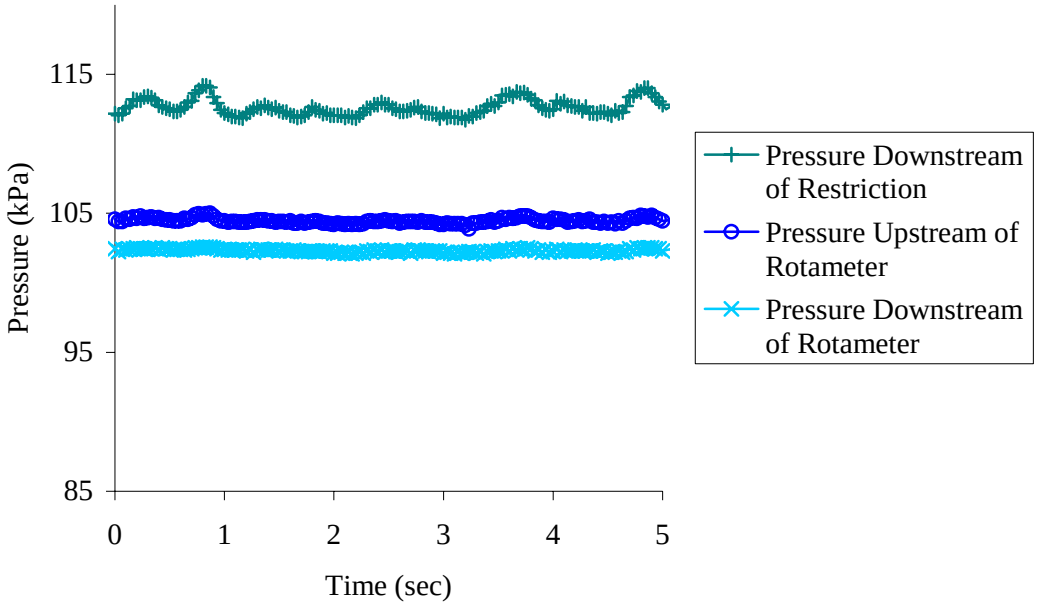

Figure 5.29 Plot of downstream pressure variations using a metering valve and flashing fuel.

The metering valve has more complex geometry and heated fuel relative to the saturated tank temperature. The geometry and heated fuel conditions promote more complex flow through the throat of the restriction than the orifice. The result is evident in the downstream of restriction pressure trace that shows variations in the amplitude and frequency that is not seen in the orifice pressure trace. It is therefore not a surprise that the pressure pulsations are more erratic when viewed on a time history plot as shown in Figure 5.29. No discernable resolution to the source of the frequency production or

pressure variations are evident aside from an extrapolation of the effects seen by the orifice into more complex geometry flow and higher saturated fuel temperatures than the tank temperature that produce two-phase flow.

At the end of the investigation, the root cause of the pulsations is still not explicitly clear. The two most likely causes are not the sole root cause. The engine intake events are at a different and faster frequency. The pulsations still exist without the flashing of the fuel when dry nitrogen is used. The flashing fuel increases the magnitude of the variations so flashing is important to variations. The point of the flashing fuel is at the flow restriction. Therefore, the flow restriction is the most likely candidate for causing the variations. This cause would also allow for an increase in amplitude given flashing flow when compared to pure gaseous flow as well as additional pressure variation frequency peaks. Given this lack of clarity and the alignment of the flashing fuel frequency through a 50 micron orifice similarity to the flow of dry Nitrogen through a 50 micron orifice and no similarity to the other flashing frequencies, an investigation into flow dynamics was completed. This search produced investigation into the Strouhal number. This number is a dimensionless parameter that relates the frequency of vortex shedding to the flow characteristics. The Strouhal number is dependant upon the flow regime and thus related to the Reynolds number. The Reynolds number noted for the flows of this work is on the order of 1000. The equation to translate the average velocity of the fuel into a vortex shedding frequency for an orifice is given below (21).

$$St\# = \frac{\omega * D_h}{v_{fluid}} \tag{10}$$

For the orifice sizes of this work, the numbers align as shown in Table 5.1. The Strouhal number must be compared with research that investigated the vortex shedding of a small orifice on the order of 50 microns with gaseous and flashing flow at the flow rates of this work. The Reynolds number of the flow of this work falls in the region of eight hundred to two hundred thousand. At this flow regime, the flow has a low and high

frequency Strouhal number. This could be a source, alternative to engine intake events, of the variation in the sinusoid pressure variations (21). That investigation is beyond the scope of this research.

Table 5.1 Calculated Strouhal number based on observed data.

Orifice Diam (m)	Fluid Velocity (m/s)	Observed Freq (Hz)	Strouhal Number
0.00003	103.98	4	0.0001
0.00005	37.89	5	0.0002
0.00010	9.36	8	0.0015

As a result of the investigation of the pressure variations, it is determined that the phenomenon viewed in the dry Nitrogen data and accentuated in the flashing fuel flow data is caused by vortex shedding off of the flow restriction.

5.7. UNCERTAINTY

The quality of the data is an important consideration to determine the reliability of the above results. An uncertainty analysis for some of the results is presented below. These results are further adjusted via an uncertainty multiplier derived from the error of measurement from the applicable sensor, DAQ unit, or display device. The multiplier is an adjustment of standard deviation to relate the deviation to a confidence level. This confidence level provides a number that gives a bracket around the mean. The confidence level is a statement about the certainty that data will fall within the confidence bracket. This multiplier is a step in the uncertainty analysis that is applied to the standard deviation to adjust the anticipated range to confidence intervals based upon sample size.

The first measurement that has large variability in the measured data is the flow rate measurement. The rotameter data reveals that the flow rate fluctuated over 80 % of the full measurable scale of the rotameter at the most extreme variability. These large

variations were the result of higher vaporized flow rates. The magnitude of the flow variation does diminish for smaller vaporized flow rates. Also, higher flows showed the ability to freeze the downstream vapor fuel line, the fuel may not be completely flashing at high vaporizing flows due to the extremely cold temperature of the heat exchanger and thus flashing in the downstream vapor fuel line. This flashing at high flows could cause larger pressure pulse amplitudes. As a result, the standard deviation for the data at the higher flow rate is larger than the mean. Variation also stems from the pressure variation discussed previously. This variability does not mean the data are irrelevant as the flow is simply variable. The measurement data presented with the standard deviation of the means of several test runs is shown below in Figure 5.30. The standard deviation is higher than the mean. This shows how much variation is in the flow through the flashing device.

An uncertainty analysis is not conducted because the method of data acquisition and the flow characteristics were not compatible. Essentially the limited scope of the research did not allow for fast data acquisition of the flow rate. The option of measuring flow via a rotameter did not allow the measurement to be taken fast enough to capture all of the fluctuations in the cycle. As a result, the data points in the average flow rates can be from any point in the varying cycle. Therefore, the random points can only be averaged and the standard deviation is a measure of the cyclic variability. To reiterate, this does not mean the measurements are inaccurate. It simply means that only variability can be captured due to the inability to capture variation cycles to compare for uncertainty. The result of this limitation does not allow for uncertainty to be conducted on the flow rate data. As a result of the variability, this data does not provide significant insight into a comparison between the flow model and the actual flow for the fuel system. Figure 5.30 shows the standard deviation range bars on the mean flow value as discussed previously. As is evident in the plot of Figure 5.30, no discernable trend in the data can be realized.

The variable flow data is also a result of visual observation of the instrument via the subjective observer eye. Freezing the outside of the rotameter, which makes accurate measurements impossible, further exasperates this condition. The space between the external acrylic tube and the interior glass flow path would freeze from ambient

humidity. This frost was not accessible to be cleaned during testing. The cause of the freezing was the higher cooling supplied by higher vapor flow rates.

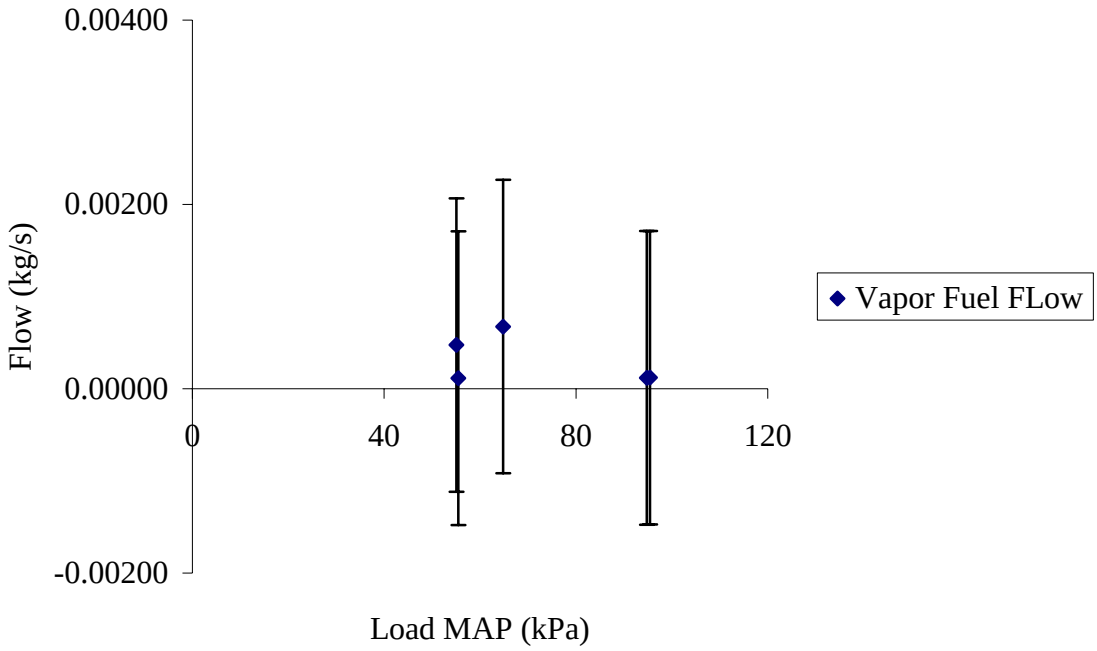

Figure 5.30 Magnitude of the uncertainty of the vapor flow rate relative to the average flow rate.

The additional cooling was not fully utilized in the heat exchanger and thus the exhausted vapor flow from the heat exchanger to the flow meter was cold enough to freeze the ambient humidity onto the rotameter as shown in Figure 5.31. Therefore, the only data available is on lower vapor flow test conditions. Additionally, the previously discussed pressure fluctuations caused oscillations in the rotameter measurement that permeated the remaining low flow data.

The next set of variable data is recorded by the DAQ and therefore offers more insight into the quality of the data. This data references the pressures of the fuel system. While there are noticeable fluctuations to the pressure data, the standard deviation is not larger than the mean. Also, the DAQ system allows the data trends to be captured and variability to be measured within each data set. As a result, uncertainty can be calculated using the mean of variability from multiple data sets. The standard deviation of the data

variability is 0.02 times the mean for high pressure measurements and 0.2 for low pressure measurements. A measurement uncertainty factor is applied to the average of the mean values of the variable data sets. These pressure data and uncertainty range bars are evident in Figures 5.32 and 5.33.

Figure 5.31 Picture of the frozen rotameter.

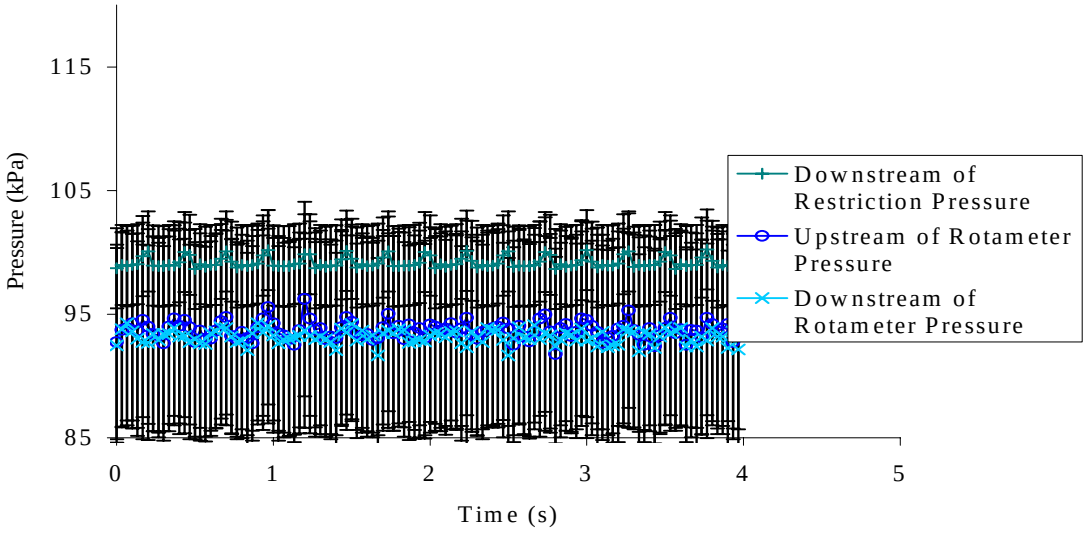

Figure 5.32 Figure showing down stream pressures with uncertainty range bars.

The uncertainty numbers for Figures 5.32 are 3.24 kPa for the Downstream of restriction data and 7.87 kPa for both of the pressure sensors adjacent to the rotameter. The variation of the data within a test run is between 1 and 1.5 kPa for all three pressure sensors.

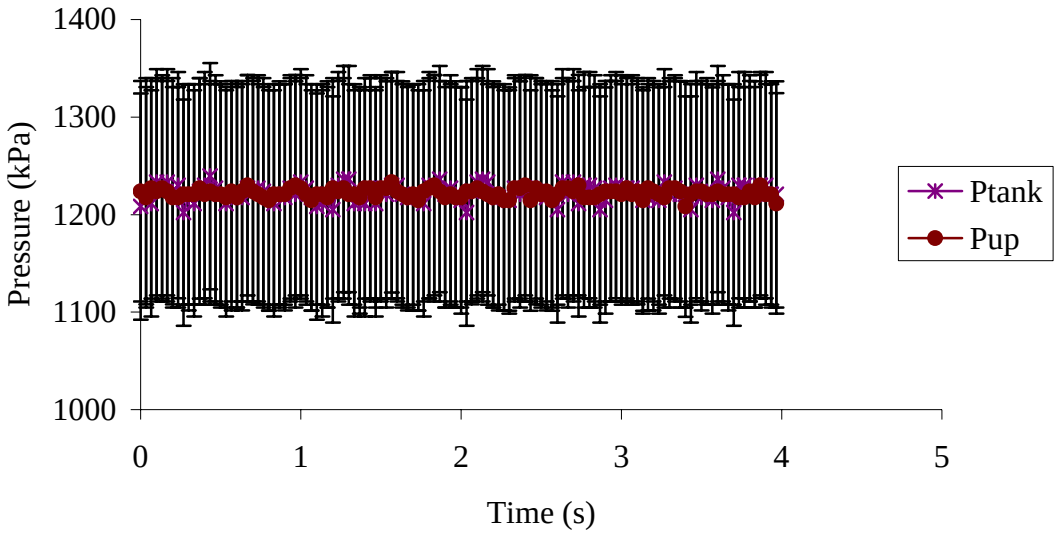

Figure 5.33 Figure depicting the upstream pressure variations with uncertainty range bars.

The uncertainty numbers in Figure 5.33 are 116 kPa for the tank pressure and 113 kpa for the pressure upstream of the flow restriction. The variability with in the data set is 124 kPa for the tank pressure and 42 kPa for the pressure upstream of the flow restriction.

The downstream of the flow restriction pressure region shows a lower mean and is therefore subject to a larger standard deviation relative to the mean. Also, the amplitude of the downstream pressure fluctuations are on the same order of magnitude as the upstream pressure variations. It is important to note that the pressure data upstream is reliable by virtue of a large mean relative to the uncertainty. The upstream pressure drives the flow through the pressure restriction more than the downstream pressure. This

pressure is also important in considering the saturation condition at the injector. The upstream pressure is reliable.

Fortunately, the temperature data is the most steady data that has been acquired in this research. After applying uncertainty, the error range of the data is orders of magnitude less than the resolution of a degree of temperature as shown in Figure 5.34.

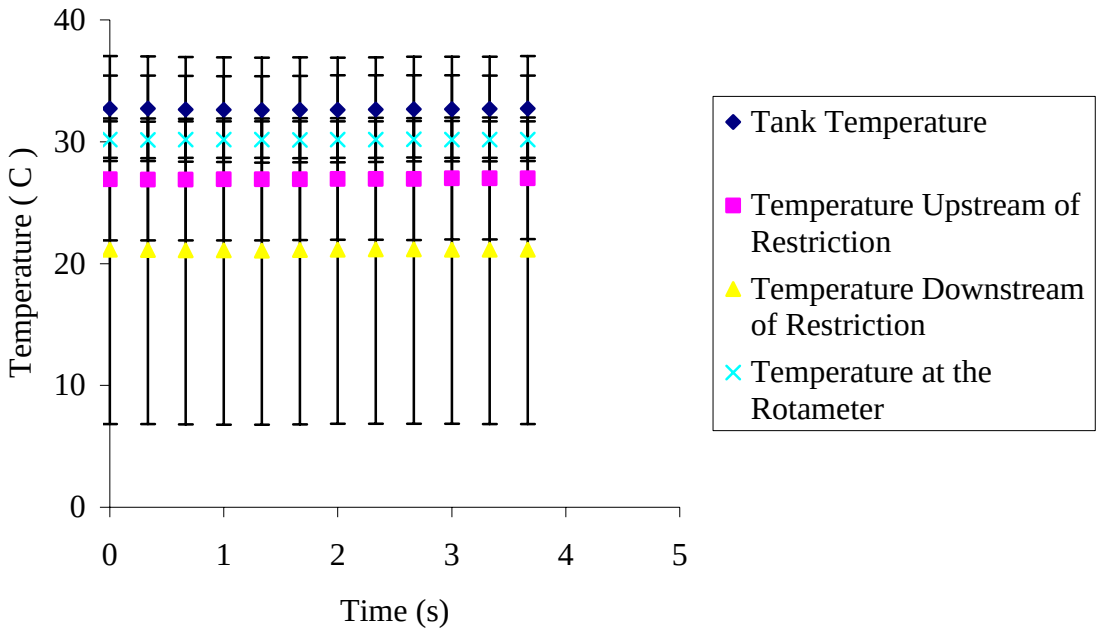

Figure 5.34 Figure showing the DAQ temperatures, with uncertainty range bars, employed to validate the fuel system requirement of –5 K injector temperature relative to the tank temperature.

The uncertainty numbers in Figure 5.34 are all between 1.5 and 5 degrees Celsius except for the temperature immediately after the flow restriction. This temperature has an uncertainty of 14 degrees Celsius. The variability with in the data set is between 0.16 and 0.25 degrees Celsius.

Therefore, the data that reveals the temperature at critical locations is reliable. Most importantly, temperature data that measures exhaust temperatures and intake manifold temperatures are also stable. This realization validates the claims of fuel system

effectiveness on lowering the intake charge temperature as the exhaust temperatures are rising. Additionally, the fuel system conclusions are supported by the stable temperature data. The measurement locations required for the conclusions of this work are the upstream temperature, the tank temperature, and the injector temperature. These data locations are shown in the Figure 3.5 above. The stability of these Temperature and upstream pressure data sets show that the initial assumption of saturated fuel is released from the fuel tank. Then, the injector temperature at that saturation pressure is stable and as discussed earlier is sub-cooled by 5 degrees Celsius so that it is liquid at the injector. Additionally, the assumption of liquid before the injector can be verified to validate the use of the Bernoulli equation to approximate vaporizing fuel flow. As discussed previously the upstream of the flow restriction temperature is also sub-cooled and is dependable via the small variations that are experienced during acquisition.

In addition to the data that was taken with the DAQ unit, the data that was recorded by hand are investigated with an uncertainty analysis. This is done to investigate the reliability of the charge cooling of the intake flow relative to the exhaust temperatures. Figure 5.35 shows the post-injection temperature in the intake manifold with standard deviation bars. These data points are the result of manual recording like the flow rate.

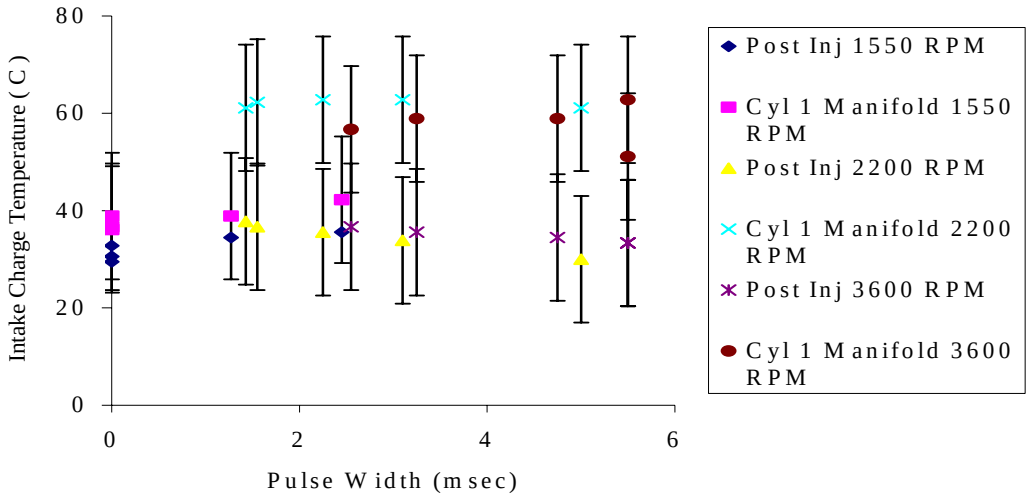

Figure 5.35 Plot showing the standard deviation of the intake manifold temperature data.

The other pivotal plot from the validation discussion for the heat exchanger and thus a thermally controlled liquid propane fuel injection system is the effect of the exhaust. Figure 5.35 shows the variation of the data that shows a reduction in the intake manifold as load is increased on the engine. Figure 5.36 shows the variation of the data that shows the increasing environmental temperature of the exterior of the intake manifold given increased engine load.

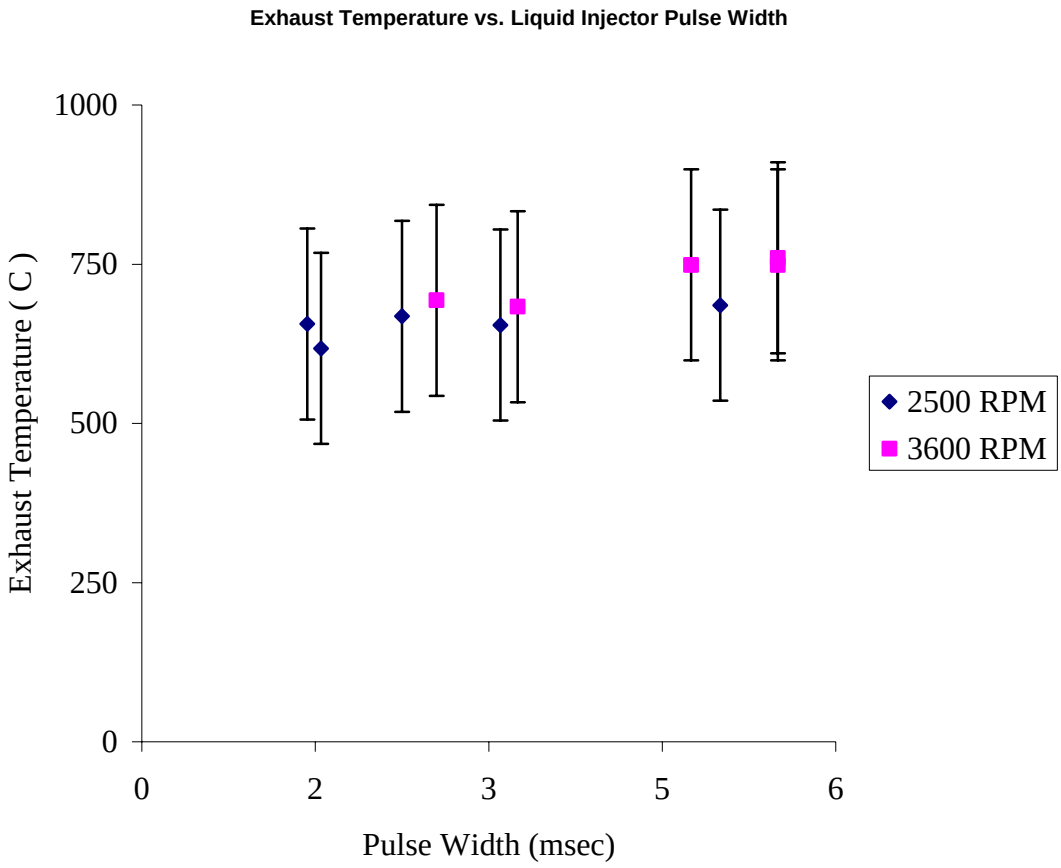

Figure 5.36 Plot showing the standard deviation of the exhaust temperature data.

The uncertainty analysis demonstrates the variation of the data that has been used to validate a sacrificial cooling heat exchanger concept for a liquid injected propane system. The tank pressure that drives the saturation condition of the fuel in the saturated sections of the fuel system is stable enough to produce a saturation pressure to which a

requisite temperature can be calculated that would ensure liquid at vital locations such as the injector and immediately before the flow restriction. Additionally, the temperature data is also very stable and as a result the temperatures that are 5 degrees Celcius lower than the saturation temperature reliably denote a liquid condition. Therefore, the conclusions made in this research about the viability of this fuel system concept are reasonable given the stability of the data.

6. CONCLUSIONS

The use of temperature subcooling to enable liquid LPG injection has been shown. The fuel distribution issue is minimized for the inherent bias of the unbalanced V-twin engine. The liquid injection of the fuel is referenced against pure vapor flow with high mixing for determination of fuel distribution. The flashing flow concept is able to maintain liquid at the injector as the goal of maintaining an injector temperature that is 5 degrees Celsius below the tank temperature is accomplished. Moreover, 70% of the resultant flow of fuel is supplied as a liquid at WOT where cooling is most beneficial. Liquid injection supplies the cooling that allows a temperature drop in the intake manifold temperature of 5 degrees Celsius from idle to WOT given a rise in exhaust temperatures of 50 degrees Celsius through the same conditions. Also, the fuel system is interfaced with a computer to control the injector given ambient temperature of the intake manifold and the manifold pressure. The fuel system can accommodate a metering valve or an orifice as the vaporizing device. These vaporizing devices have been studied and modeled using the Bernoulli equation. The Bernoulli equation can predict the average flow rate of the flashing device.

Currently the system is not a stand-alone fuel system that can be applied to existing or production engines. The computer for the injector does not have the capability to adjust the pulse width of the injector for a change in fuel pressure brought on by a change in temperature to the saturated fuel in the tank. Also, the fuel system demonstrates pressure and flow rate fluctuations in the vapor flow line. These fluctuations alter the fuel air ratio in the intake manifold and create instability in engine operation. Moreover, the fuel system has not been tested for start up conditions. This is an extremely important qualification for a liquid LPG system to become a viable fuel system. This all leads to work that still needs to be done on the development of a thermally controlled liquid LPG system.

7. FUTURE WORK

The first issues that should be addressed by future work on the fuel system are those in the steady state. The fuel system computer should be further developed to adjust pulse width for changes in fuel pressure i.e. tank temperature. This requires the development of a three dimensional fuel table to replace the current two-dimensional table. Testing this issue requires temperature control of the entire fuel system. This can be cost intensive if a climate chamber is required. Also, the flashing device is subjected to the same pressure issues and can be tested in a similar method of controlled temperature. Moreover, the flashing device can be a metering valve that can be automated and controlled by the fuel system computer. This is again verified by the same testing already described. Another issue of the steady state should address the variability to the air fuel ratio of the engine given the flow rate variability caused by pressure fluctuations in the fuel system. The engine intake pressure pulses must be better isolated from the flashing device and a more in depth study of the flashing process should occur for a more stable fuel system.

The transient response of the fuel system is the final stages of making the system viable for operation. This task is formidable considering all of the conditions that must be addressed for any given start-up condition. The most typical are cold start and hot-soak delay start. These conditions do not allow assumptions of liquid phase of the fuel at any point in the fuel system. Moreover, the hot soak delay assumes only vapor in the liquid line to the injector as hot soak assumes engine heat has boiled all the fuel after an engine shut down.

The system warrants further development as the current system offers solution possibilities to all of the future work concerns. Simple verification testing can build a three-dimensional fuel map for the injector and the flashing device. The pressure fluctuations can be minimized with surge tanks and an array of small flow flashing devices in place of the larger single device. Investigation can find pressure fluctuation sources in the fuel system as well. Finally, the transient solution could simply be to open a metering valve further and the injector to provide enough vapor flow under the tank pressure to satiate rich starting conditions for an engine.

APPENDIX A.
MODEL CODE

```
!ccccccccccccccccccccccccccccccccccccccccccccccccccccccccccccccccccccccccccc
!       Vaporization Flow Model for Single Component(Propane) Two-Phase
!       Critical Flow Through an Orifice.
!       Brian Applegate
!       11/03/2005
!       This is the article of my thesis that will soon be directly linked
!       to my sudden loss of sanity.  Hopefully, there will not be too many
!       innocent victims slaughtered on my psychopathic rage and I will be
!       subject to an expedient trial and subsequent execution.
!ccccccccccccccccccccccccccccccccccccccccccccccccccccccccccccccccccccccccccc

implicit none

!       Declare variables

Real    Tin, mapv, Ttank, Tinj, Tup, Pup, Tdown, Pdown, mdotmin, size
Real    avevel, Pabs, Mass, Blackbox, Prints, Trns
Character loop

!       Get into main program loop

loop = 'y'
do while (loop .ne. 'n' .and. loop .ne. 'N')

!       Ask for user input

        print *,'Prepare to be awestruck by the intense brilliance that'
        print *,'is about to be bestowed upon you.  You should thank God'
        print *,'that the intellectual prowess of the programmer is'
        print *,'buffered by the mediocre limitations of computer'
        print *,'programming.  Otherwise, your brain would certainly melt'
```

```
      print *,'down from attempting to maintain such an elevated,'
      print *,'enlightened level of consciousness that is required to'
      print *,'even contemplate the depth of genius of this fearless'
      print *,'programmer.  Quite honestly, however, your head would not'
      print *,'melt down but, deflagrate upon the moment of interaction'
      print *,'with such perception, insight, and wisdom.'
      print *,'Please input intake air temperature in K.'
      read *,Tin
      print *,'Please input the manifold absoulte pressure in kPa.'
      read *,mapv
      print *,'Please input the tank temperature in K.'
      read *,Ttank
      print *,'Please input the injector temperature in K.'
      read *,Tinj
      print *, 'Please input the absolute pressure in kPa.'
      read *,Pabs

!     This is the black box input for the model of the orifice

      print *,'Please input the upstream propane temperature in K.'
      read *,Tup
      print *,'Please input the upstream propane pressure in kPa.'
      read *,Pup
      Pup = Pup*1000
      print *,'Please input the downstream propane temperature in K.'
      read *,Tdown
      print *,'Please input the downstream propane pressure in kPa.'
      read *,Pdown
      Pdown = Pdown*1000

!     This is the subroutine that will return the minimum mass flow
```

```
!       requirement for orifice to produce.

        call Mass (Tin, mapv, Ttank, Tinj, mdotmin, Pabs)

!       This is the subroutine that is my Houdini magic trick.  It is
!       the black box of the model I am referencing for a base model.

        call Blackbox (Tup, Pup, Pdown, mdotmin, size, avevel, Trns)

!       This is the subroutine that I will use to print my output.

        call Prints (Tup, Pup, Tdown, Pdown, size, avevel, Trns)

!       This is the question to the user about rerunning the program

        print *,'Do you want to go again Pilgrim?'
        read '(a)', loop

        do while (loop .ne. 'n' .and. loop .ne. 'N' .and. loop .ne. 'y' .and. loop .ne.
'Y')

                print *,'Try again genious'
                read '(a)', loop

        end do

!       End main loop

end do

!       End main program
```

```
end

!ccccccccccccccccccccccccccccccccccccccccccccccccccccccccccccccccccccccccccccc

!       This is the subroutine that will calculate the minimum amount of
!       vaporizing fuel that is required to satiate operating conditions.
!       The larger value of the two parameters idle fuel flow versus fuel
!       flow required for WOT cooling will be returned as the minimum fuel
!       flow parameter.

subroutine Mass (Tin, mapv, Ttank, Tinj, mdotmin, Pabs)
implicit none

Real    Tin, mapv, Ttank, Tinj, mdotmin, Cp, HOV
Real    wotsp, wotload, engspI, engspW, mairI, mairW, mfuelI
Real    mfuelvapW, mfueltotW, Qdot, Qeff, Pabs, voleffI, voleffW

!       First calculate fuel flow requirements for an engine setpoint at A/F
!       ratio of 13.01.  Designate another subroutine since this is used again
!       for WOT case.  This returns the minimum mass fuel flow rate for idle
!       speed combustion.  Idle is a MAP of ~2V ~~54.8 kPa.  This

        voleffI=0.1815 ! --flow data
        engspI=1550

call fuel (Tin, mapv, mfuelI, voleffI, engspI)

!       Now recall that subroutine so that the combustion fuel flow requirement
```

```
!       is known for the WOT case.  This is only the total fuel flow for the
!       engine combustion, not the amount of vaporizing fuel needed to cool the
!       liquid fuel line.

        voleffw=0.778 ! --flow data
        engspW=3600

call fuel (Tin, mapv, mfueltotW, voleffW, engspW)

!       This the part that uses the engine fuel requirement for WOT to calculate
!       a mandatory vaporizing fuel flow requirement to maintain liquid at the
!       injector.  This assumes none of the vaporizing fuel will enter the engine
!       so that a conservative estimate of the orifice size will result ensuring
!       that liquid will be maintained at the injector.  Moreover, the vaporized
!       fuel percentage is on the order of 1 % of the fuel flow in this case, so
!       the assumption is reasonable.


!       Find the heat sink of the liquid fuel as a rate
!       Find the mass flow rate in copper tube given volume (ID of copper tube)
!       Use mass flow rate, Cp, and delta T to approximate Qdot

        Cp=2.54         !  1.679 is Cp in kj/kg*K
        Qdot=(mfueltotW*(Ttank-Tinj)*Cp)*1.4      ! Loss to environment

!       Use Qdot and Heat of vaporization to determine necessary fuel vaporized
!       assuming no losses.  Add a heat transfer gain from surrounding of about
!       1/0.8 times the Qdot.

!       Get fuel vaporized vaporized
```

```
        HOV=425.31  ! HOV is in kj/kg
        mfuelvapW=Qdot/HOV

!       Compare idle fuel vs. vapor requirements (kg/s)

        if (mfuelI > mfuelvapW)  then
                mdotmin = mfuelI
        end if
        if (mfuelvapW > mfuelI)       then
                mdotmin = mfuelvapW
        end if

!       return mass of fuel to main to be used in the black box subroutine

print *,mfuelvapW
print *,mfuelI
end subroutine Mass




!ccccccccccccccccccccccccccccccccccccccccccccccccccccccccccccccccccccccccccccccc

!       This is the subroutine that calculates fuel requirements for combustion.

subroutine fuel (Tin, Pabs, mf, voleff, engsp)
implicit none

Real    voleff, mair, Pabs, mf, AF, engsp, volair, Tin

if (engsp > 2000) then
```

```
        AF = 13.01
        else
                AF = 14.67
        end if
volair=(engsp/(2*60))*.000494*voleff
mair = volair*(Pabs/(.287*Tin))
mf = mair/AF

end subroutine fuel



!ccccccccccccccccccccccccccccccccccccccccccccccccccccccccccccccccccccccccccccc

!       This is the subroutine that calculates the orifice size

subroutine Blackbox (Tup, Pup, Pdown, mdotmin, size, avevel, trns)
implicit none

Real    Tup, Pup, Tr, Pdown, mdotmin, size, avevel, Tc, sig
Real    vf, vg, SIGMA, volume, tension, rof, Trns, Pi
Real    A, B, D, dAdz, dout
Double Precision K, C, C1, C2, A1, A2, Areaf, Ai, SIGMAi
Double Precision delta, Pf, temp, ref

!       Define Constants and terms used in the equation
Tc      =       369.8
Tr = Tup/Tc
!       K = 1.380658 * (10**-23) need to pre-root K to not get a zero

K = 0.000000000003715       !3.71572065688*(10**(-12))
```

```
!       Call the subroutine that will return the liquid and vapor phase
!       specific volumes.

Call Volume (Tup, Pup, vg, vf)

!       Call the subroutine that will return the surface tension parameter
!       and the liquid density parameter before the restriction

Call tension (Tup, sig, vf, rof)

!       This is the Bernoulli estimate of the flow area for liquid propane as
!       it is assumed to be saturated liquid that will flash after the
!       restriction.  This estimate will be used to benchmark the solving
!       equations.  This is all set in a loop to allow convergence of effective
!       area calculation

Ai = mdotmin/sqrt(2*rof*(Pup-100000))       !1000kg/m*s^2 = kPa
dout = 2*(sqrt(Ai/3.141596))
print *, dout
!       Typical valve height at the moment is the average from dA/dz.

dAdz = 0.000039

!       This is the pressure reduction equation (3) from the published model
!       that has been solved for the depressurization rate.  It is broken
!       into components for easier debugging.

B = (K*sqrt(Tc))/(sig**1.5)
C1 = 1-(vf/vg)
C2 = Tr**13.73
```

```
C = C1/C2
D = 1/0.8

Areaf = 0.000000001
delta = 1
ref = 0.0000000001
do while (delta > ref)

  SIGMAi =
((mdotmin**3)*dAdz)/(((rof**2)*(Ai**4))*((10**6)*101.325*1000))

!       Find the Pf value to then reverse and find final area.

  Pf = Pup-(0.253*((1/B)*(1/C)*sqrt(1+(14*(SIGMAi**0.8)))))

  A = (Pup-Pf)/0.253

  SIGMA = ((((A*B*C)**2)-1)/14)**D

!       This is the depressurization rate equation (4) from the published
!       model that has been solved for cross-sectional area.  Also, the dA/dz
!       term is 3.9*10^-5.  (4) is broken into components for debugging.

  A1 = (rof**2)*SIGMA*((10**6)*101.325*1000)  ! Units satiation
  A2 = (mdotmin**3)*(dAdz)
  Areaf = (A2/A1)**0.25

!       Find delta to check for loop

  temp = Areaf - Ai
  Ai = (Areaf+Ai)/2.0
```

```
  delta = abs(temp)

!       End loop

end do

!       This is the typical area of a circle equation to output orifice size

size = sqrt((Areaf*3.141596)/4)

!       This is the subroutine that is an extension of the trick for
!       a metering valve as opposed to a simple orifice.  The valve
!       is a swagelock ss-ss4.  Valve specific parameters are located in the
!       subroutine.

print *,mdotmin
call valve (Areaf, SIGMA, rof, mdotmin, Trns)

!       End this mystical montage of mesmerizing manipulations.

end subroutine Blackbox



!ccccccccccccccccccccccccccccccccccccccccccccccccccccccccccccccccccccccccccc

!       This is the subroutine that handles the case statements to find the
!       specific volume of the liquid and vapor phases.

subroutine Volume (Tup, Pup, vg, vf)
implicit none
```

```
Real Tup, Pup, vg, vf

!       Set upstream temperature to C from K for this subroutine

Tup = Tup - 273.15

!       Case statement to provide more accurate densities and specific
!       volume figures relative to user input.
!       All upstream temperature less than -30 degrees C are assigned
!       saturation figures for -30 C

if(Tup<-30)then
 vf=0.001763
 vg=0.02585
 Pup=1.677*101.325*1000

!       All upstream temperature less than -10 degrees C

 else if(Tup<-10)then
        vf=0.001844
        vg=0.1309
        Pup=3.451*101.325*1000

!       All upstream temperature less than 8 degrees C

        else if(Tup<8) then
         vf=0.001931
         vg=0.07666
         Pup=6.011*101.325*1000
```

```
!       All upstream temperature less than 24 degrees C

        else if(Tup<24)then
          vf=0.002024
              vg=0.04973
              Pup=9.278*101.325*1000
!       All upstream temperature less than 40 degrees C
              else if(Tup<40)then
               vf=0.00214
               vg=0.0331
               Pup=13.69*101.325*1000
!       All upstream temperature 40 C or above are assigned data for
!       60 C saturation

               else
                vf=0.00234
                vg=.02015
                Pup=21.16*101.325*1000
end if
end subroutine Volume



!ccccccccccccccccccccccccccccccccccccccccccccccccccccccccccccccccccccccccccccc

!       This is the subroutine that will extract a surface tension value from
!       a case statement as well as the liquid density value before the
!       restriction.

subroutine Tension (Tup, sig, vf, rof)
implicit none
```

```
Real Tup, sig, rof, vf

sig = 0.01594          !       In N/m for Propane at 15 degrees C
rof = 1/vf                     !       In kg/m^3

end subroutine Tension



!ccccccccccccccccccccccccccccccccccccccccccccccccccccccccccccccccccccccccccccccc

!       This is the subroutine that will calculate the turns out on a
!       metering valve for a given flow rate.  This is for the Swagelock
!       800771001 SS-SS4 metering valve.

subroutine valve (Areaf, SIGMA, rof, mdotmin, Trns)
implicit none

Real SIGMA, rof, mdotmin, TotalTrns, Trns, dA, alpha, Dnot
Real h, hmax
Double Precision Areaf

!       Solve the depressurization rate equation (4) for dA/dz.

dA=(SIGMA*(rof**2)*(Areaf**4))/(mdotmin**3)

!       Solve the dA/dz equation (5) for h which is the valve lift.  This
!       quantity will be used to find the turns out of the metering valve as
!       a function, relevant to a specific valve style, that describes lift
!       against turns on the valve (or radians).
```

```
hmax = 5.66/1000                    ! Measured valve lift 5.66 mm
TotalTrns = 12.5                    ! Valve specific -- literature says 10
alpha = 1*(3.141596/180)     !??? Valve specific -- literature says 1 degree taper
Dnot = 0.81/1000                    !??? Valve specific --literature says 0.81 mm

h=((2*(cos(alpha))**2)/(3.1415968*(sin(2*alpha))**2))*(((3.141596*Dnot*sin(a
lpha))/(cos(alpha)))-dA)

!       This is a personal magic trick that intends to accurately relate the
!       required valve lift to the physical number of turns on the valve
!       required by the valve to obtain that lift.  The first attempt is a
!       direct proportion of valve turns over total possible number of valve
!       turns related to lift required over total lift available.  The literature
!       supplies a flow coefficient vs. valve turns chart.  It is fairly linear
!       for valve turns greater than or equal to five so this approximation
!       should be acceptable

Trns = TotalTrns*(h/hmax)

!       End this marvelous subroutine

end subroutine valve


!ccccccccccccccccccccccccccccccccccccccccccccccccccccccccccccccccccccccccc

!       This is the subroutine that prints the data to the screen..

subroutine Prints (Tup, Pup, Tdown, Pdown, size, avevel, Trns)
implicit none
```

```
Real     Tup, Pup, Tdown, Pdown, size, avevel, Trns

print *, size,'     ',Trns

!        The future may encompass more fancy how do ya do formatting, but this
!        approach is functional and acceptable at this juncture.
!print 100 (size, avevel)

!100             Format ('O. size',size,'avg. vel.',avevel

!        End the printing subroutine
end subroutine Prints
```

APPENDIX B.
ORIFICE DATA

200 Micron orifice w/o injection

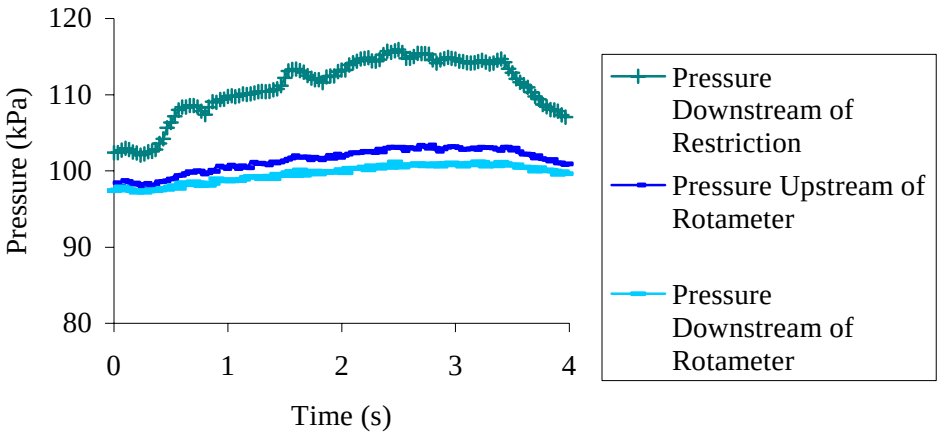

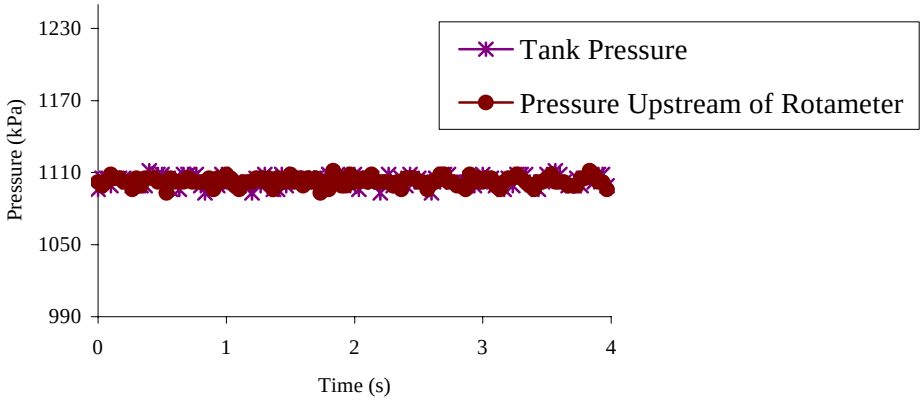

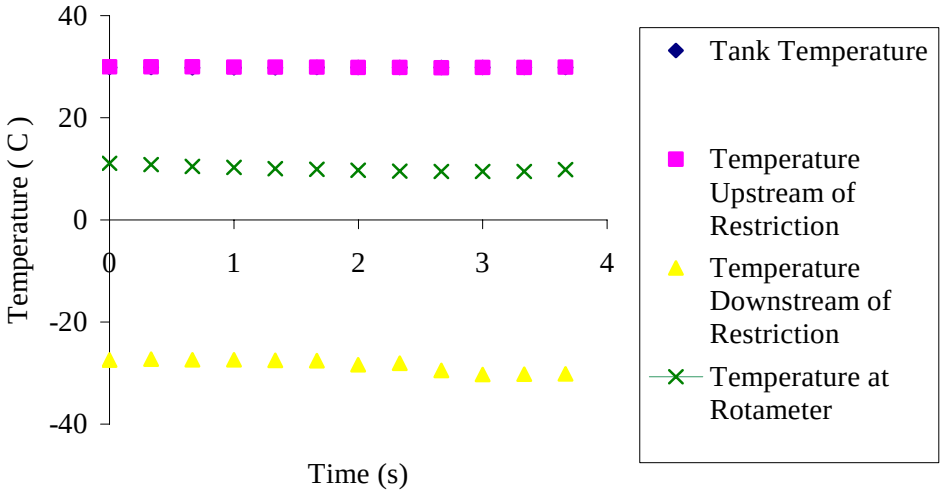

200 Micron orifice with injection

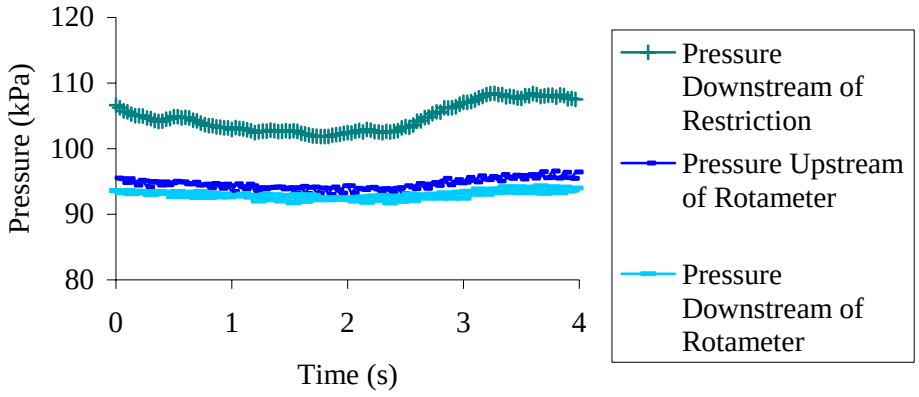

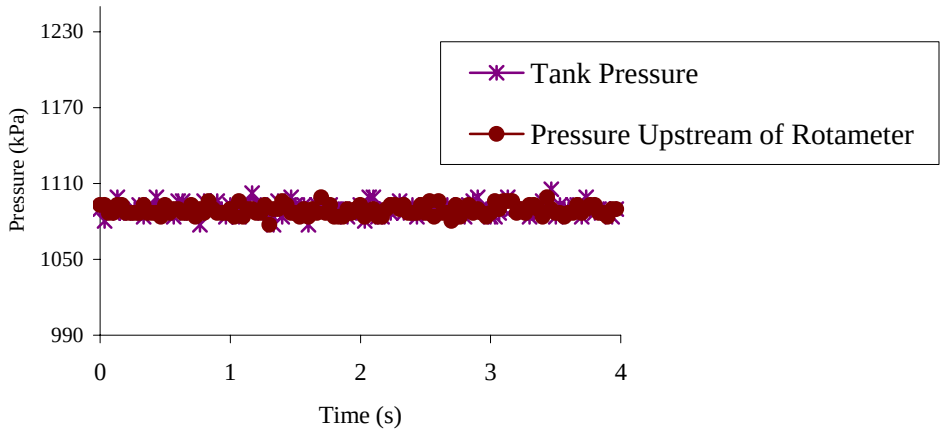

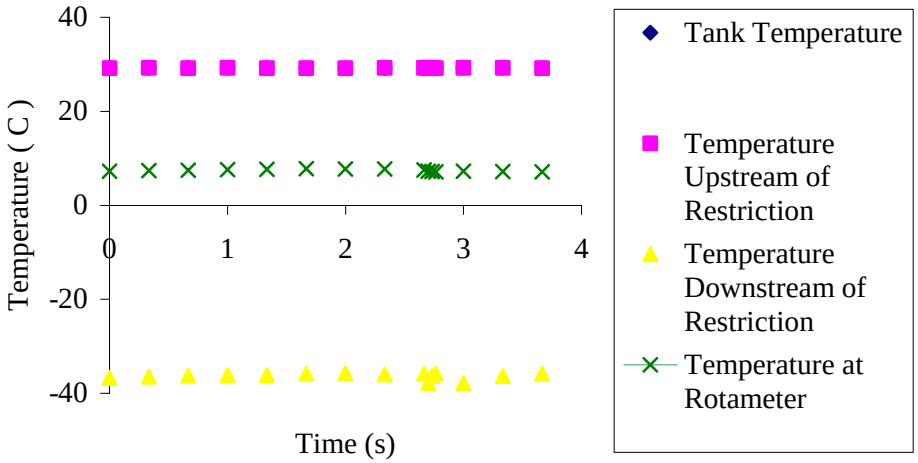

150 micron orifice w/o injection

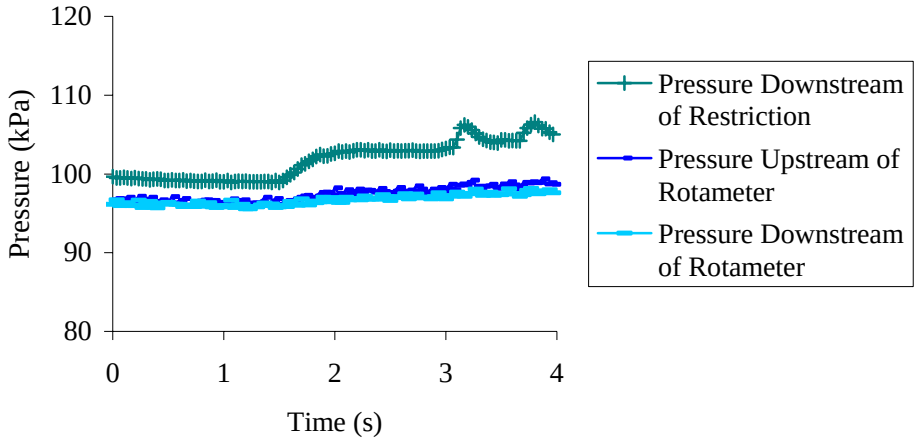

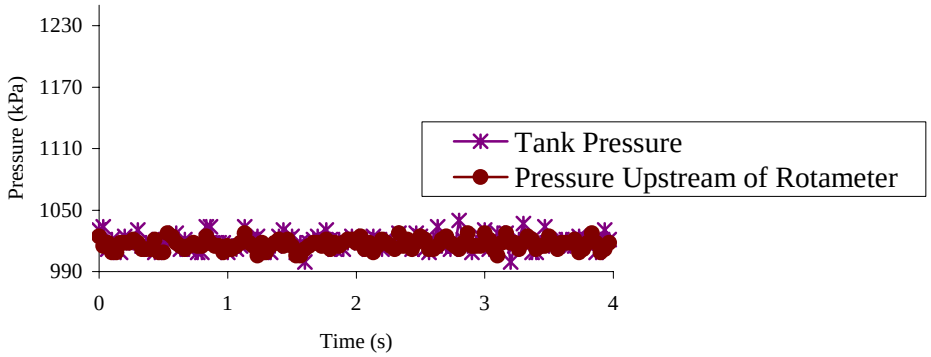

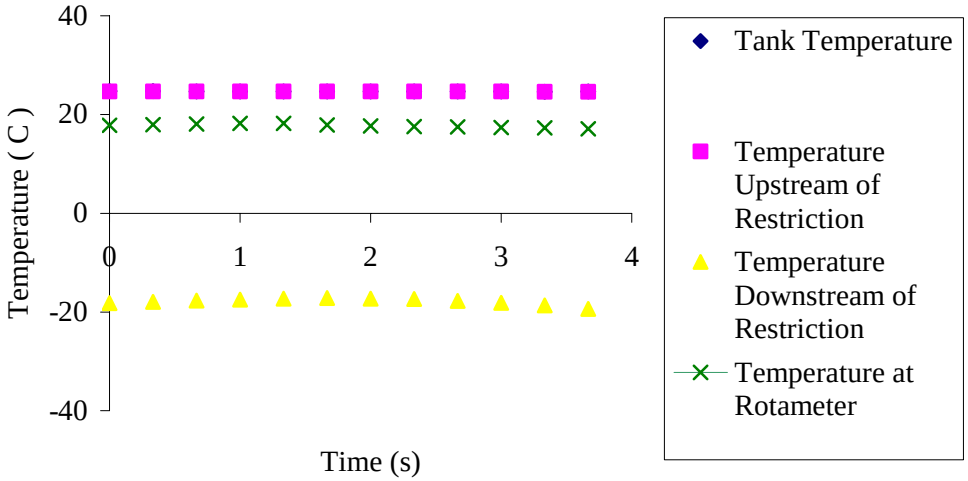

150 micron orifice with injection

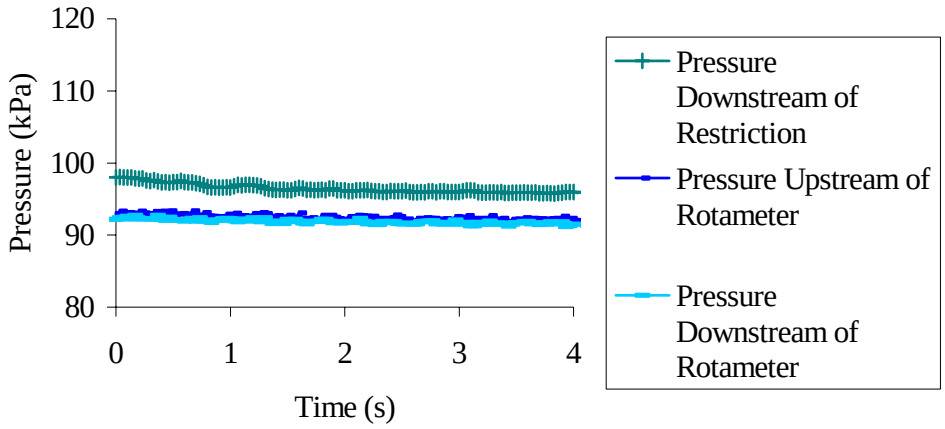

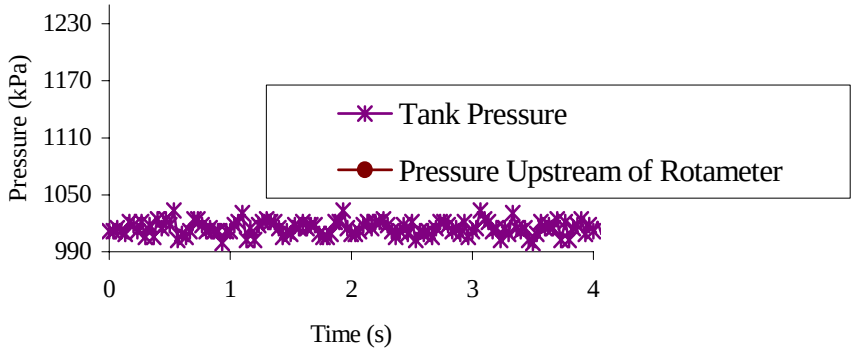

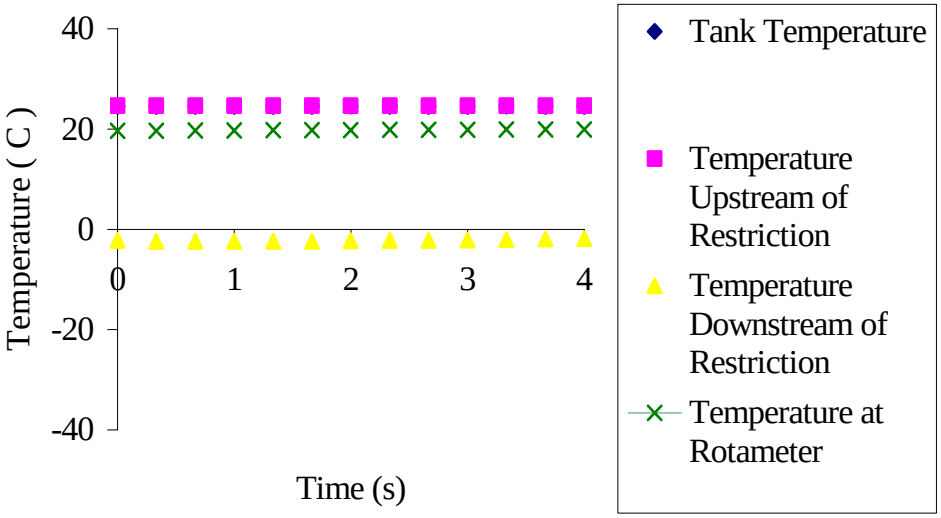

100 micron orifice w/o injection

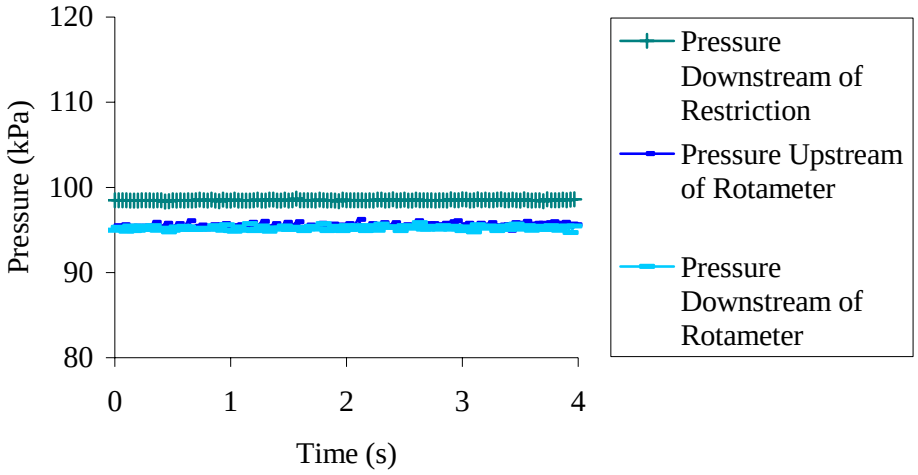

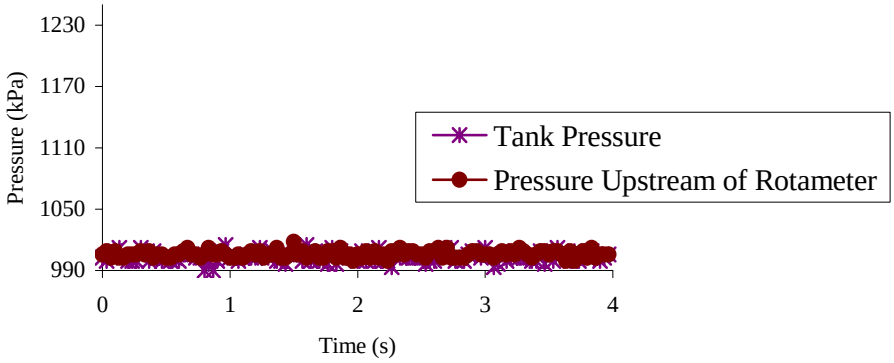

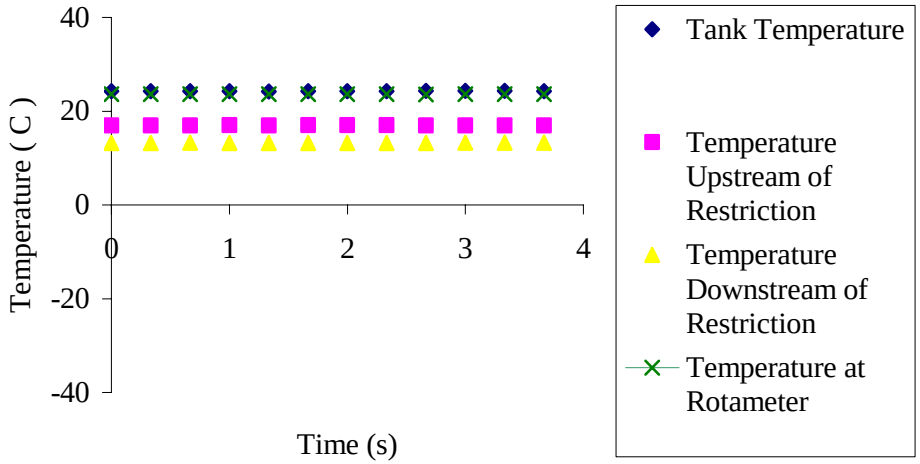

100 micron orifice with injection

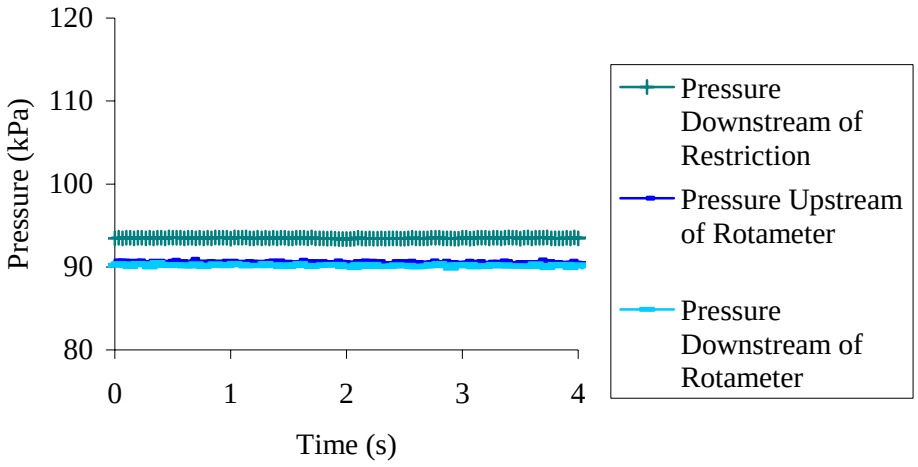

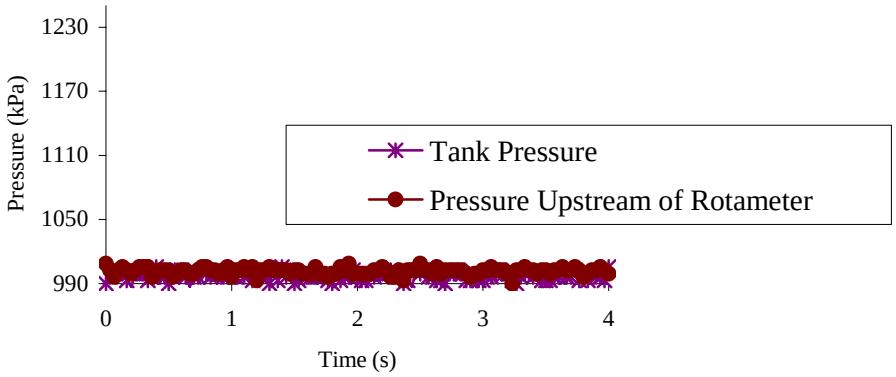

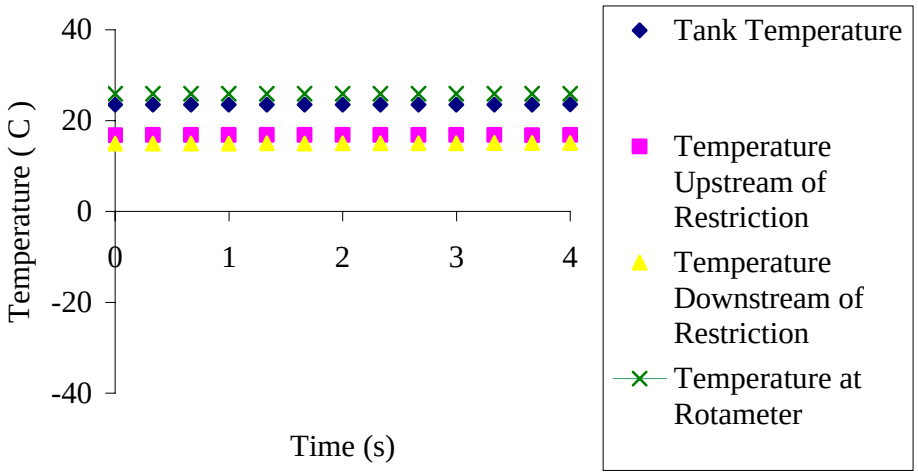

75 micron orifice w/o injection

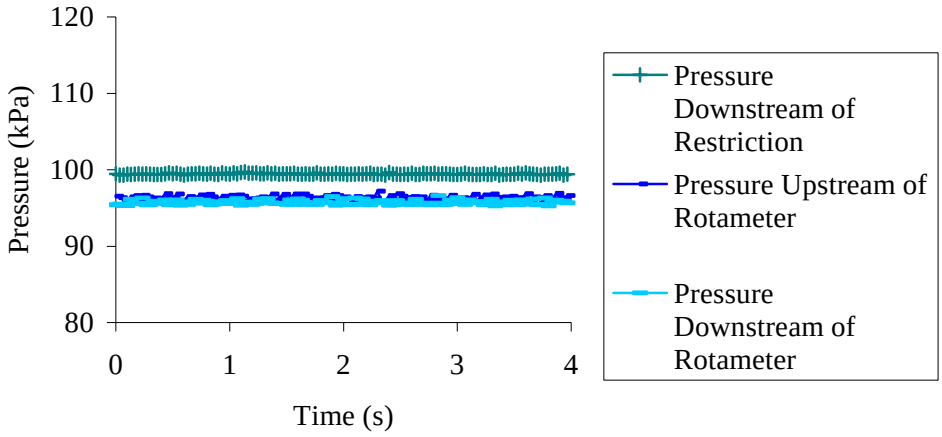

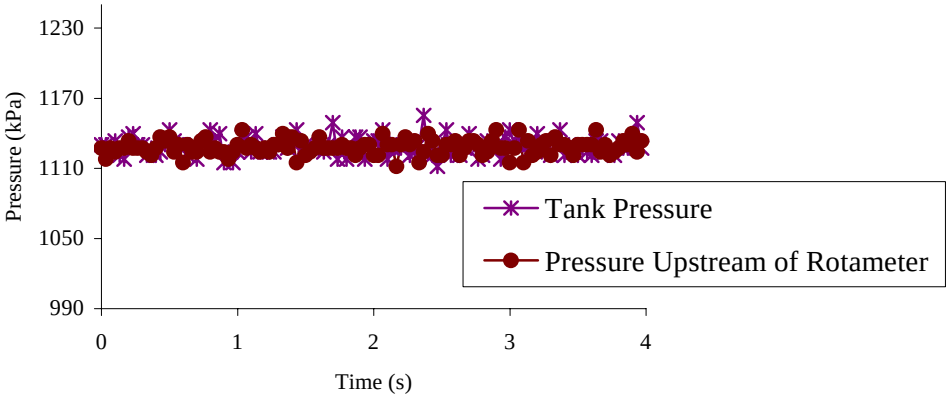

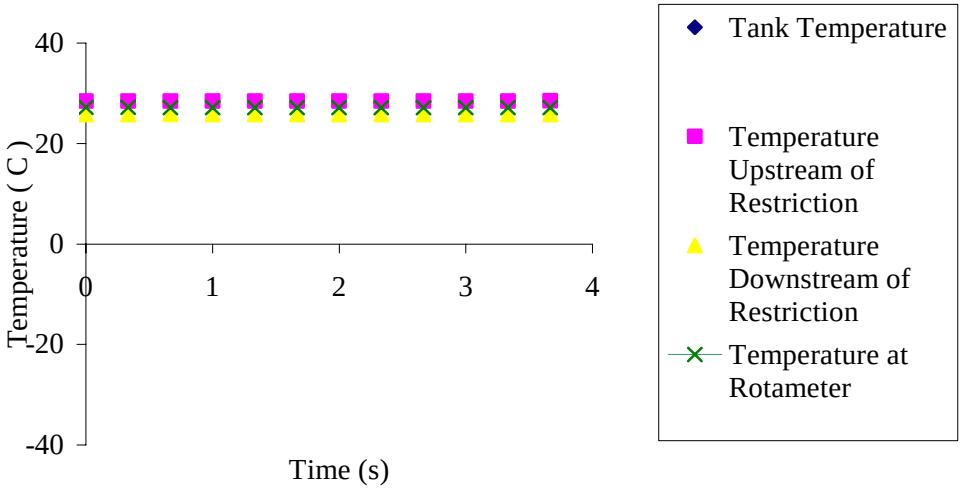

75 micron orifice with injection

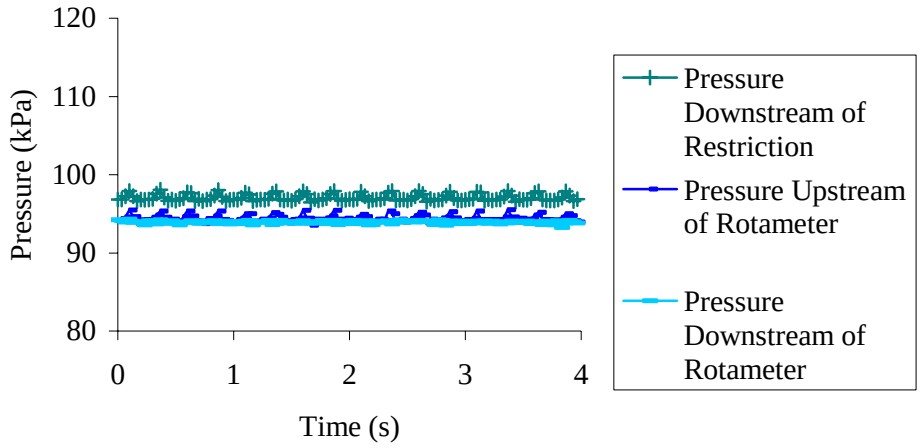

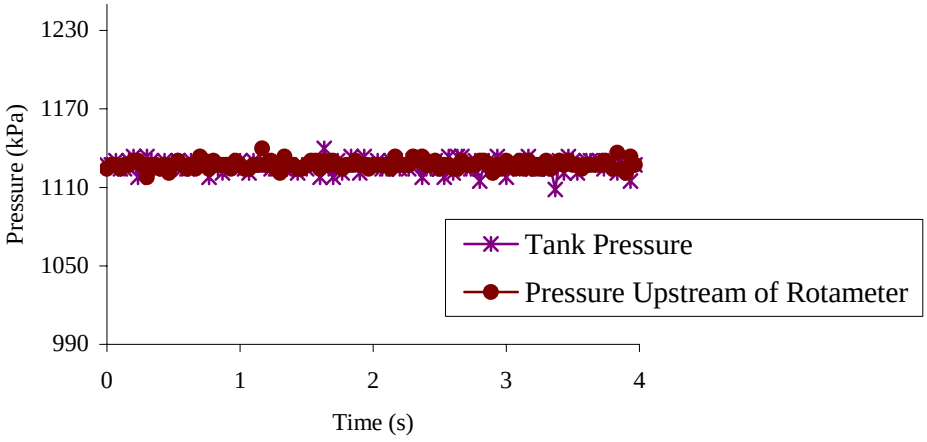

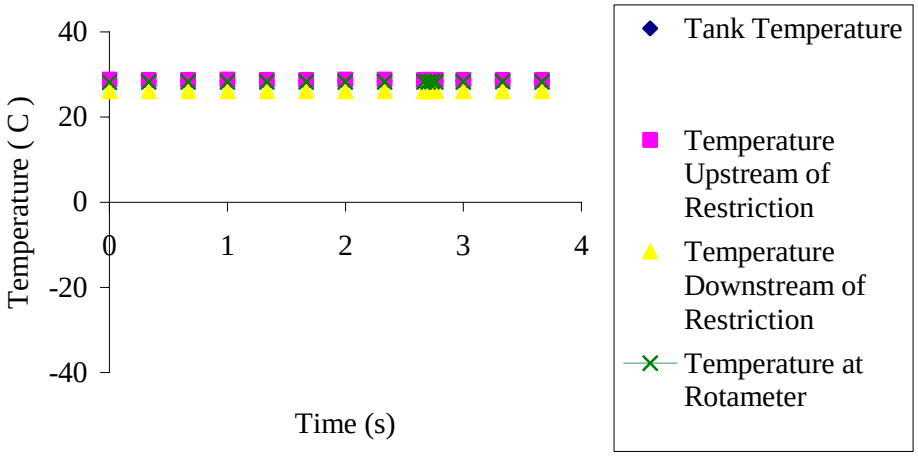

50 micron orifice w/o injection

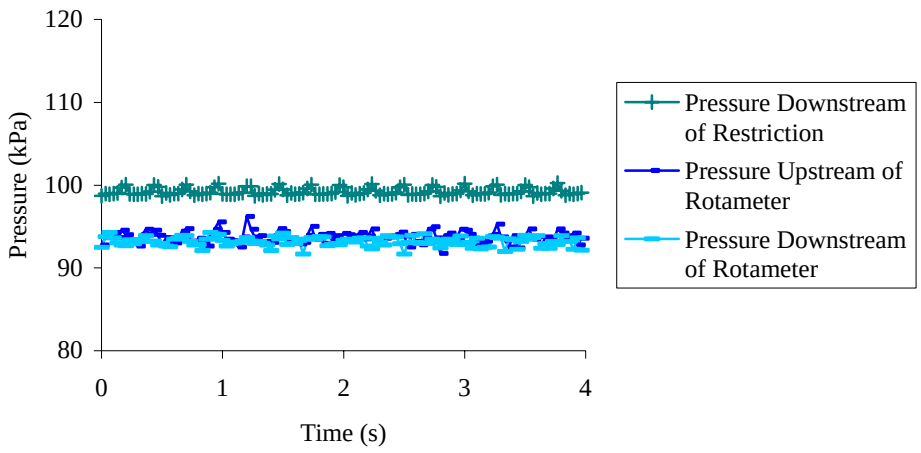

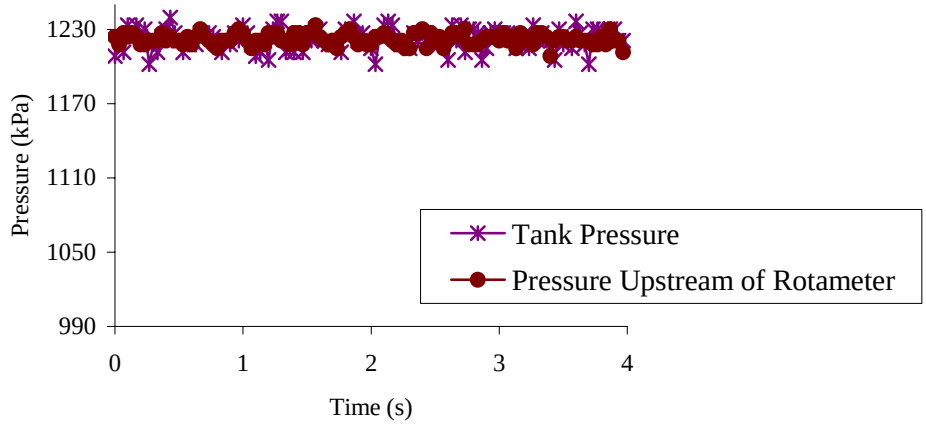

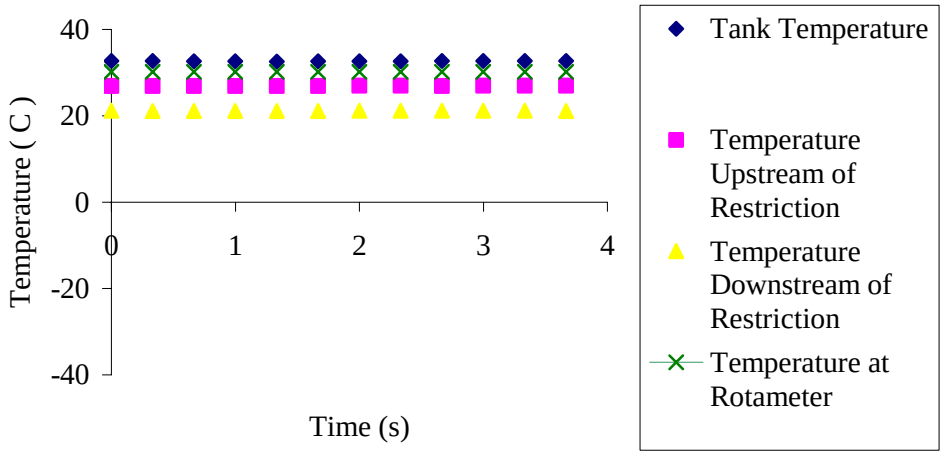

50 micron orifice with injection

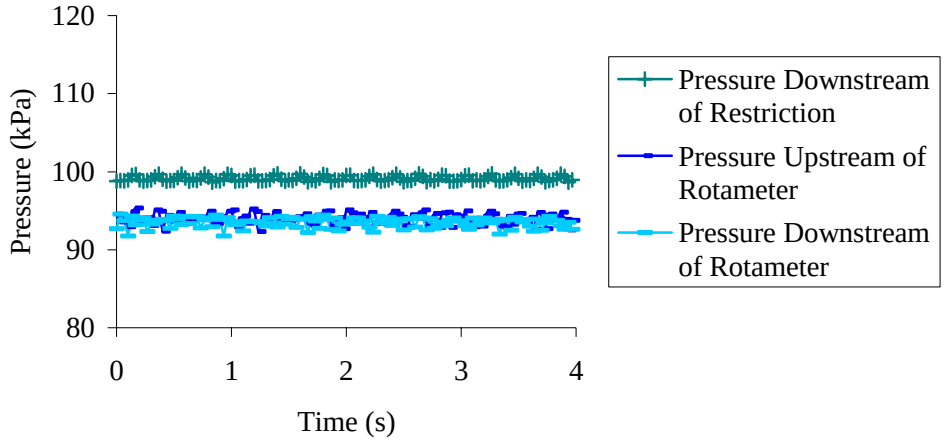

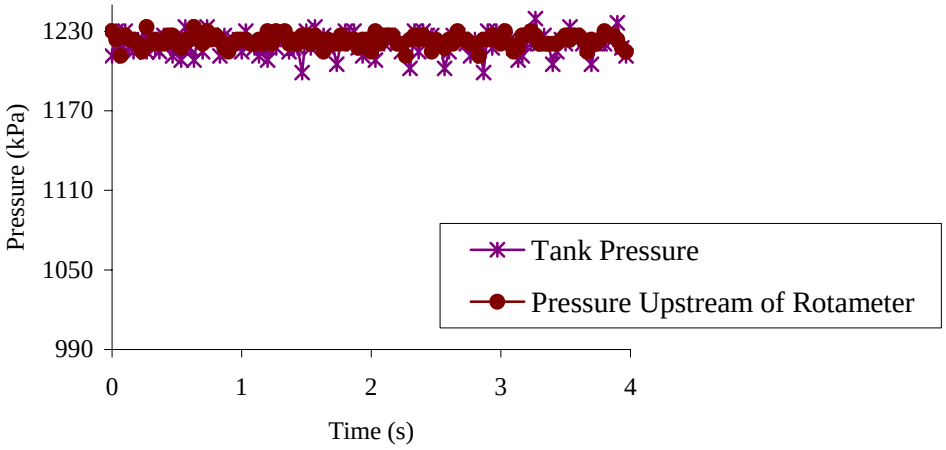

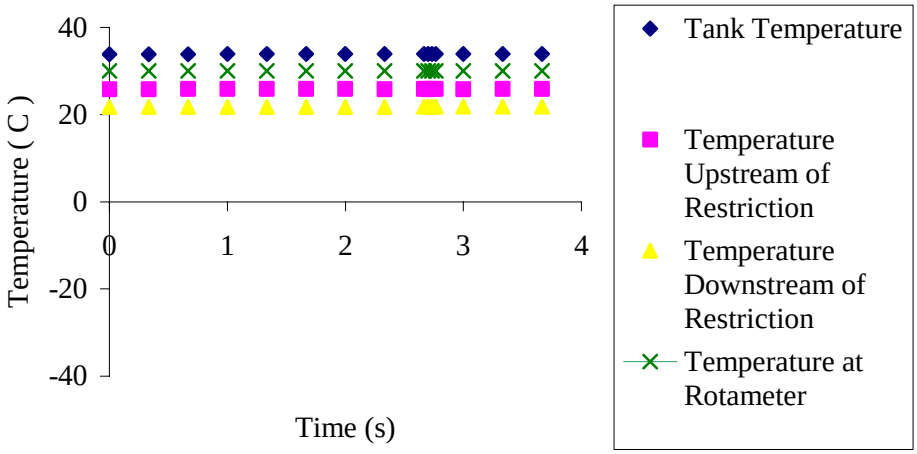

35 micron orifice w/o injection

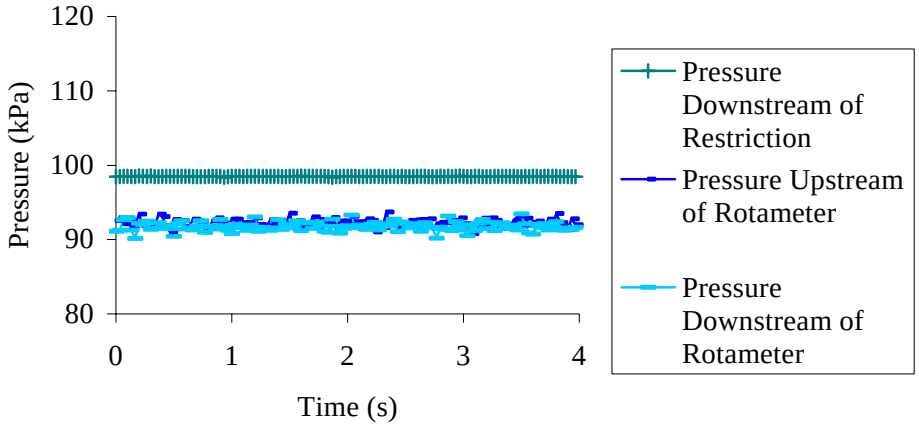

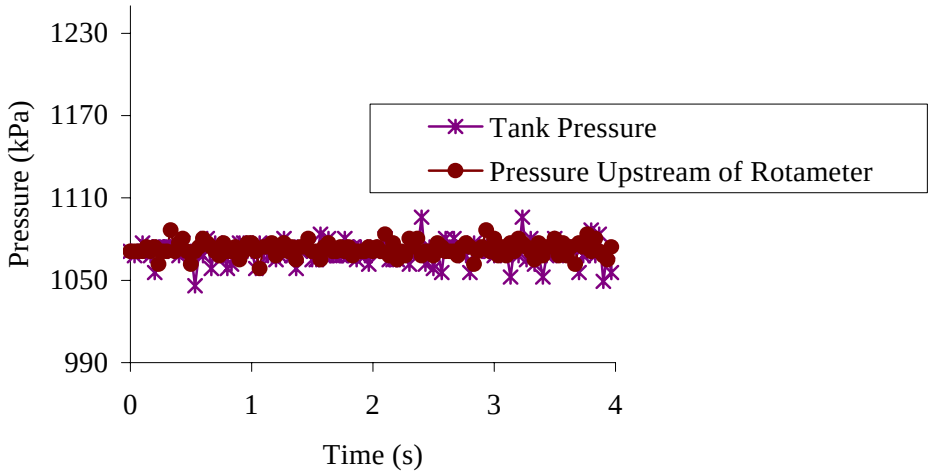

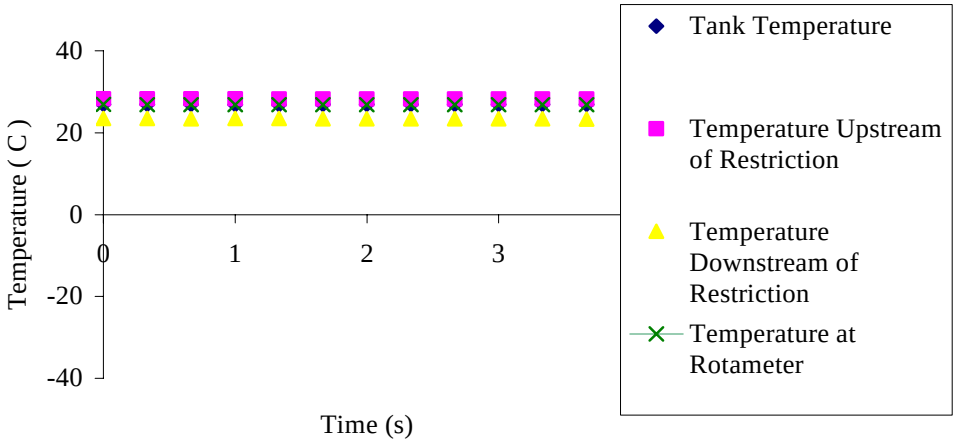

35 micron orifice with injection

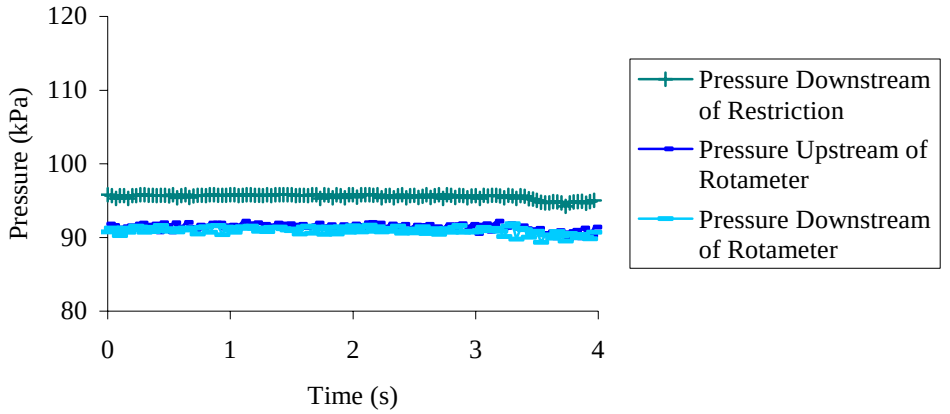

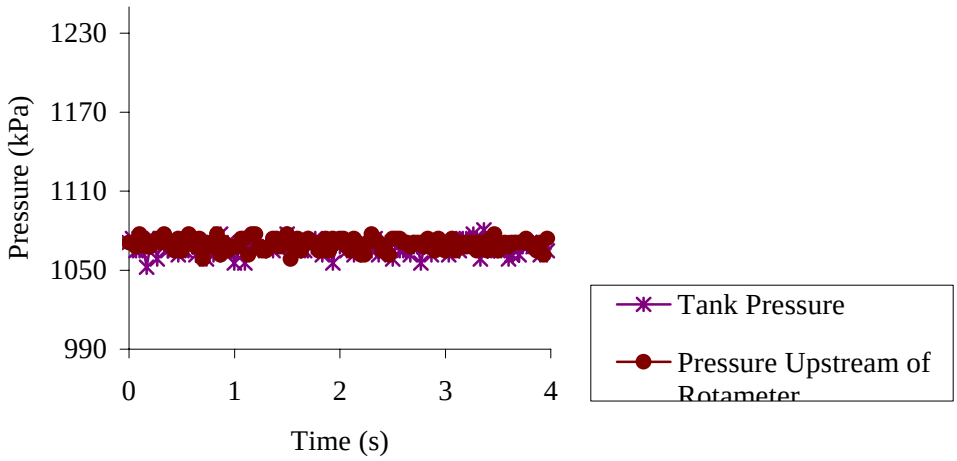

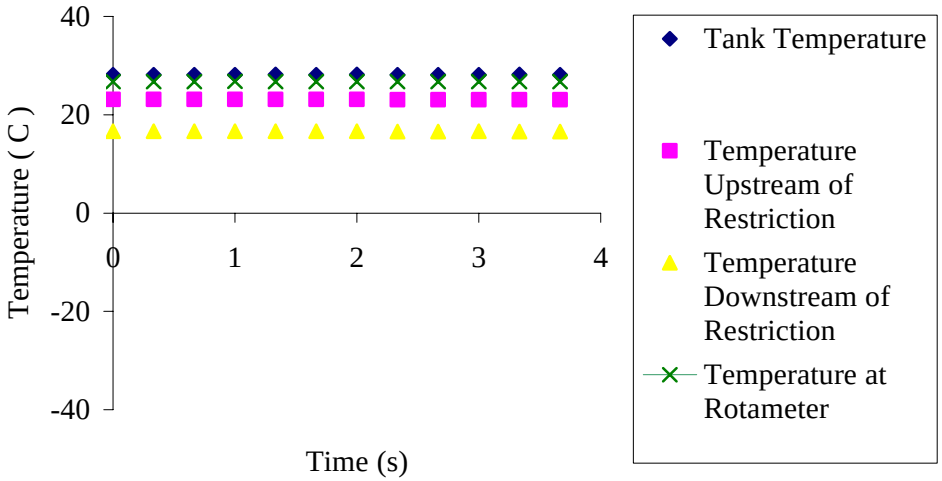

30 micron orifice w/o injection

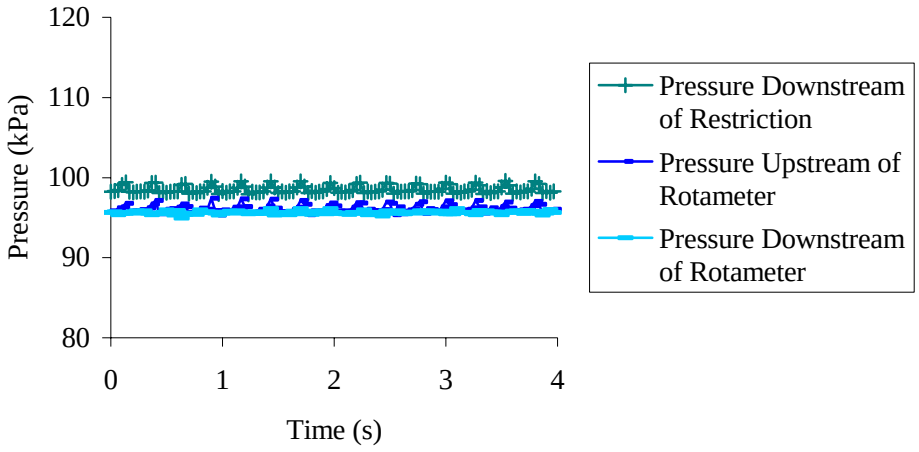

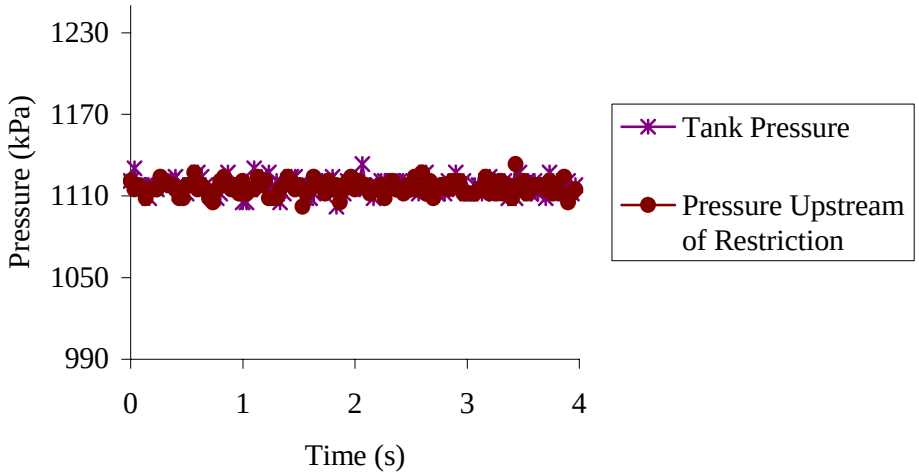

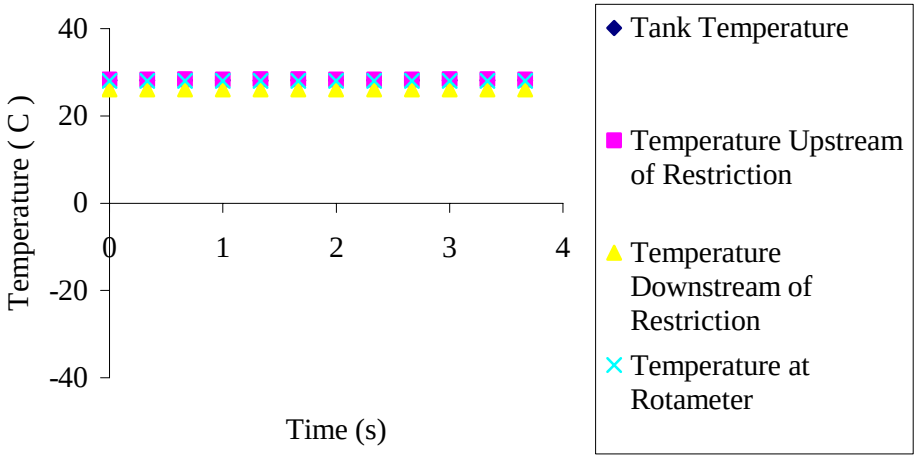

30 micron orifice with injection

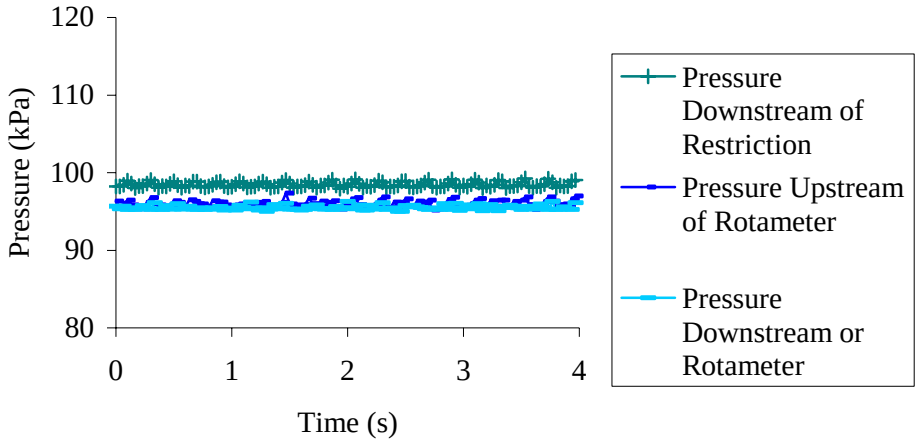

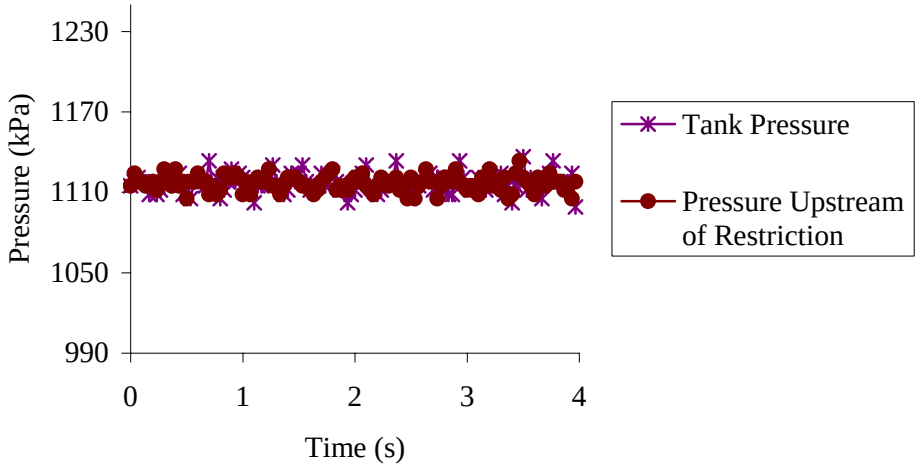

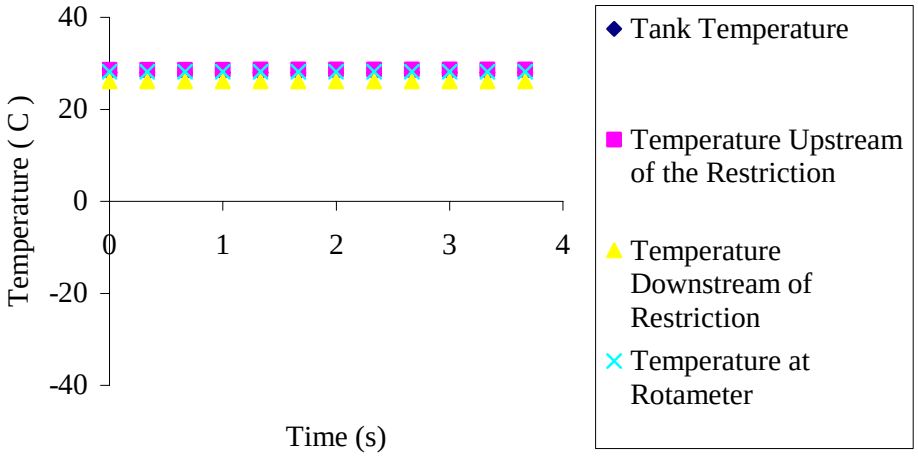

APPENDIX C.
METERING VALVE DATA

Metering valve w/o injection - closed

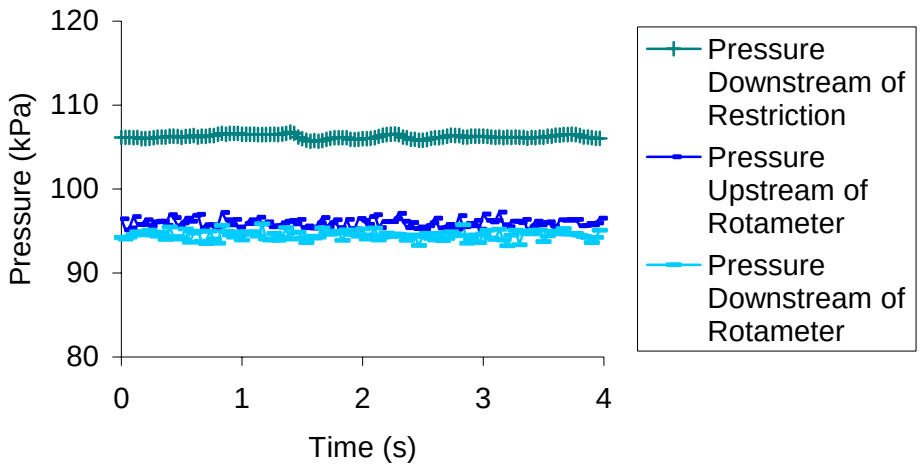

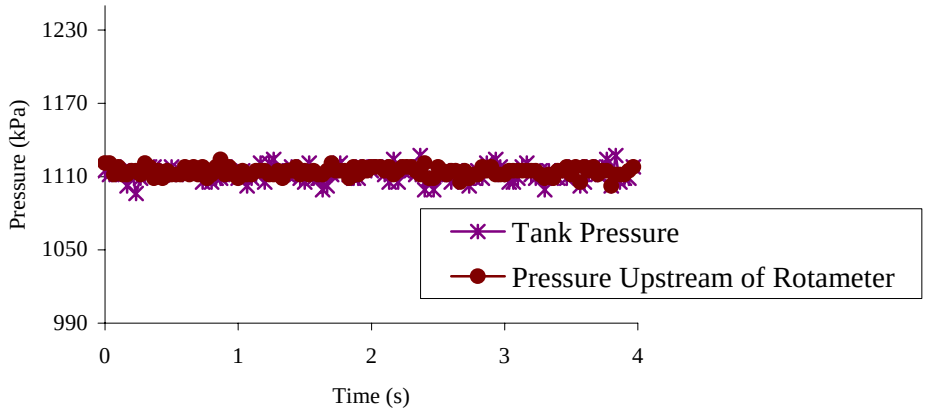

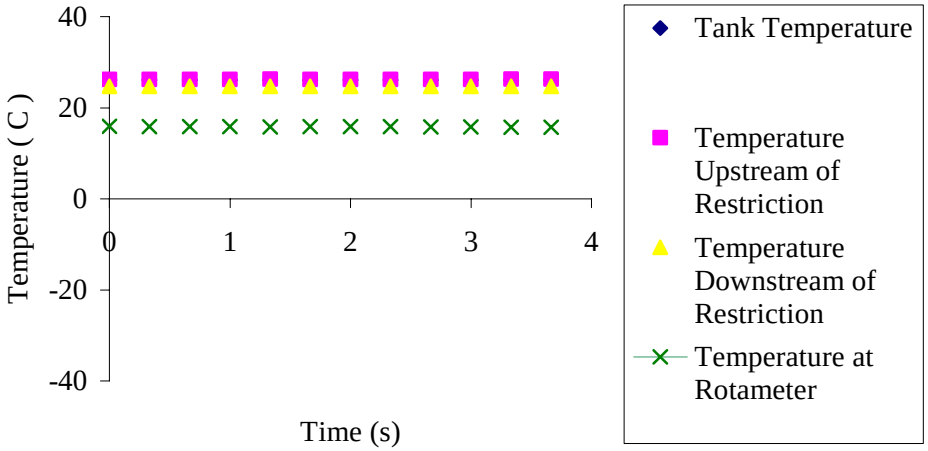

Metering valve with injection - closed

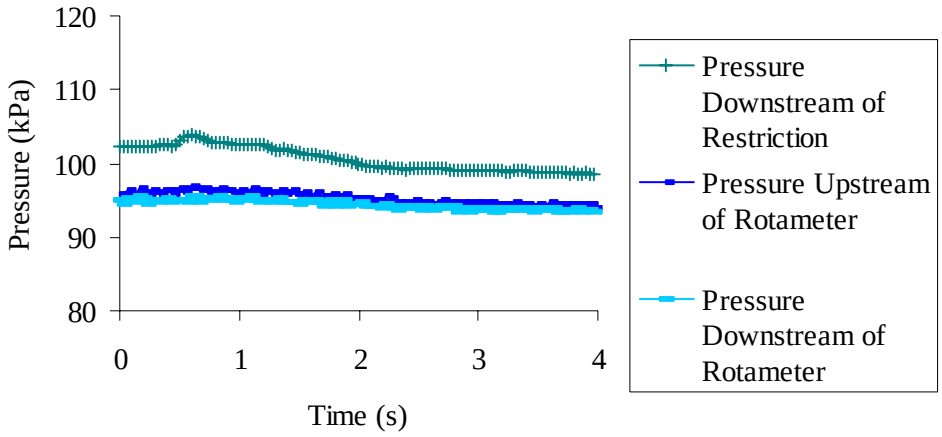

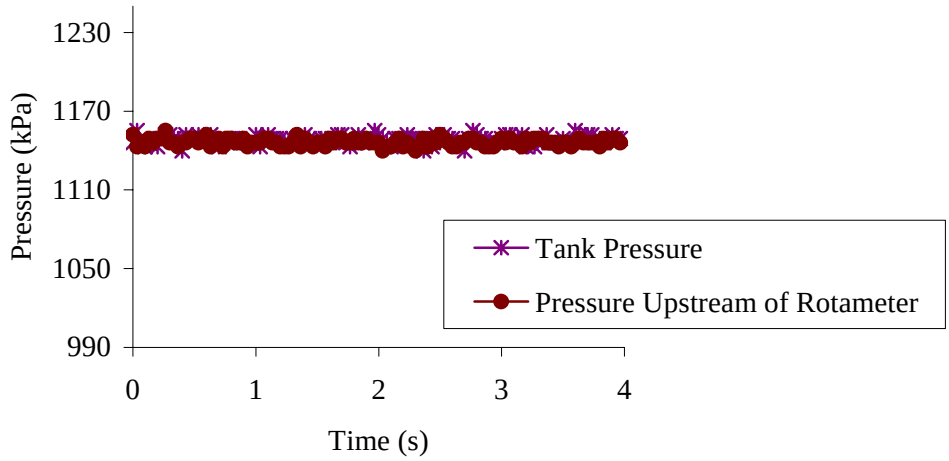

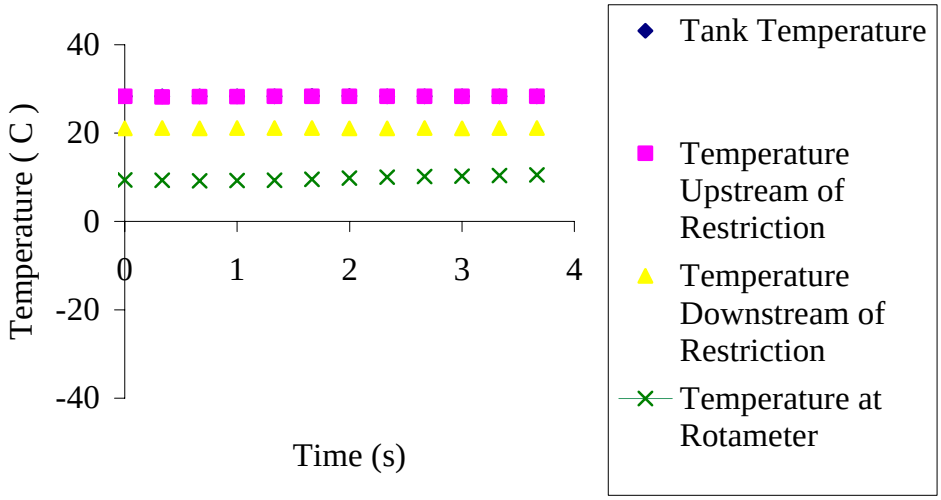

Metering valve w/o injection – 1 turn open

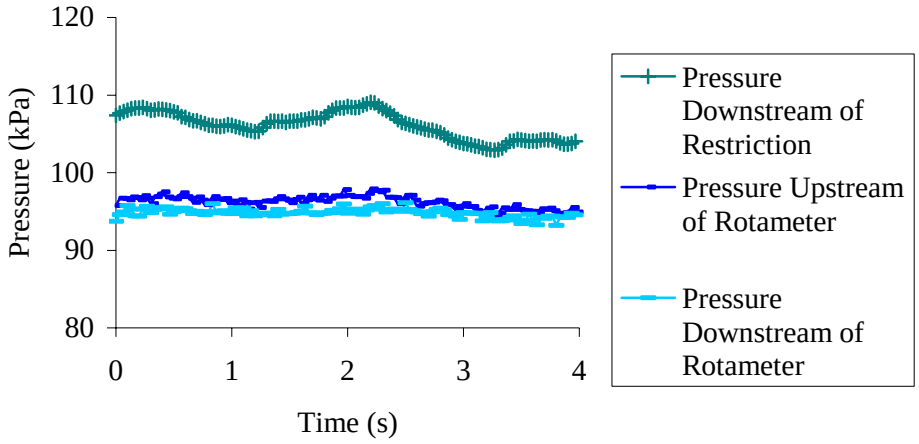

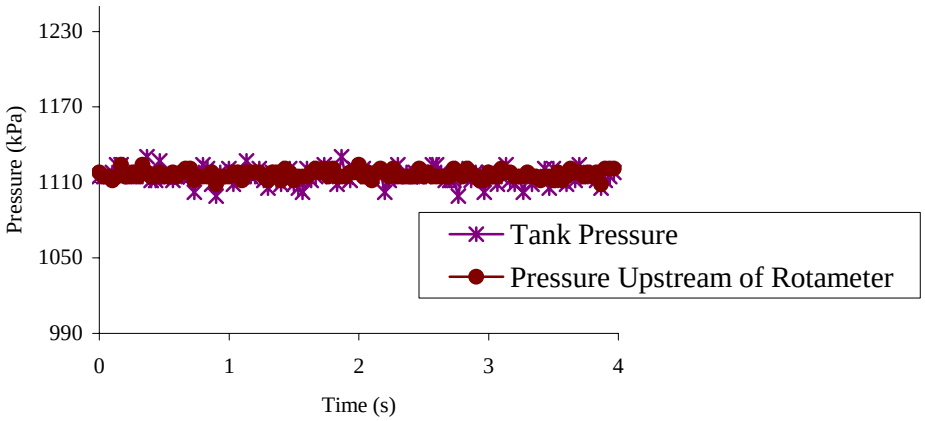

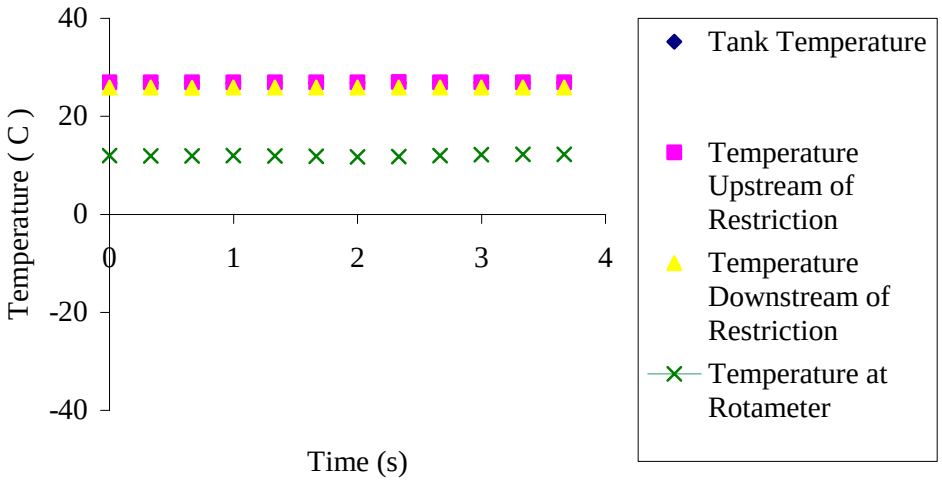

Metering valve with injection – 1 turn open

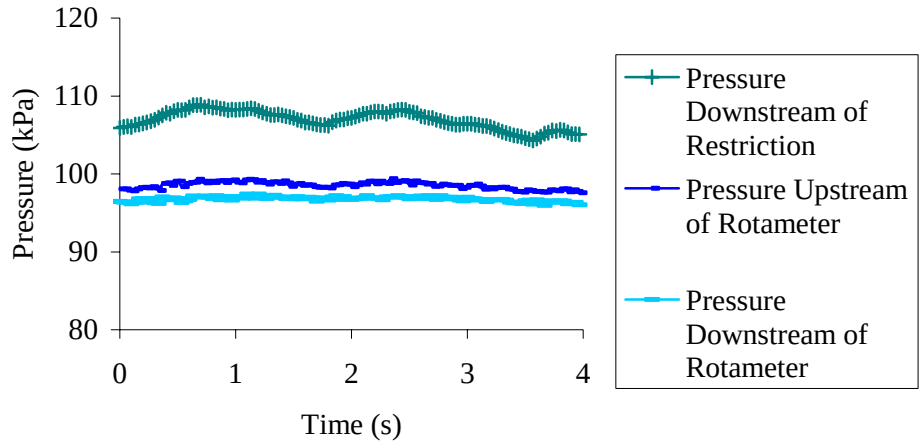

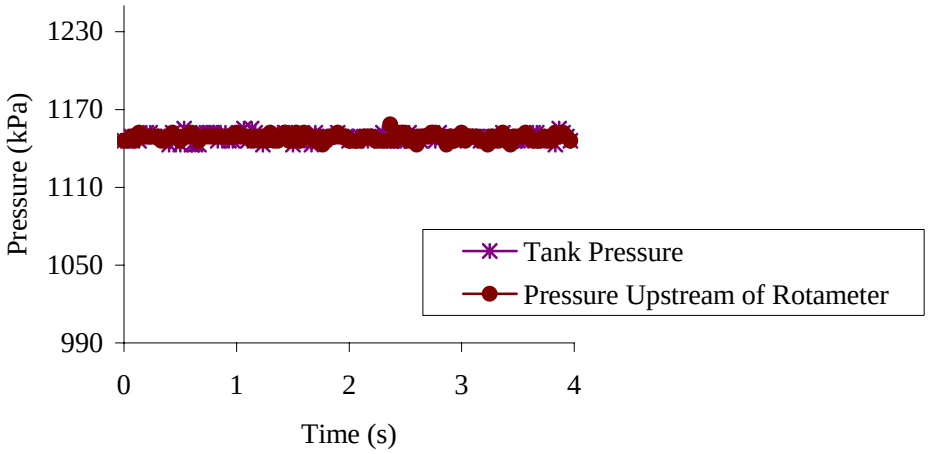

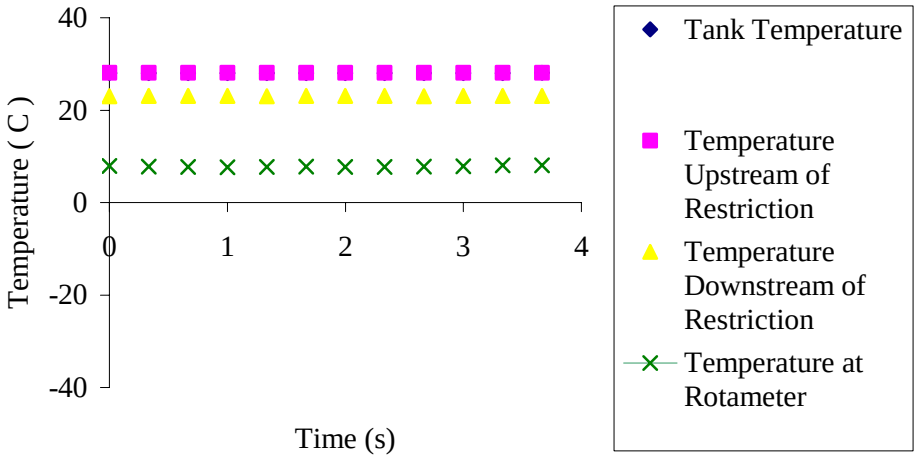

Metering valve w/o injection – 2 turns open

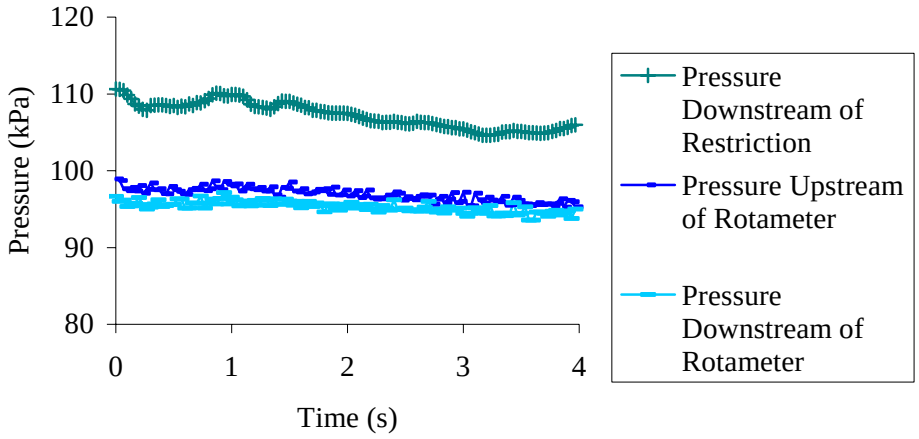

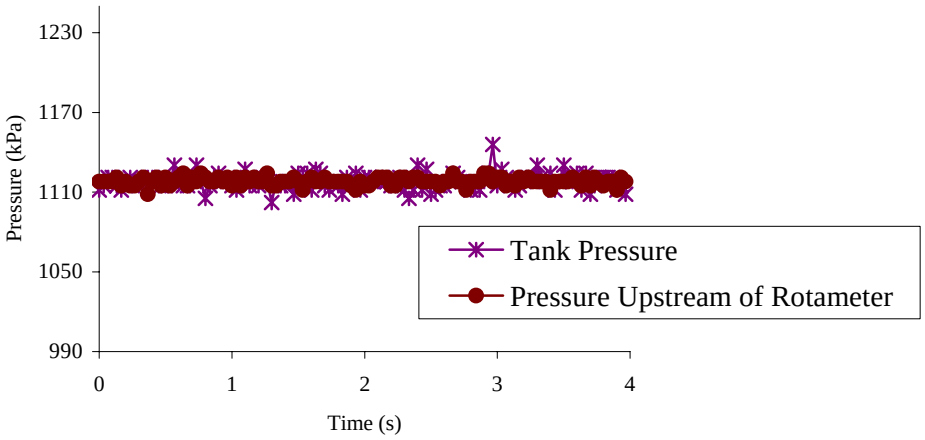

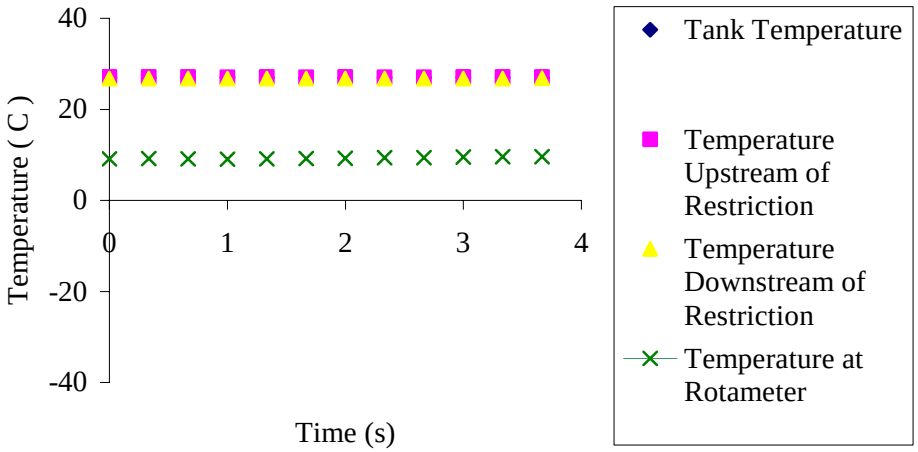

Metering valve with injection – 2 turns open

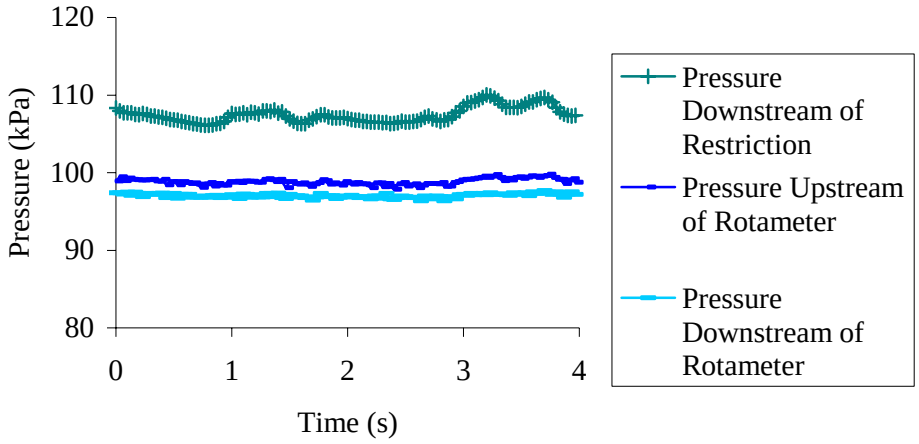

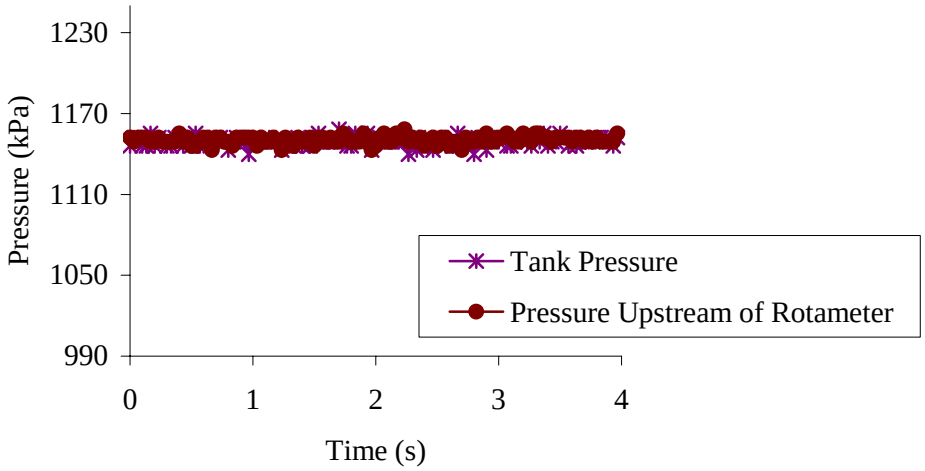

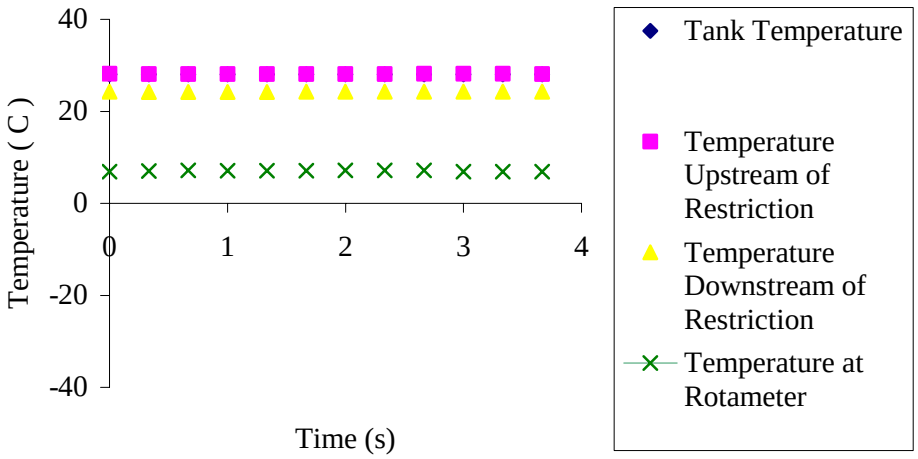

Metering valve w/o injection – 3 turns open

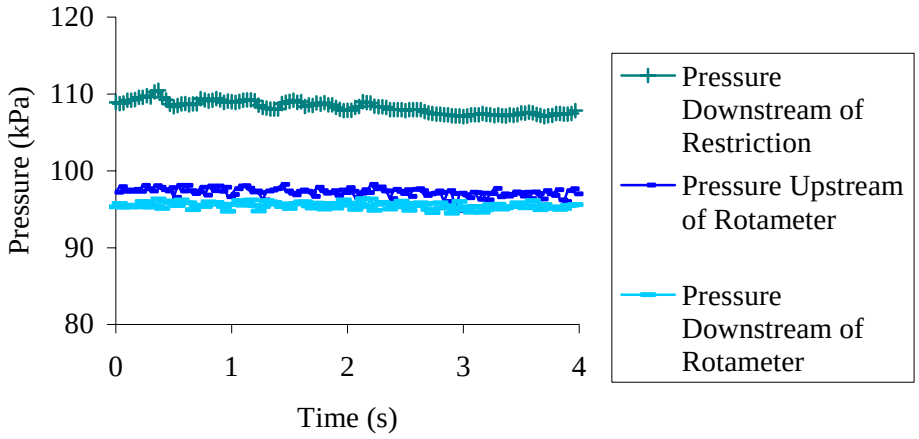

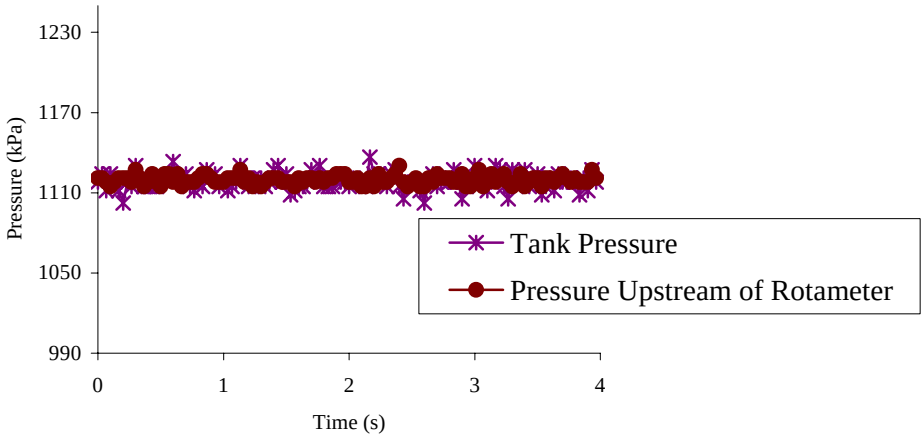

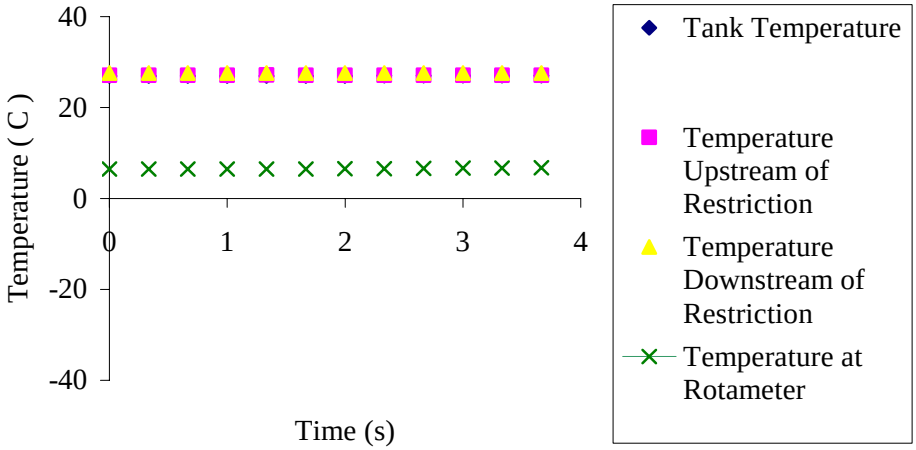

Metering valve with injection – 3 turns open

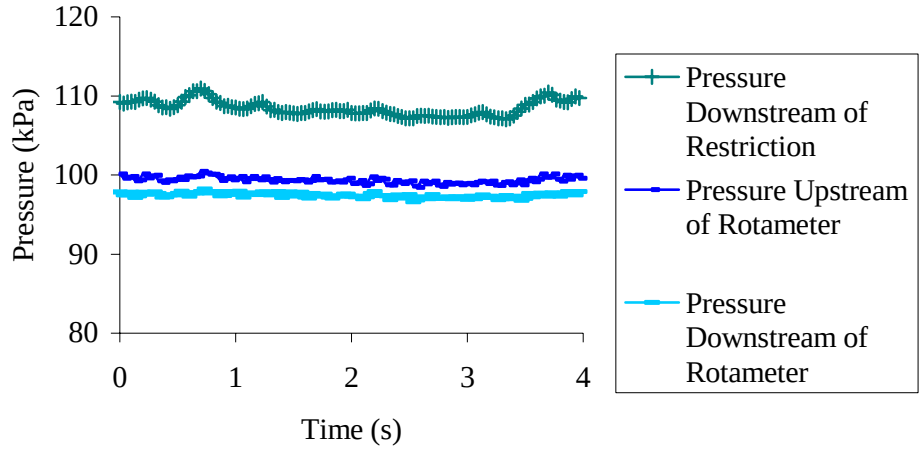

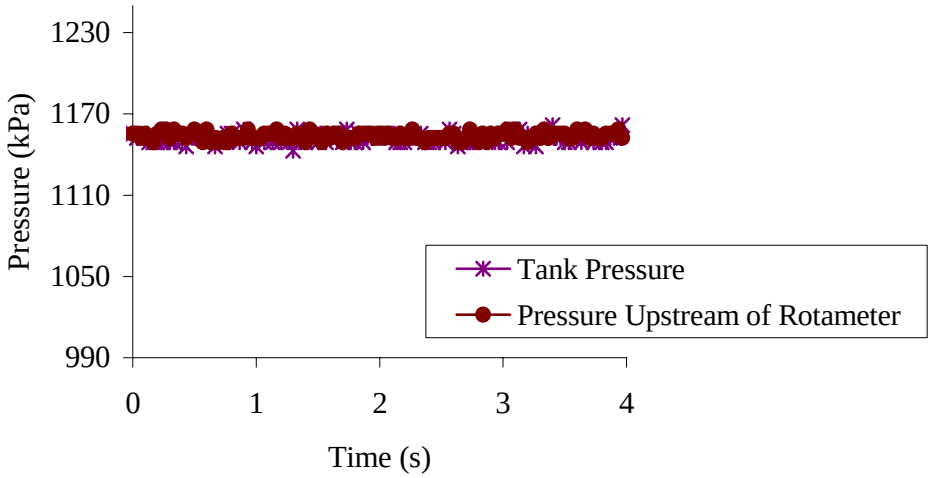

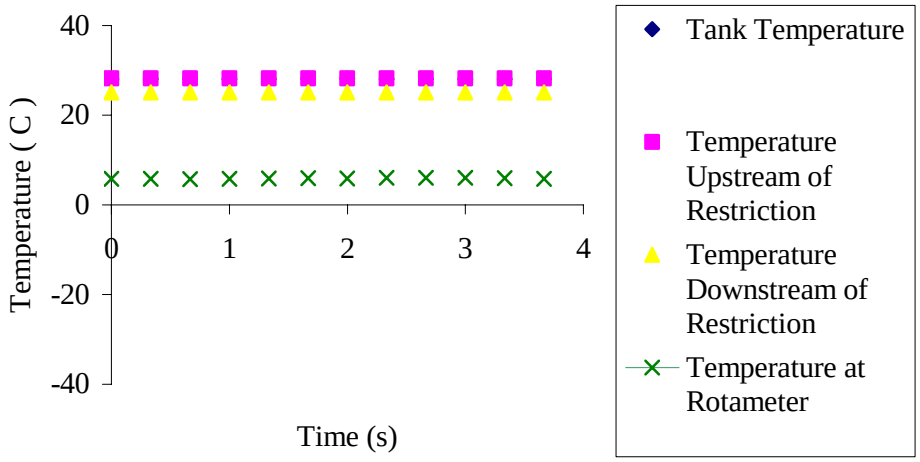

Metering valve w/o injection – 4 turns open

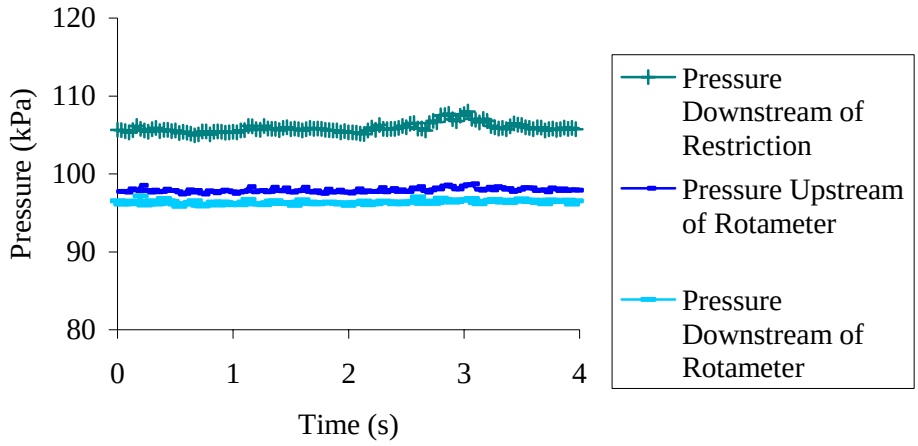

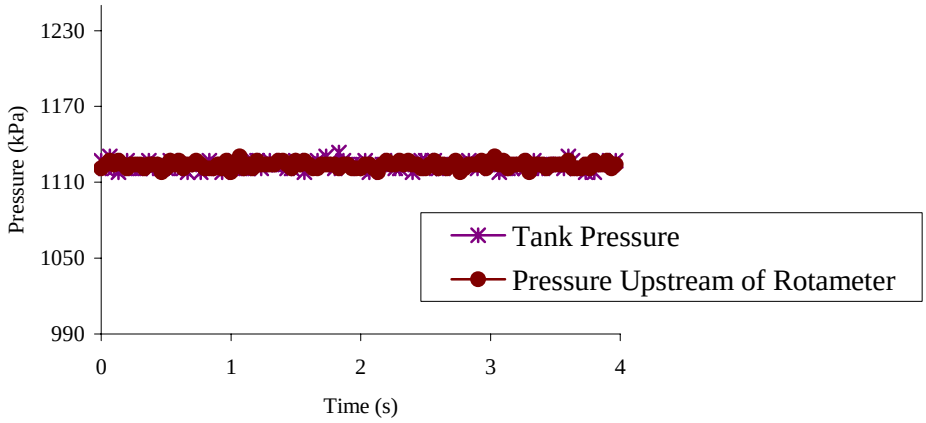

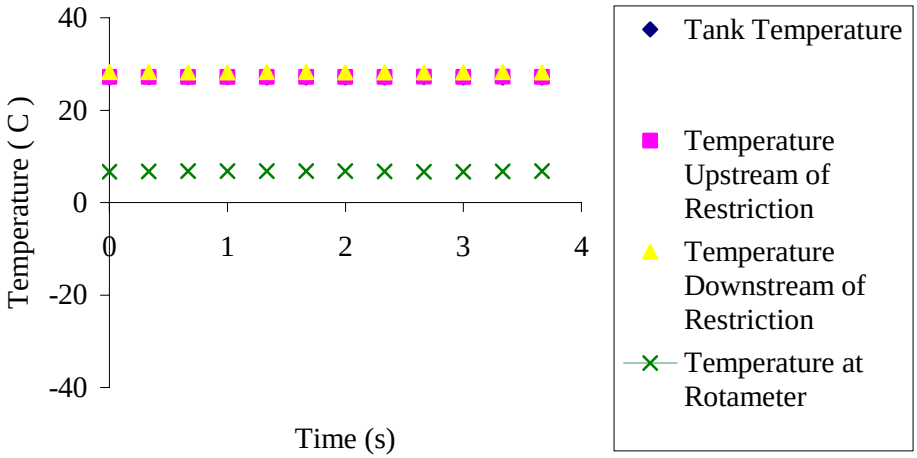

Metering valve with injection – 4 turns open

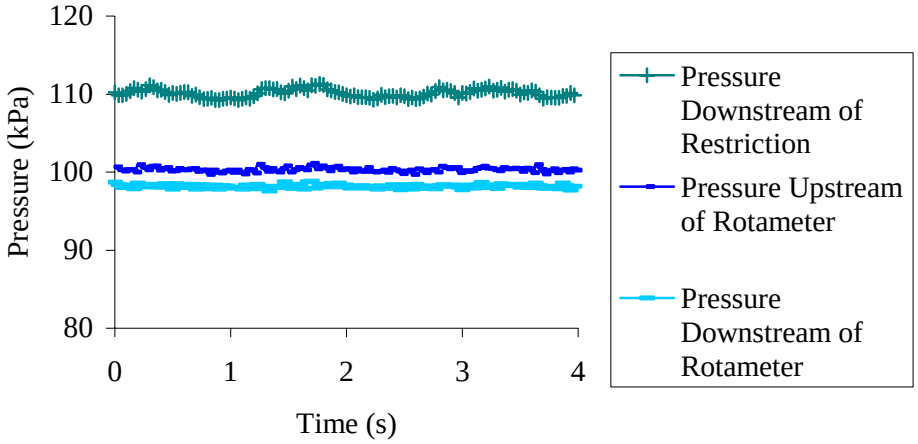

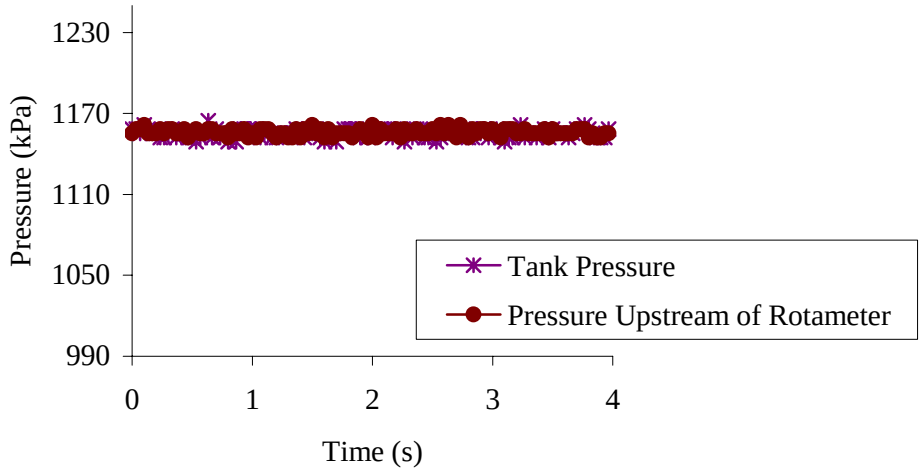

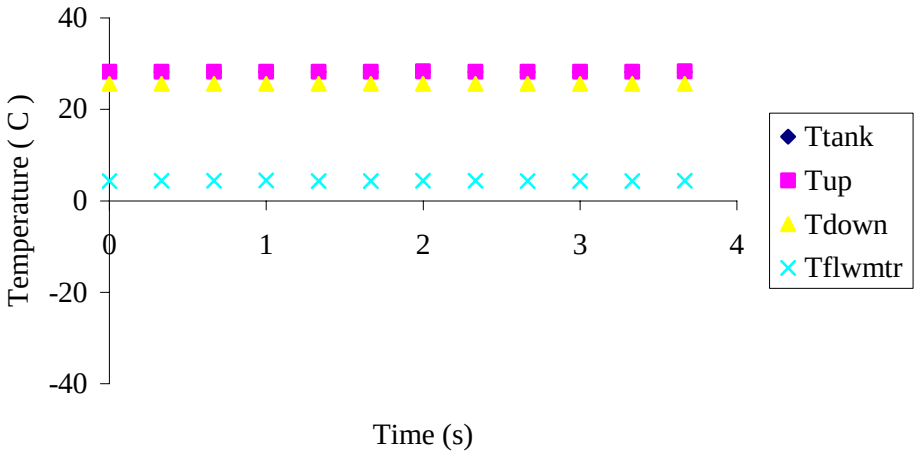

Metering valve w/o injection – 5 turns open

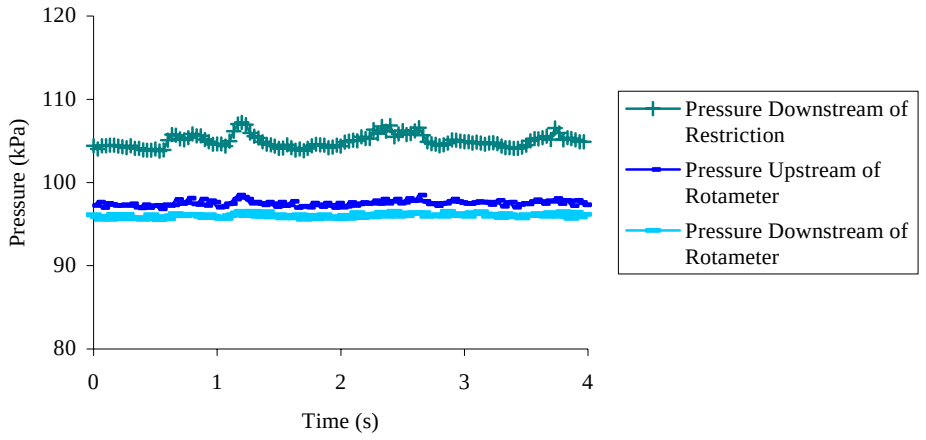

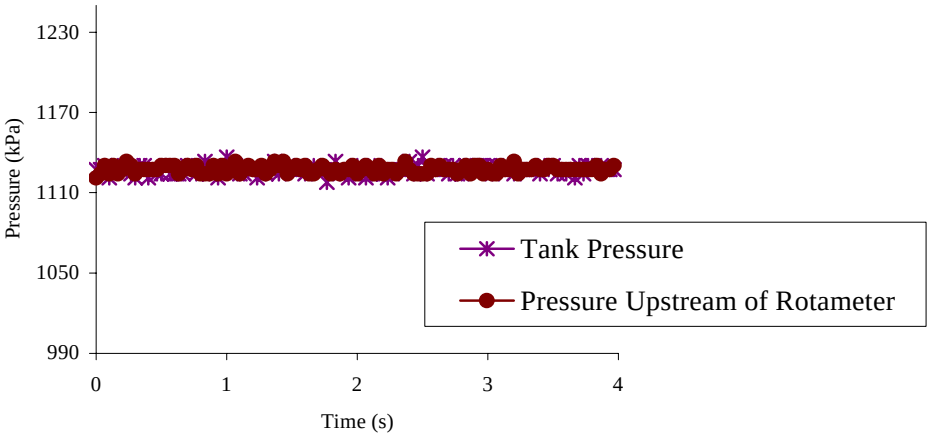

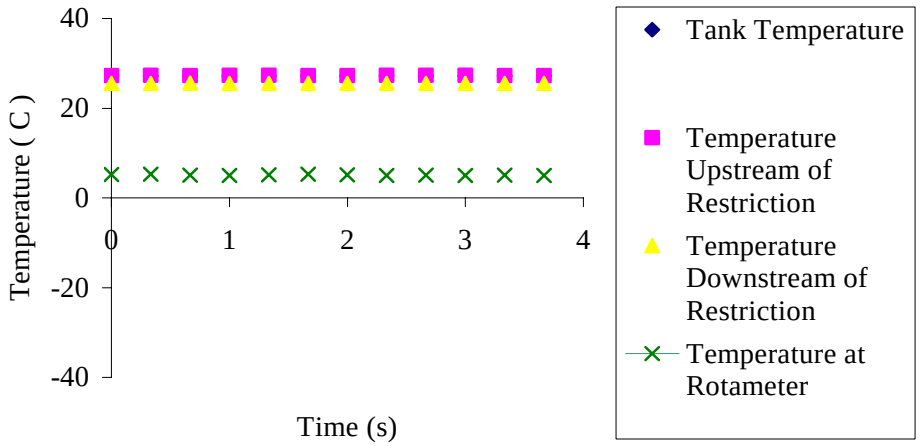

Metering valve with injection – 5 turns open

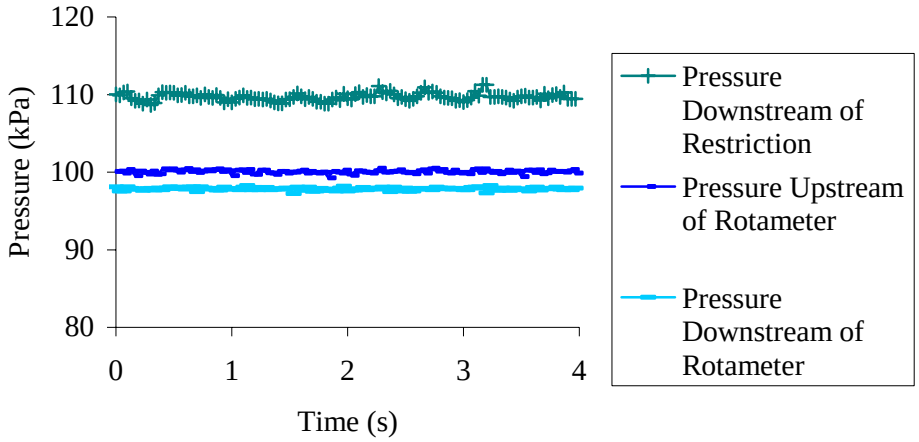

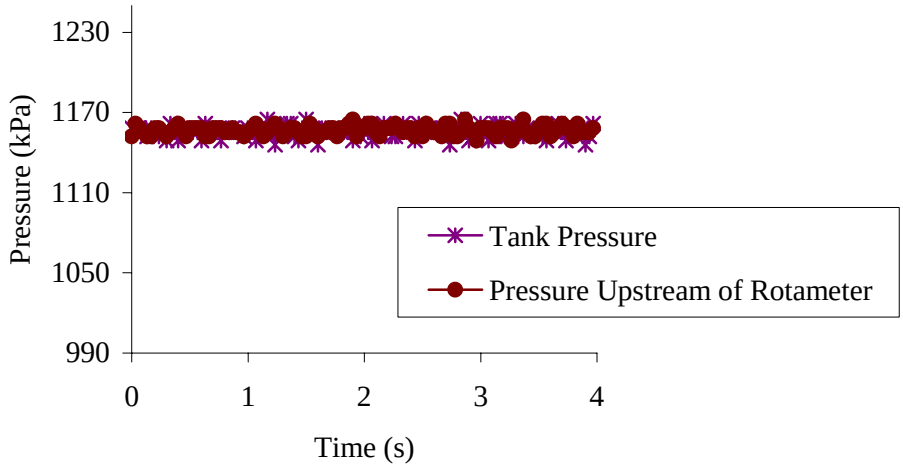

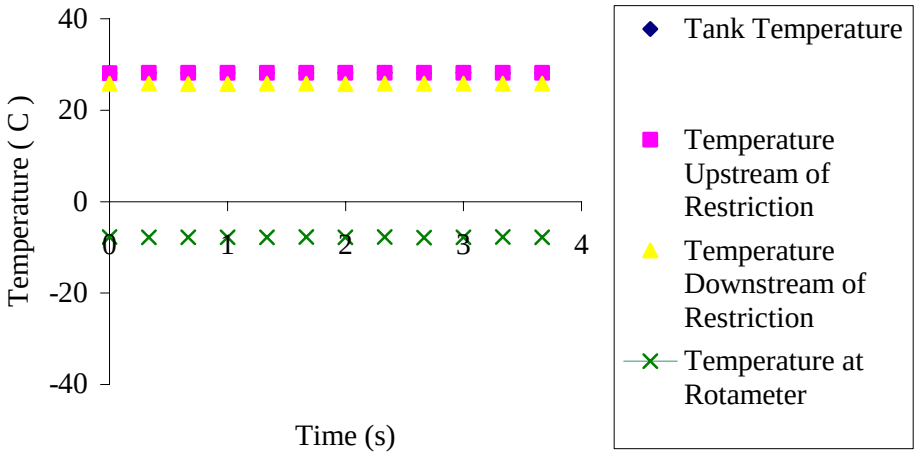

Metering valve w/o injection – 6 turns open

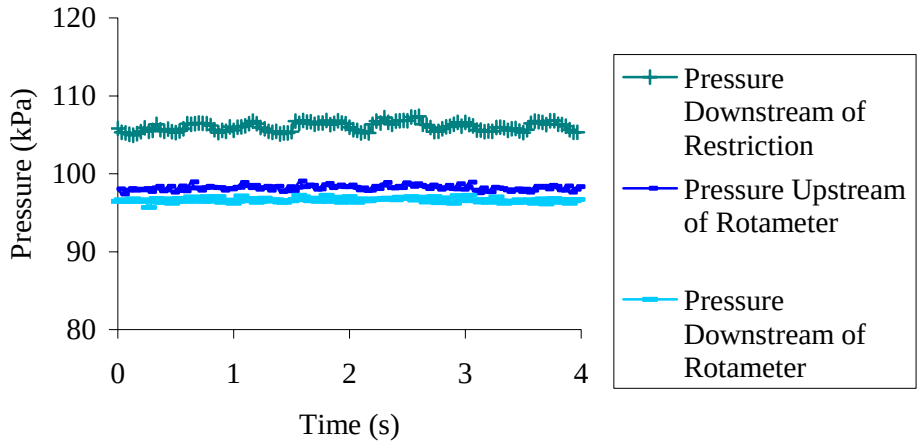

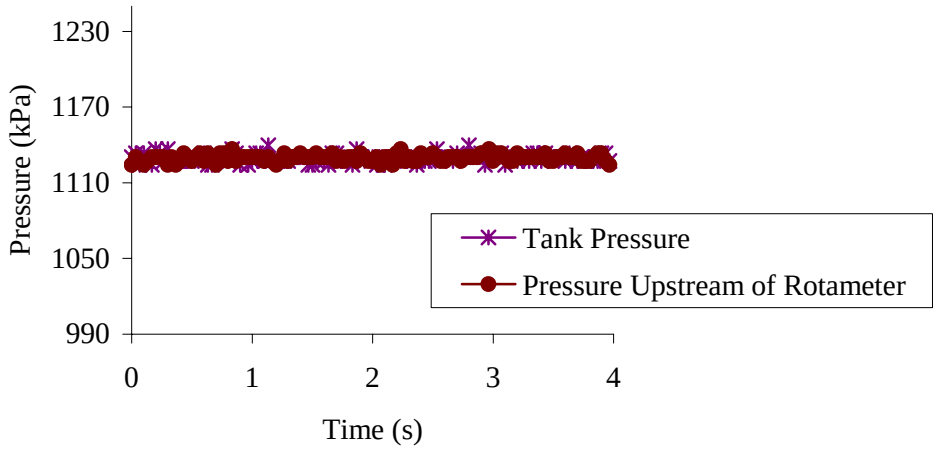

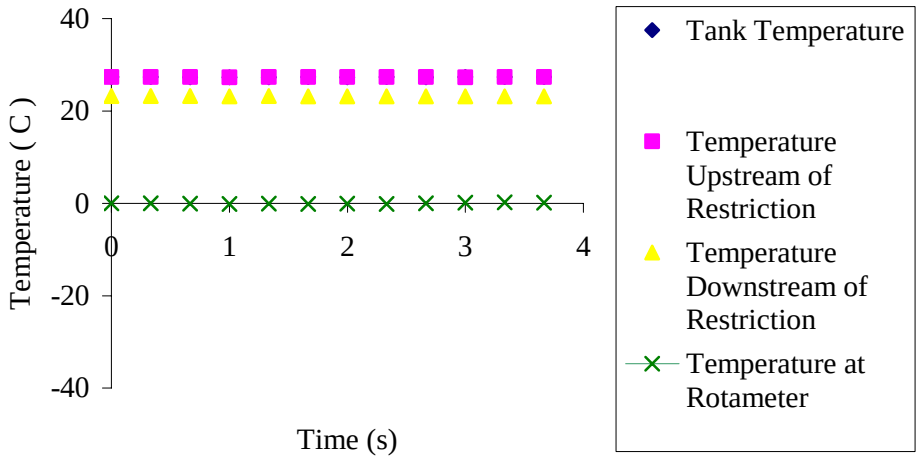

Metering valve with injection – 6 turns open

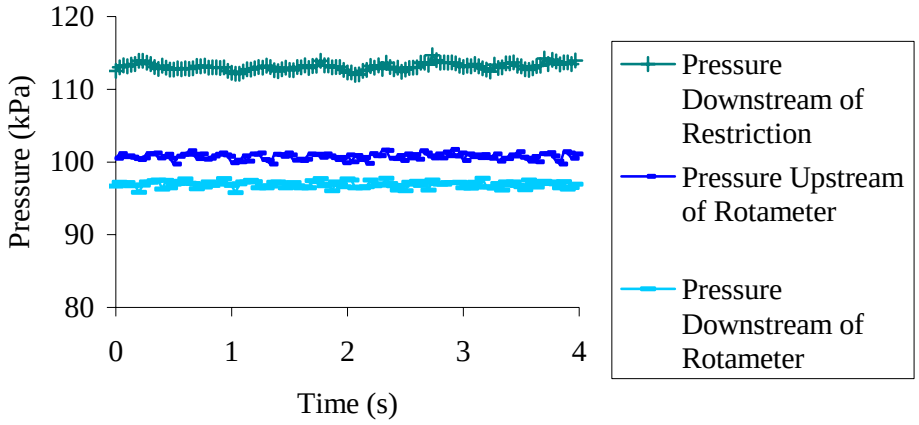

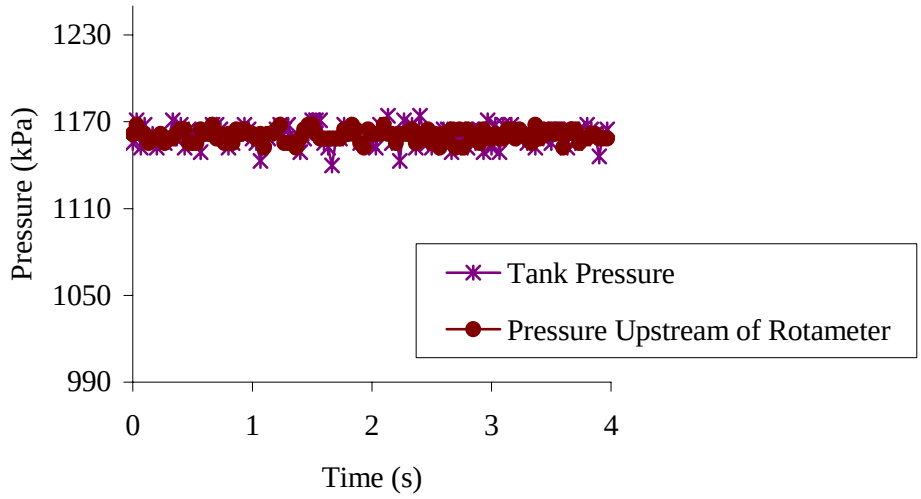

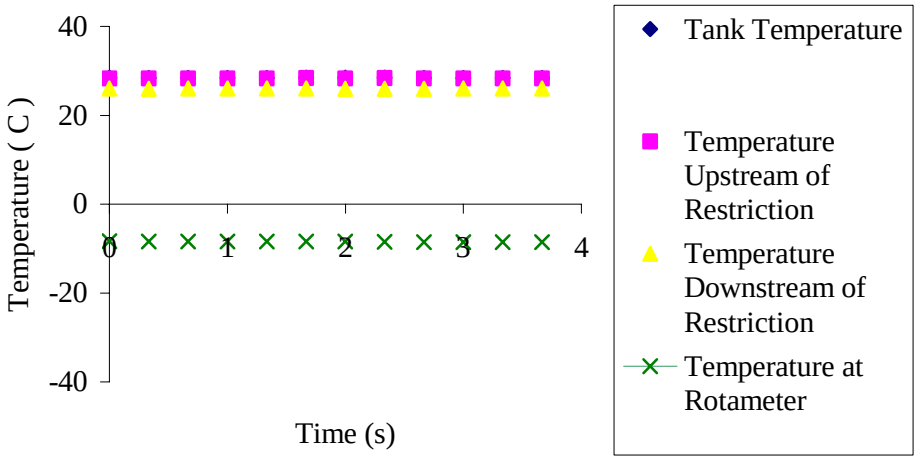

Metering valve w/o injection – 7 turns open

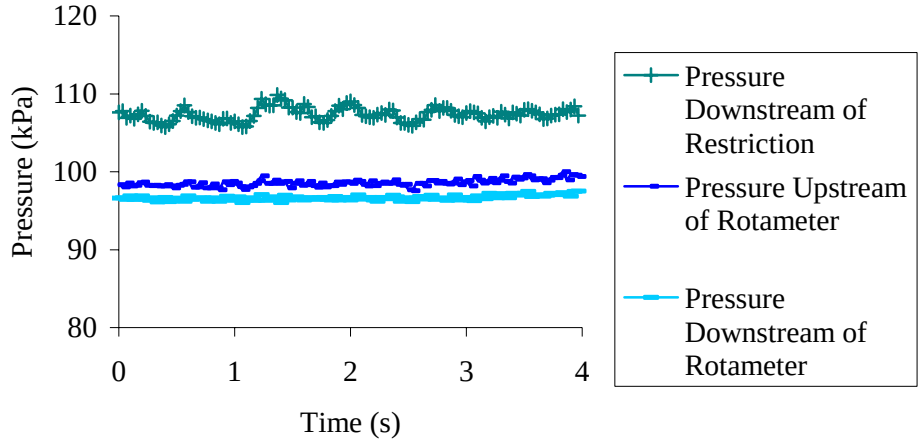

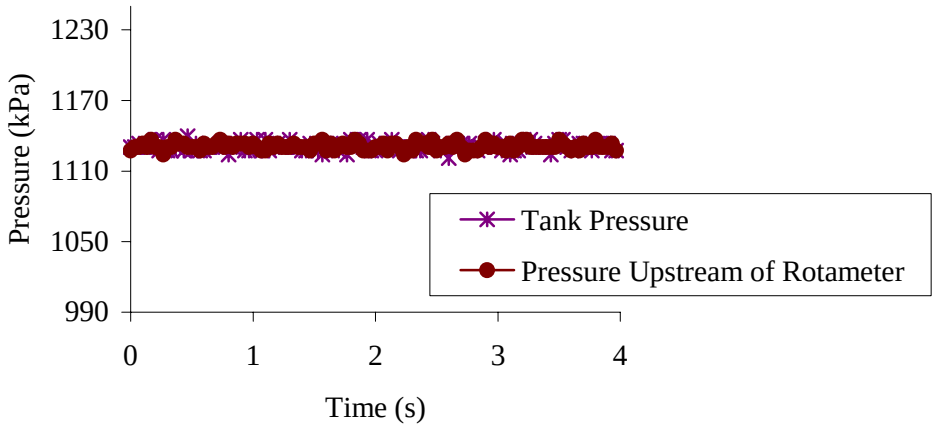

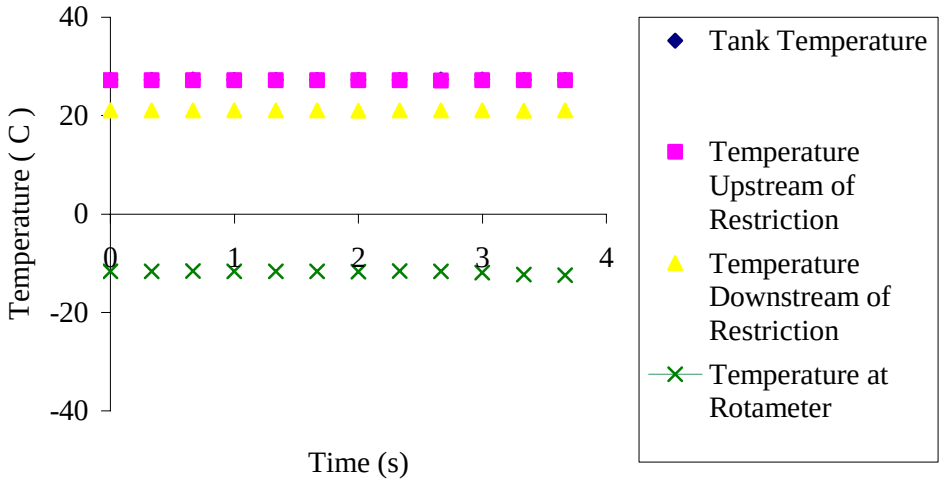

Metering valve with injection – 7 turns open

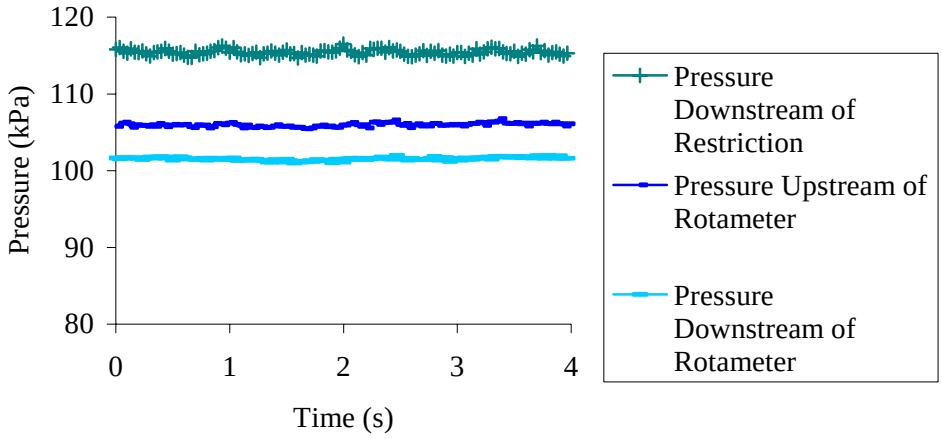

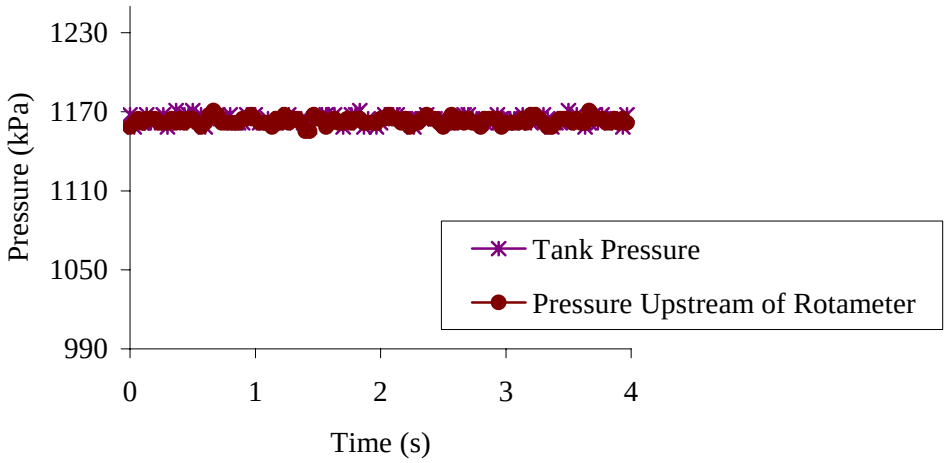

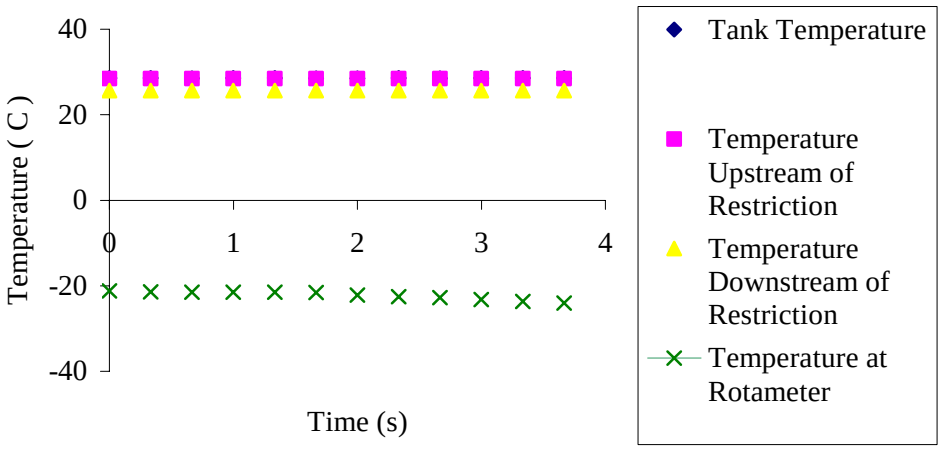

Metering valve w/o injection – 8 turns open

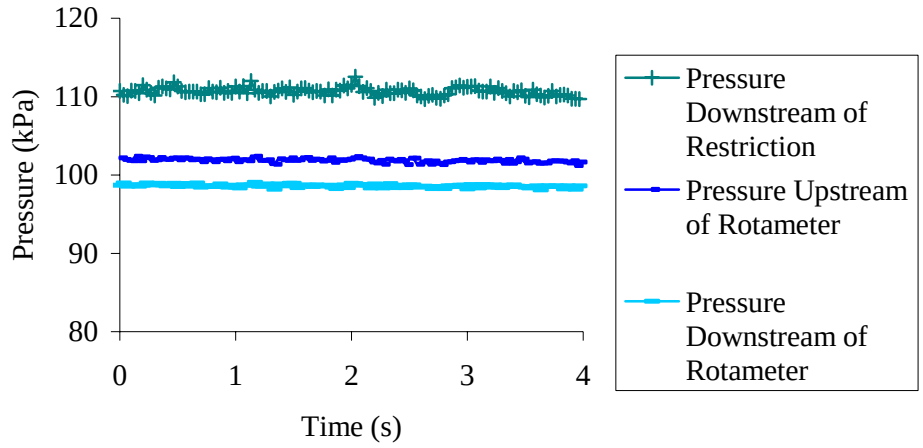

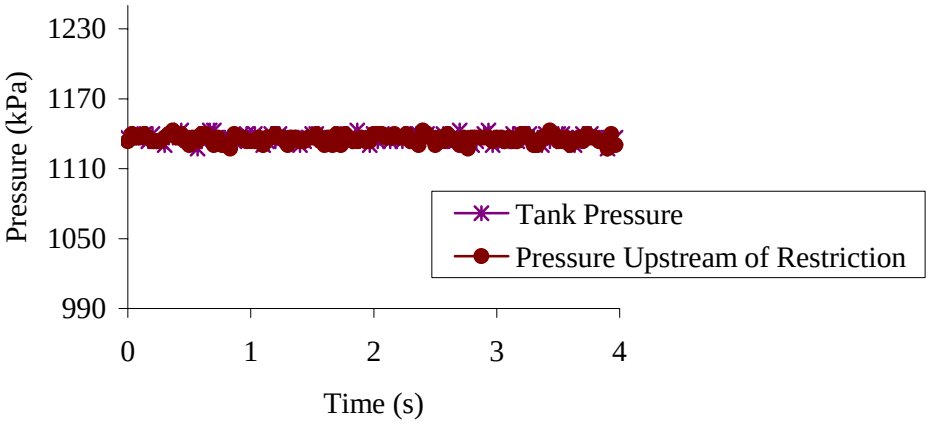

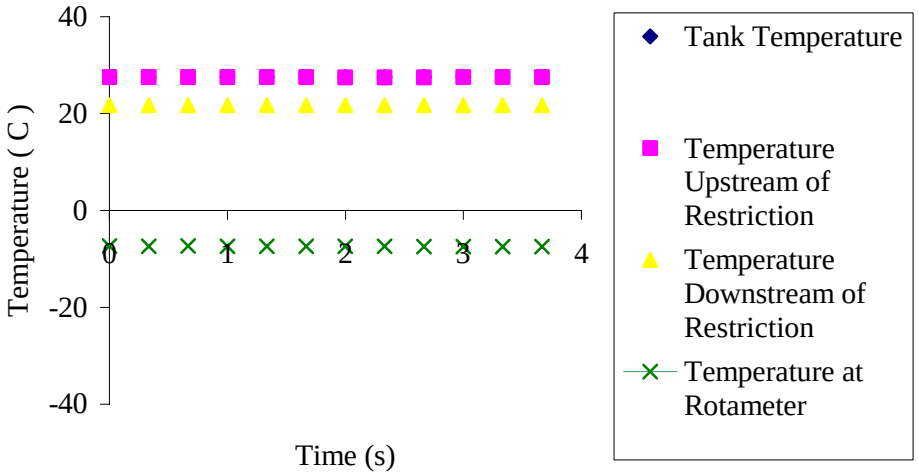

Metering valve with injection – 8 turns open

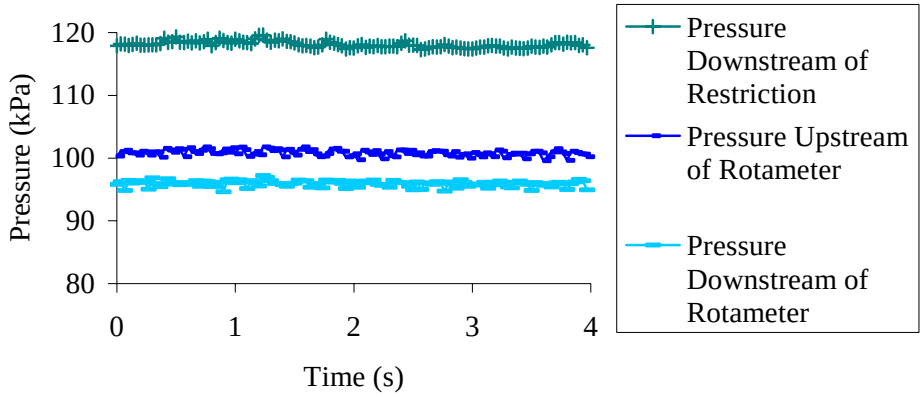

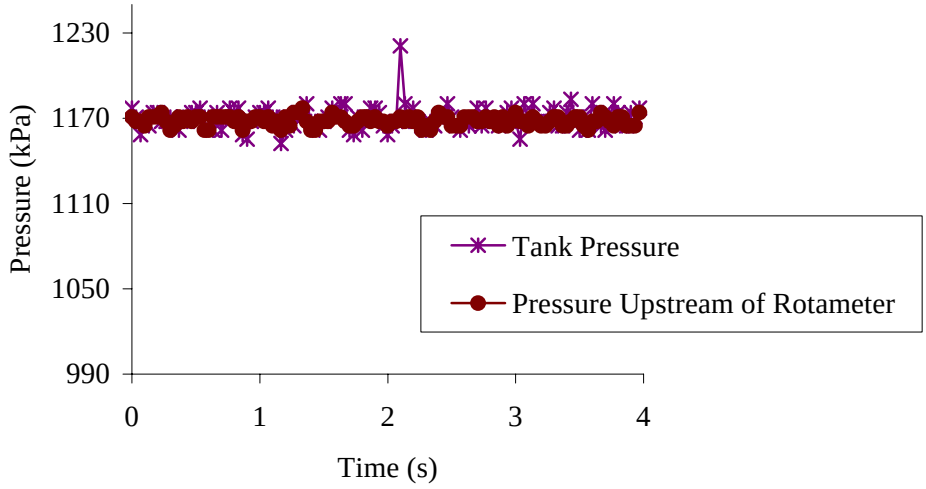

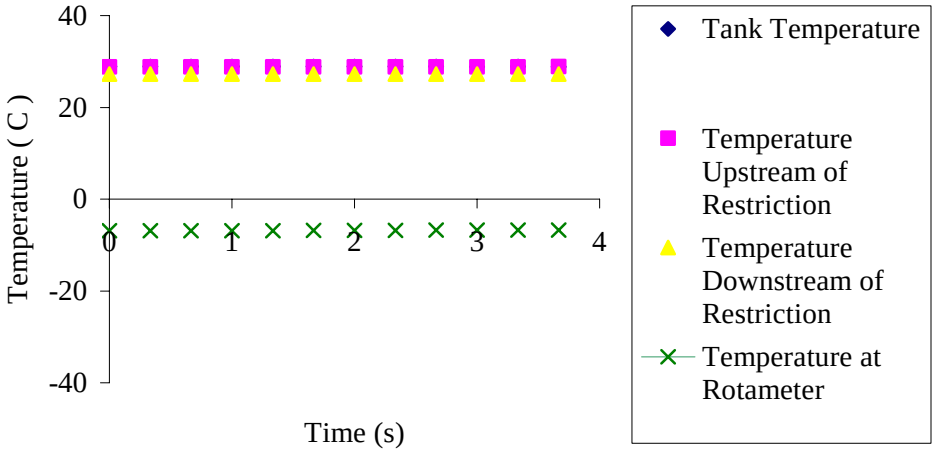

APPENDIX D.
FUEL SYSTEM PICTURES

Perpendicular to intake air flow axis with engine fan cowling removed

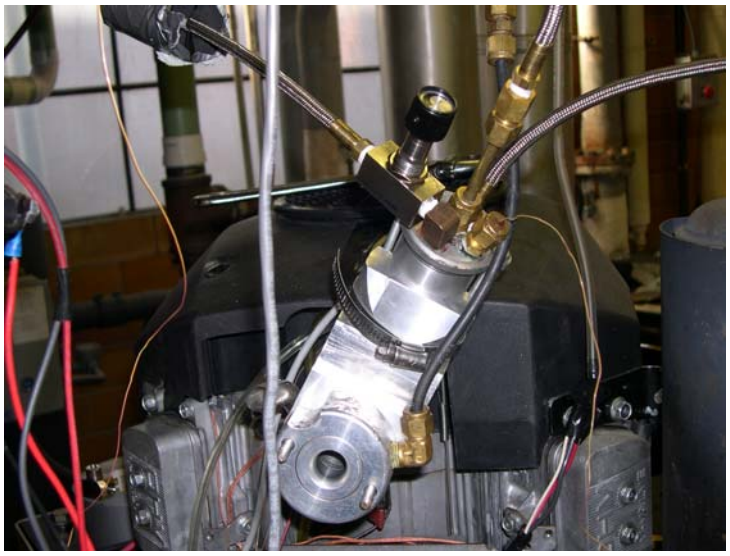

Intake venture orifice

Perpendicular to intake air flow axis with engine fan cowling on.

BIBLIOGRAPHY

[1] R. Sierens, “An Experimental and Theoretical Study of Liquid LPG Injection,” SAE Technical Paper Series, 922363, pp. 79-88, October 1992.

[2] Jacob L. Brann, “Fuel System Development for Liquid-Phase Injection of Liquefied Petroleum Gas on Small Displacement Engine,” University of Missouri-Rolla Thesis, 2002.

[3] Smith, W. J., Timoney, D. J., and Lynch, D. P., “Emissions and Efficiency Comparison of Gasoline and LPG Fuels in a 1.4 Litre Passenger Car Engine,” SAE Technical Paper Series, 972970, October 1997.

[4] Caton, J. A., McDermott, M., and Chona, R., “Development of a Dedicated LPG-Fueled Spark Ignition Engine and Vehicle for the 1996 Propane Vehicle Challenge,” SAE Technical Paper Series, 972692, August 1997.

[5] Wu, D- Y., Matthews, R. D., Popova, E. T., and Mock C., “The Texas Project, Part 4 – Final Results: Emissions and Fuel Economy of CNG and LPG Conversions of Light-Duty Vehicles,” SAE Technical Paper Series, 982446, October 1998.

[6] Dean Nelson, “Development of a Dual Fueled (Gasoline or Propane) Air Cooled, Spark Ignited Utility Engine,” SAE Technical Paper Series, SAE 1999-01-3335 SAE 9938090, September 1999.

[7] Roberto Cipollone and Carlo Villante, “A/F and Liquid-Phasse Control in LPG Injected Spark Ignition ICE,” SAE Technical Paper Series, 2001-01-2974, October 2000.

[8] Lutz, B. R., Stanglmaier, R. H., Matthews, R. D., Cohen, J., and Wicker, R., “The Effects of Fuel Composition, System Design, and Operating Conditions on In-System Vaporization and Hot Start of a Liquid-Phase LPG Injection System,” SAE Technical Paper Series, 981388, May 1998.

[9] Van Der Meer, “Simulation of a Refrigerant Evaporator,” Technishe University Ph. D. Thesis, 1987.

10] H. Miyamoto and K. Watanabe, “A Thermodynamic Property Model for Fluid-Phase Propane,” International Journal of Physics, Vol. 21 no. 5, pp. 1045-1072, 2000.

[11] J. T. Jeong and S. R. Choi, “Axisymmetric Stokes Flow Through a Circular Orifice in a Tube,” Physics of Fluids17, 053602, 2005.

[12] C-L. Zhang and L. Yang, "Modeling of Supercritical CO2 Flow Through Short Tube Orifices," Transactions of the ASME, Vol. 127, pp. 1194-1198, November 2005.

[13] M. Lorcher and D Mewes, "Atomization of Liquids by Two-Phase Gas-Liquid Flow Through a Plain-Orifice Nozzle: Flow Regimes Inside the Nozzle," Chem. Eng. Technol. 24, pp. 167-172, 2001.

[14] Bahajji, M. A., Corberan, J. M., Urchueguia, J.,Gonzalvez, J., and Santiago, J., "Study About Flashing Process Through a Metering Expansion Valve," Experimental Thermal and Fluid Science 29, pp. 757-763, 2005.

[15] M. W. Benjamin and J.G. Miller, "The Flow of Saturated Water Through Throttling Orifices," Transactions of the ASME, July 1941.

[16] D. A. McNeil, "Two-Phase Flow in Orifice Plates and Valves," Proc. Instn. Mech. Engrs., Vol 214, pp. 743-756, 2000.

[17] J. A. Perry, "Critical Flow Through Sharp-Edged Orifices," Transactions of the ASME, pp. 757-764, October 1949.

[18] Robert E. Henry and Hans K. Fauske, "The Two-Phase Critical Flow of One-Component Mixtures in Nozzles, Orifices, and Short Tubes," Journal of Heat Transfer, pp. 179-187, May 1971.

[19] H. Uchida and H. Nariai, "Discharge of Saturated Water Through Pipes and Orifices," A.S.M.E.

[20] Koederitz, Kyle R. "Investigation of Hydrocarbon Sources and Reduction in Small Four-Stroke Spark Ignition Engines," Ph.D. Dissertation, University of Missouri-Rolla, 2003.

[21] Wikepedia, http://en.wikipedia.org/wiki/Strouhal_number, June 24, 2007.

[22] Md. Alamfir and J.H. Lienhard, "Correlation of Pressure Undershoot During Hot-Water Depressurization," Transaction of the ASME, Vol. 103, February 1981.

[23] C. Buffone and K. Sefiane, "IR Measurements of Interfacial Temperature During Phase Change in a Confined Environment," Experimental Thermal and Fluid Science 29, pp. 65-74, January 2004.

[24] Frigiola, R. S. and Beasley, D. E., "Theory and Design for Mechanical Measurements," John Wiley and Sons, 4th Edition, 1994.

[25] Gemci, T., Yakut, K., Chigier, N., and Ho, T. C.,"Flash Atomization of Water/Acetone Solutions," Atomization and Sprays, Vol. 14, pp. 459-475, 2004.

[26] Omer L. Gulder, “Correlations of Laminar Combustion Data for Alternatives S.I. Engine Fuels,” SAE Technical Paper Series, 841000, August 1984.

[27] K. Hara and H. Yonetani, “CNG Utilization in Small Engines,” SAE Technical Paper Series, 940763, February 1994.

[28] John B. Heywood, “Internal Combustion Engine Fundamentals,” McGraw-Hill, Inc., 1988.

[29] Zaki D. Hussain, “Theoretical Uncertainty of Orifice Flow Measurement,” Proceedings of the International School of Hydrocarbon Measurement, Is. 72, 1997.

[30] St. Korner and L. Friedel, “Assessment of the Maximum Possible Liquid Superheat During Flashing Leak Flow,” Elseveir Science Ltd., 0950-423(97)00024-7.

[31] H. R. Linden and D. F. Othmer, “Air Flow Through Small Orifices in the Viscous Region,” Trasaction of the ASME, pp. 765-772, October 1949.

[32] D. B. Rhodes and J. C. Keck, “Laminar Burning Speed Measurements of Indolene-Air-Diluent Mixtures at High Pressures and Temperature,” SAE Technical Paper Series, 850047, March 1985.

[33] Sonntag, R. E., Borgnakke, C., and Van Wylan, G. J., “Fundamentals of Thermodynamics,” John Wiley and Sons, Inc., 5th Ed., 1998.

[34] B. N. Taylor and C. E. Kuyatt, “Guidelines for Evaluating and Expressing the Uncertainty of NIST Measurement Results,” NIST Technical Note 1297, 1994.

[35] S. A. G. Watson and S. McCahan, “An Experimental Study of the Injection of Preheated Dodecane Through a Transparent Converging –Diverging Nozzle,” University of Toronto.

[36] Xiaojin, Huanzhen, and Qiaoxinqi, “A Model of Atomization on a Flash Boiling Spray with Fuel Containing CO2,” Proceedings of the 10th Annual Conference on Liquid Atomization and Spray Systems, pp. 249 –254, October 2005.

VITA

Brian Charles Applegate was born October 15, 1979 in St. Louis, MO. His current education includes a B.S. in Mechanical Engineering in 2003 along with a B.S. in Economics in 2003. This work completed Brian's work on a M.S. in Mechanical Engineering in 2007. Currently, Brian is working for Caterpillar Inc. in the Engine Research department in Mossville, IL.

Brian is the son of Walter and Teresa Applegate. He grew up in St. Louis, MO where he grew up watching the Cardinals with his brother Jeremy Applegate. Through his natural curiosity and open minded influence of his parents, Brian is a student of many endeavors and can therefore be found in any one of many favored activities that range from automotive repair and modifications to photography, landscaping, woodworking, running, lifting, cooking, church work, charity work or any other 'wild hare' projects that peak his interest.

His future will hopefully include some land in the country where he can enjoy the wide open spaces with family. Brian hopes to further his career with Caterpillar, make notable contributions to technological advancement, and donate time and resources to worthy causes in gratitude to the blessings he enjoys. If Brian could give advice, it would be to always pursue options. Options give the beholder power to shape their future.